UNIVERSITY OF CALIFORNIA

Los Angeles

Adipose tissue lipolysis and the regulation of hepatic lipid metabolism

A dissertation submitted in partial satisfaction of the

requirements for the degree Doctor of Philosophy

in Molecular, Cellular, and Integrative Physiology

by

Sicheng Zhang

2023

ABSTRACT OF THE DISSERTATION

Adipose tissue lipolysis and the regulation of hepatic lipid metabolism

by

Sicheng Zhang

Doctor of Philosophy in Molecular, Cellular, and Integrative Physiology

University of California, Los Angeles, 2023

Professor Claudio J. Villanueva, Chair

The communication between adipocytes and liver plays a crucial role in the physiological regulation of metabolism and understanding the basis of this dynamic inter-organ communication has the potential to advance clinical therapies. This is particularly important for conditions like obesity, fatty liver disease, and type 2 diabetes, which have emerged as global metabolic disorders. Consequently, the investigation of the communication between the liver and adipose tissue has been a hot point in metabolic research for many years (Azzu, Vacca et al. 2020).

Numerous studies have investigated adipose tissue and its secretome composition, however, a comprehensive global analysis of the lipidome was still absent. In this study, we used the beta-3-adrenergic receptor agonist, CL-316,243 (CL), to stimulate adipose tissue lipolysis in both in *vivo* and *in vitro* settings (Zhang, Williams et al. 2023). A single dose of CL treatment was deemed an appropriate model to mimic acute adipose tissue lipolysis. Additionally, we conducted a time course analysis to investigate the dynamic changes in the adipose tissue

lipolysis lipidome and its impact on hepatic lipidome, considering the lipid flux originating from adipose tissue lipolysis. We also utilized ATGL adipose tissue-specific knockout mice as a model to underscore the significance of adipose tissue lipolysis in hepatic lipid remodeling (Kim, Tang et al. 2016). Our study provides a comprehensive perspective on how adipose tissue lipolysis remodels the hepatic lipidome. Furthermore, we identified specific lipid alterations of interest, including the accumulation of linoleic acid and the release of odd-chain free fatty acids.

Another pivotal aspect of the study on the interaction between adipose tissue and the liver is how the liver responds to adipose tissue lipolysis. In this investigation, we applied RNA-seq and subsequent bioinformatic analysis to detect novel hepatic regulators. In addition to the well-established regulators such as PPARa, HNF4a, and SREBP1c, we identified hepatic glucocorticoid receptor (GR) as another critical transcription factor involved in this process, which is activated by the hypothalamic-pituitary adrenal (HPA) axis. Furthermore, it appears that hepatic GR plays a crucial role in regulating ketogenesis and triglyceride accumulation during adipose tissue lipolysis. Notably, our research revealed that Plin5 serves as a downstream target whose expression is controlled by hepatic GR directly. And absence of hepatic Plin5 also impedes ketogenesis. This suggests that the Adipose-HPA-GR-PLIN5 axis may represent an important regulatory pathway in ketogenesis.

In addition to RNA-seq, we employed Assay of Transposase-Accessible Chromatin ATAC-seq as an additional tool to investigate hepatic regulators. Our findings suggest that a novel transcription factor, Elk4, may potentially have a role in hepatic metabolism, specifically in glucose metabolism and pyruvate metabolism. However, given the limited knowledge available about Elk4, further research is warranted to understand more about its functions and mechanisms.

The dissertation of Sicheng Zhang is approved.

Tamer I. Sallam

Thomas Aguiar Vallim

Xia Yang

Claudio J. Villanueva

University of California, Los Angeles

2023

Table of Contents

CHAPTER ONE.....1

ADIPOSE TISSUE LIPOLYSIS REGULATES HEPATIC LIPIDS REMODELING.....1

1.1 INTRODUCTION.....2

1.1.1 NAFLD and Obesity.....2

1.1.2 Adipose Tissue Lipolysis.....4

1.2 ADIPOSE TISSUE LIPOLYSIS IN THE PHYSICAL CONTROL OF COLD, FASTING, AND EXERCISE.....7

1.3 ADIPOSE TISSUE LIPOLYSIS RELEASES THE SIGNALS AND LIPIDS SOURCE FOR HEPATIC LIPIDS REMODELING.....9

1.4 CELLULAR ORGANELLES IN HEPATOCYTES RESPONDING TO ADIPOSE TISSUE LIPOLYSIS.....10

1.5 TRANSCRIPTION REGULATION AND TRANSCRIPTION FACTORS ACTIVATION PROCESS.....13

1.5.1 Transcription factors.....13

1.5.2 Co-transcription factors.....17

1.5.3 Histone modifications.....18

1.6 SUMMARY.....19

CHAPTER TWO.....21

ACUTE ADIPOCYTE LIPOLYSIS AND DYNAMIC LIPID REMODELING OF LIPIDOME IN THE LIVER.....21

2.1 INTRODUCTION.....22

2.2 TARGETED QUANTITATIVE LIPIDOMIC ANALYSIS USING LC-MS OF WHOLE MOUSE SERUM AFTER ACUTE ACTIVATION OF ADIPOCYTE LIPOLYSIS.....24

2.3 HEPATIC LIPID REMODELING DYNAMIC.....28

2.3.1 Time Dependent Changes in Serum and Liver Lipids Highlight Dynamic Lipid Remodeling...29

2.3.2 Adipocyte lipolysis promotes the expression of genes involved in lipid handling and hepatic lipid remodeling.....29

2.3.3 Adipocyte lipolysis increases energy expenditure and oxidation of both endogenous and dietary-derived lipids. 34
2.4 THE IMPACT OF BLOCKING ADIPOCYTE LIPOLYSIS ON HEPATIC LIPID REMODELING 36
2.4.1 Blocking adipocyte lipolysis prevents hepatic lipid remodeling induced by b3-AR activation. .36
2.4.2 Blocking adipocyte lipolysis attenuates triglyceride accumulation in the liver. 40
2.5 TARGETED LIPIDOMIC ANALYSIS FOR DIFFERENTIATED WHITE ADIPOCYTE AND HEPATOCYTES IN VITRO 41
2.5.1 Targeted lipidomic analysis of lipid secretome of differentiated white adipocyte. 41
2.5.2 Conditioned media from activation of lipolysis leads to lipid remodeling of hepatocyte lipidome. 43
2.6 DISCUSSION 46
CHAPTER THREE 52
ADIPOSE-LIVER CROSSTALK SIGNALING PROMOTES GR-PLIN5 AXIS TO REGULATE KETOGENESIS 52
3.1 INTRODUCTION 53
3.4 HEPATIC GR IS ESSENTIAL REGULATORS RESPONDING TO ADIPOSE TISSUE LIPOLYSIS. 64
3.4.1 Hepatic GR deficiency results in aberrant gene expression in the liver in response to adipose tissue lipolysis. 64
3.4.2 Hepatic GR deficiency impedes adipose tissue lipolysis induced ketogenesis and triglyceride metabolism. 67
3.4.3 The absence of hepatic GR hinders the induction of ketogenesis by dexamethasone. 70
3.5 HEPATIC PLIN5 DEFICIENCY HAMPERS THE INITIATION OF KETOGENESIS DURING ADIPOSE TISSUE LIPOLYSIS. 72
3.6 DISCUSSION 75
CHAPTER FOUR 79

ADIPOSE-LIVER CROSSTALK SIGNALING TRIGGERS HEPATIC CHROMATIN REMODELING, ACTIVATING ELK4 TO MODULATE GLUCOSE METABOLISM.....79

4.1 INTRODUCTION 80

4.2 ATAC-SEQ REVEALS THAT ADIPOSE TISSUE LIPOLYSIS PROMOTES HEPATIC CHROMATIN ACCESSIBILITY. 81

4.2.1 Quantification of ATAC-Seq result reveals the impact of adipose tissue lipolysis on regulating hepatic chromatin accessibility. 82

4.2.2 Adipose tissue lipolysis remodels hepatic chromatin accessibility exposing new binding sites of transcription factors. 83

4.3 ADIPOSE TISSUE LIPOLYSIS ELEVATES ELK4 BINDING SITES IN THE LIVER, AND HEPATIC ELK4 MIGHT BE CRITICAL IN GLUCOSE METABOLISM. 86

4.4 DISCUSSION 89

CONCLUSIONS AND OUTLOOK 91

LIMITATION OF THE STUDY 98

METHODS 99

SUPPLEMENT FIGURES.....105

List of Figures

Figure 1-1. Abstract of human white adipose tissue.

Figure 1-2. Adipose tissue lipolysis activation and molecular mechanism abstract.

Figure 1-3. Abstract of hepatic transcription regulation responding to non-esterified fatty acids (or NEFAs) sensing.

Figure 2-1-1. Quantitative lipidomic analysis of serum with acute activation of adipose tissue lipolysis.

Figure 2-1-2. Quantitative analysis of fatty acid composition from WAT after acute activation of adipose tissue lipolysis. Non-esterified fatty acids (NEFA) and triacylglycerol were measured in inguinal white adipose tissue (WAT) 30 minutes after saline or 1 mg/kg CL-316,243 administration (n=4, *: $p<0.05$, **: $p<0.01$, ***: $p<0.005$).

Figure 2-2-1. Time-dependent changes in serum and liver lipids after CL-316,243 administration.

Figure 2-2-2. Fatty acid composition of serum and liver triglycerides after CL administration.

Figure 2-2-3. Dietary palmitate and linoleate utilization in response to activation of lipolysis.

Figure 2-3-1. Targeted Lipidomic analysis of serum and liver from mice with selective deletion of ATGL in adipocytes.

Figure 2-3-2. Inhibition of adipose tissue lipolysis prevents lipid remodeling in the liver.

Figure 2-3-3. Quantitative changes in lipids from serum and liver in $Pnpla2^{F/F}$ and $Pnpla2^{F/F}$::$Adipoq^{CRE}$mice.

Distribution of significant serum lipids (A) and liver lipids (B) by lipid classes. The Y-axis represents the lipid concentration after CL treatment, and X-axis represents the lipid concentration with vehicle treatment. Dot diameter represents –log10(p-value). (n=5-7).

Figure 2-4-1. Quantitative lipidomic analysis of conditioned media from differentiated white adipocytes.

Figure 2-4-2. Lipidomic analysis of hepatocytes treated with adipocyte conditioned media.

Supplement Figure 2-1-1. The concentration of specific lipid species in serum after 30 minutes of vehicle or CL-316,243 administration. A-J. The concentration of targeted lipid species in serum.

Supplement Figure 2-1-2. Serum and liver metabolites after 30 minutes of (CL) CL-316,243 administration.

Supplement Figure 2-2-1. Time Course for serum and liver after CL Administration. Cluster analysis showing a heatmap from mouse serum lipids (A) and liver (B) after CL administration.

Supplement Figure 2-2-2. Dietary palmitate and linoleate utilization in response to activation of lipolysis.

Supplement Figure 2-3-1. Comparative analysis of serum lipids from $Pnpla2^{F/F}$ mice and $Pnpla2^{F/F}$::$Adipoq^{CRE}$ mice. A

Supplement Figure 2-3-2. Quantitative analysis of serum lipids in $Pnpla2^{F/F}$ and $Pnpla2^{F/F}$::$Adipoq^{CRE}$ mice after 5hrs CL administration. Mice were administered a single dose of Saline or 1mg/kg CL-316,243 and sacrificed after 5 hours (n=5-7).

Supplement Figure 2-3-3. Quantitative analysis of liver lipids in $Pnpla2^{F/F}$ and $Pnpla2^{F/F}$::$Adipoq^{CRE}$ mice after 5hrs CL administration. Mice were administered a single dose of Saline or 1mg/kg CL-316,243 and sacrificed after 5 hours (n=5-7).

Supplement Figure 2-4-1. Metabolite analysis of condition media from differentiated adipocytes.

Supplement Figure 2-4-2. Quantitative lipid analysis of condition medium of differentiated adipocytes after vehicle or CL-316,243 administration. (n=6, *: $p<0.05$, **: $p<0.01$, ***: $p<0.005$)

Supplement Figure 2-4-3. Quantitative lipid analysis of hepatocytes treated with adipocyte conditioned media. Adipocytes were treated with saline or CL-316,243 in. (n=6, *: $p<0.05$, **: $p<0.01$, ***: $p<0.005$)

Figure 3-1-1. An analysis of liver transcriptions in mice with targeted removal of ATGL in adipocytes revealed that GR, or Glucocorticoid Receptor, shows promise as a potential regulator in the liver's response to the breakdown of fats in adipose tissue.

Figure 3-1-2. In vitro model for identifying GR function responding to adipose tissue secretum.

Figure 3-2. GR was activated after CL administration.

Figure 3-3-1. Hepatic GR deficiency mice in response to adipose tissue lipolysis.

Figure 3-3-2. Time course for gene expression and ketogenesis from hepatic GR deficiency liver in response to adipose tissue lipolysis.

Figure 3-3-3. Hepatic GR deficiency in response to Dexamethasone treatment.

Figure 3-4. Hepatic Plin5 deficiency mice in response to adipose tissue lipolysis.

Figure S3-1-1. Transcription analysis from mice liver with selective deletion of ATGL in adipocytes.

Figure S3-1-2. Imaging to assess the accumulation of lipids in different mutated hepatocyte cell lines after treating them with conditioned medium for 6 hours (Green: BPDIPY, Blue: DAPI, n=3). (*Ppara, myc*, and *Rorc*)

Figure S3-2. Time course for additional GR targeted genes (n=4).

Figure S3-3-1. Hepatic GR deficiency mice has no significant body and organs weight change.

Figure S3-3-2. Time course for gene expression from hepatic GR deficiency liver in response to adipose tissue lipolysis.

Figure 4-1-1 ATAC-Seq reveals that adipose tissue lipolysis promotes hepatic chromatin accessibility.

Figure 4-1-2 Downstream analysis of ATAC-seq, Peaks Distribution and Homer Motif Enrichment.

Figure 4-2 Conduct a brief assessment of the metabolic function of hepatic Elk4.

Acknowledgments

I would like to express my gratitude to several individuals and groups who have played a significant role in my academic journey and personal life during my thesis and Ph.D. studies.

First and foremost, I extend my heartfelt thanks to Dr. Claudio Villanueva and his research team at UCLA. Their invaluable advice, insightful discussions, and generous sharing of reagents and resources have been instrumental in my academic growth. Dr. Villanueva's professional guidance and unwavering support have been pivotal in shaping me into the researcher I am today.

I am also deeply grateful to my lab colleague, Mirian Krystel, for her extensive assistance with my experiments. Her collaboration and expertise have been indispensable to the success of my research.

I extend my appreciation to my committee members and all the faculty members who have offered their assistance and guidance. Your support has been crucial in overcoming the obstacles I encountered during my experiments and moving my project forward. Special thanks go to K. Williams, G. Su, and the UCLA Lipidomics core for their contributions to the lipidomics analysis.

In addition to my academic mentors and colleagues, I would like to acknowledge my parents. Although we have not been in contact since I underwent gender transition, I understand the conservative culture in my hometown and the discrimination faced by transgender individuals in China. Despite this, I hold onto the hope that my mom and dad may someday accept me, and we can reunite in the future.

I owe a debt of gratitude to my best friend, Weiye Iris Dai, who has been my guardian angel during these past few years. Her unwavering support has helped me rise above the challenges of depression, and I look forward to a bright future for both of us.

I also want to extend my thanks to all my dear friends who have stood by my side and offered their support. To Qinxin Sherry Li ,Shiyin Mia Li, Bichen Kou, Chi Pham, Canbin Tam, Gloria Bian, Tianlu Cui, Lawren GLNS Zhang, Perry Zhang, Ran Deng, Xiaoyuan Li, Amy Orwall, Tacoma Ruolan Feng, Carol Hu, Lu Chen, JY Huang, Goldenfish Liao, Yi Liu, Sherry Yang, Jimmy Chiu, Amber Capybara, Taotao Lin, Suzie Chen, Huasheng Sookie, Jin Xu, Aijia Zhang, Uzi Yan, Weiwei Xu, Wenjuan Liao, Yiwei Zhang, Jiawei Catone Wang, Wenjia Gu, and Xuanming Zhang—your friendship and encouragement have meant the world to me.

Thank you all for being a part of my journey and contributing to my personal and academic growth.

VITA

EDUCATION

Years	Degree	Institution (Area of Study)
2016	B.S.	Shandong Agricultural University (Biological Science) Tai'an, China (GPA 3.42)
2018	M.S.	School of Medicine, Tulane University (Biochemistry and Molecular Biology) (GPA 3.89) New Orleans, LA
2018 - present	Ph.D.	IBP& metabolism theme, UCLA, Los Angeles, CA (GPA 3.8)

TEACHING EXPERIENCE

09.2020-12.2020

03.2021-06.2021 Teaching Assistant, Dr.Huang Pham. GENETICS LS107. UCLA. Taught

09.2022-12.2022 weekly discussion sections and assisted students in understanding fundamental concepts of molecular cloning and genetic engineering.

JOURNAL ARTICLES

1. Hou, Xiaoyang, Xiaoning Yu, Binghai Du, Kai Liu, Liangtong Yao, **Sicheng Zhang**, C. Selin, W. G. D. Fernando, Chengqiang Wang, and Yanqin Ding. "A single amino acid mutation in Spo0A results in sporulation deficiency of Paenibacillus polymyxa SC2." Research in microbiology 167, no. 6 (2016): 472-479.

2. Xiao, Xu, John Paul Kennelly, Alessandra Ferrari, Bethan L. Clifford, Emily Whang, Yajing Gao, Kevin Qian, **Sicheng Zhang**, Claudio J Villanueva, Peter Tontonoz et al. "Hepatic nonvesicular cholesterol transport is critical for systemic lipid homeostasis." Nature Metabolism 5, no. 1 (2023): 165-181.

3. **Zhang, Sicheng**, Kevin J. Williams, Amandine Verlande-Ferrero, Alvin P. Chan, Gino B. Su, Erin E. Kershaw, James E. Cox et al. "Acute activation of adipocyte lipolysis reveals dynamic lipid remodeling of the hepatic lipidome." Journal of Lipid Research (2023): 100434.

4. Zhang, Z., Cui, Y., Su, V., Wang, D., Tol, M.J., Cheng, L., Wu, X., Kim, J., Rajbhandari, P., **Zhang, Sicheng**. and Li, W., 2023. A PPAR γ/long noncoding RNA axis regulates adipose thermoneutral remodeling in mice. *Journal of Clinical Investigation*, *133*(21), p.e170072.

5. **Sicheng Zhang**, Mirian Krystel De, Yutian Zhao, Gino B. Su, Kevin J. Williams, Judith Simcox, Erin E. Kershaw, Thomas Q. Vallim, Xia Yang, Claudio J. Villanueva. "Adipose-Liver Crosstalk Signaling Promotes GR-Plin5 Axis to Regulate Ketogenesis." In progress.

ORAL PRESENTATIONS

2018,2 "Antibody-based Assays to Monitor Polycyclic Aromatic Hydrocarbon Degradation by Marine Bacteria" Gulf of Mexico Oil Spill and Ecosystem Science Conference, New Orleans, LA

2018.3 "Polycyclic aromatic hydrocarbon degradation by Cycloclasticus, as measured by a novel immunoassay, correlates with increased cell proliferation" ACS National Meeting, New Orleans, LA

2020.3 "Adipose tissue lipolysis provides signals that modulate hepatic gene expression program" (poster presentation) ASBMB Deuel Conference, San Diego, CA

2023.3 "Adipose-Liver Crosstalk Signaling Promotes GR-Plin5 Axis to Regulate Ketogenesis" ASBMB Deuel Conference, Huntington Beach, CA

Chapter One

Adipose Tissue lipolysis regulates Hepatic Lipid remodeling.

In the last decade, there has been significant attention on the interaction between the adipose tissue and liver. Specifically, the process of adipose tissue lipolysis controlling the remodeling of hepatic lipids has emerged as a focal point. This relationship is closely tied to the regulation of energy balance, the development of metabolic diseases, and the body's response to physical challenges. Additionally, hepatic lipid remodeling plays a role in regulating cellular processes and involves both transcription and post-transcriptional regulation. This chapter provides a comprehensive overview of the secretions released during adipose tissue lipolysis and the mechanisms by which the liver responds to adipose tissue lipolysis.

1.1 Introduction

The regulation of energy balance and metabolism relies heavily on the coordinated actions of multiple vital organs (Sakers, De Siqueira et al. 2022). Here, we mainly discuss two organs: adipose tissue and the liver. Adipose tissue serves as the primary organ for storing fat, while the liver assumes the critical roles of detoxifying harmful substances, facilitating digestion, and storing energy substrates (like glucose, lipids, and amino acids). To make sure their respective roles function effectively, these organs engage in constant communication through signaling pathways and substrate exchange. This intricate interplay can significantly influence the remodeling of lipids within the liver, both in the short and long term. In the short term, physical challenges can trigger transcription and post-transcription regulation and rapid lipid accumulation, while in the long term, this communication may have implications for various common chronic diseases (Azzu, Vacca et al. 2020) (Petrescu, Vlaicu et al. 2022). Comprehending the mechanisms behind the crosstalk between the liver and adipose tissue is of importance in gaining insights into the intricate regulation of energy metabolism. Such knowledge holds the key to understanding and addressing energy-related disorders and maintaining overall metabolic health.

1.1.1 Nonalcoholic fatty liver disease and Obesity

Nonalcoholic fatty liver disease (NAFLD) is one of the most common chronic liver diseases, which has become high prevalence in the world, giving new challenges in modern medicine (Brunt, Kleiner et al. 2011). More than 34.0% of people in the United States of America have NAFLD, and global prevalence in adults is estimated at 25.2% (Azzu, Vacca et al. 2020, Noureddin, Ntanios et al. 2022, Teng, Ng et al. 2022, NIDDK.NIH 2023). Unfortunately, the rate of NAFLD in the State or worldwide has increased during the past couple of decades

(Noureddin, Ntanios et al. 2022, Teng, Ng et al. 2022). In addition, NAFLD may progress to its more severe liver diseases, like nonalcoholic steatohepatitis (NASH), steatofibrosis, and ultimate cirrhosis (Younossi, Tacke et al. 2019). NAFL and NASH are both FAFLD condition, however, NASH patients could already have liver damage and inflammation. With more serious development, the patients would even have a high risk of liver cancer, like hepatocellular carcinoma (Marengo, Rosso and Bugianesi 2016). Obesity or overweight, are chronic metabolic disorders that have been defined as abnormal or excessive fat accumulation. A body mass index (BMI) over 25 is considered overweight, and over 30 is obese. 41.9 percent of adults have obesity in the United States of America (NIDDK.NIH 2023). And around 1 billion people worldwide are obese (Mohajan and Mohajan 2023). Obese conditions would significantly increase the possibility of developing metabolic disorders, such as liver disease, cardiovascular disease, inflammatory disease, and type 2 diabetes or insulin resistance (Brunt, Kleiner et al. 2011, Younossi, Tacke et al. 2019). Currently, over 90% of NAFLD associates with obesity, and over one-quarter of NASH is related to obesity conditions (Barr, Caballería et al. 2012). Obesity might upregulate the rate of fatty acid oxidation, lipid uptake, and lipid export. Therefore, at the cellular level, the risk of DNA damage, lipid droplet hypertrophy, and insulin resistance would significantly increase in hepatocytes. Moreover, obesity-related inflammation, called meta inflammation, is another factor contributing to NAFLD development, but not only due to the fatty acids over flux from adipose tissue or the circulation system. Adipose tissue contains fat cells and several other cell types, including macrophages and monocytes (Nguyen, Qiu et al. 2011). Adipokines and cytokines from adipose tissue, such as TNF-a, IL-6, and IL-8, are positively correlated to NAFLD development (Pirzgalska, Seixas et al. 2017, Azzu, Vacca et al. 2020). In the context of obesity development, adipose tissue plays a pivotal role as a major organ

responsible for fat accumulation. The physiological changes that occur within adipose tissue can significantly impact the overall metabolic homeostasis of the entire body. Acting as a crucial energy and signaling hub, adipose tissue plays a key role in regulating hepatic metabolism. The communication and interaction between adipose tissue and the liver are critical in determining whether obesity and non-alcoholic fatty liver disease (NAFLD) will be promoted or prevented. Understanding this intricate interplay is crucial in devising strategies to manage and address obesity-related health challenges and NAFLD effectively.

1.1.2 Adipose Tissue Lipolysis

Throughout mammalian evolution, three distinct types of adipose tissue have emerged as a means of safeguarding tissues against the stress in ambient temperature. These types include white adipose tissue (WAT), brown adipose tissue (BAT), and beige adipose tissue(Hilton, Karpe and Pinnick 2015, Sakers, De Siqueira et al. 2022). When subjected to cold exposure, a unique phenomenon occurs in brown and beige adipose tissue: there is a simultaneous uptake of fatty acids, glucose, and other substrates from the bloodstream. This process aids in generating heat and helps in maintaining the body's temperature during cold exposure. Conversely, white adipose tissue primarily serves as an energy reservoir, storing excess energy for future use. (Heine, Fischer et al. 2018, Panic, Pearson et al. 2020, Carpentier, Blondin et al. 2023) Interestingly, cold exposure not only affects brown and beige adipose tissues but also seems to promote the "beiging" process in white adipose tissue, which is WAT depots was induced by stimulation (like cold exposure) appear brown-like adipocytes (Harms and Seale 2013). However, the precise mechanisms governing this beiging process still require further investigation.

In the face of external stimuli challenges, such as exercise, cold exposure, fasting, and burn injury, adipose tissue lipolysis is necessary for signaling and providing substrate (Kaur, Auger and Jeschke 2020) (Migliorini, Garofalo and Kettelhut 1997, Enevoldsen, Polak et al. 2007). Adipose tissue lipolysis is essential in regulating hepatic metabolism, including triglyceride (TG) accumulation, glucose metabolism, ketogenesis, and so on. As the major site of lipid storage, adipose tissue stores TG in cytosolic lipid droplets (LD). During fasting or caloric restriction adipose tissue lipolysis is stimulated. The catecholamines, hormones adrenaline, and noradrenaline are the most common signals that stimulate adrenergic receptors (ARs). (Collins and Surwit 2001) The adrenergic receptors are expressed on the adipocyte surface as a G-protein-coupled receptor. Alpha-adrenergic receptors (a2-AR) contain inhibitory Gi subunit and beta- adrenergic receptors (b1,b2,b3-ARs) (Leach and Suzuki 2020, Collins 2022). During the activation, the Gs from G-protein interacts with adenylyl cyclase (AC). AC converts the ATP to cAMP (cyclic AMP). With the inducing intracellular cAMP levels, cAMP-dependent protein kinase, protein kinase A (PKA), is activated to phosphorylate the perilipins and cytoplasmic Hormone-sensitive lipase (HSL). In addition, the PKA pathway releases the Adipose triglyceride lipase (ATGL) co-activator, comparative gene identification-58 (CGI-58) (Kim, Tang et al. 2016). This stimulates the lipolytic cascade. Lipolysis is defined as the sequential hydrolysis of TG to free fatty acid (FFAs) and glycerol. To fully hydrolyze TGs, ATGL converts TG to diglycerides (DG), HSL converts DG to MG, and monoglyceride lipase (MGL) cleaves monoglyceride (MG) into glycerol and FFA. Typically, the first cleavage (TG to DG is completed by ATGL) is considered the rate-limiting step. Therefore, on the mechanism of molecular level study, ATGL gene-related modifications are the primary strategy to study adipose tissue lipolysis(Møller, Pedersen et al. 2015).

There have been therapeutics developed for selective and non-selective agonists to activate or inactivate adipose tissue lipolysis. For example, Dobutamine, inotropes, norepinephrine (b1-AR) (den Uil, Lagrand et al. 2014), and Dopamine, Epinephrine (Adrenaline, non-selective) are used to treat cardiogenic shock and heart failure(Capellino, Claus and Watzl 2020). Oxymetazoline (a1-AR, FDA-approved) is used to treat rosacea(Washrawirul, Puaratana-arunkon et al. 2023). CL-316,243 (b3-AR) is suggested as a potential agonist drug for the treatment of type 2 diabetes and obesity in humans(Zhu, Li et al. 2021). Unfortunately, the consequence of CL-316,243 treatment still needs more study. CL-316,243 is also an appropriate strategy to mimic adipose tissue lipolysis stimulation(Simcox, Geoghegan et al. 2017, Heine, Fischer et al. 2018).

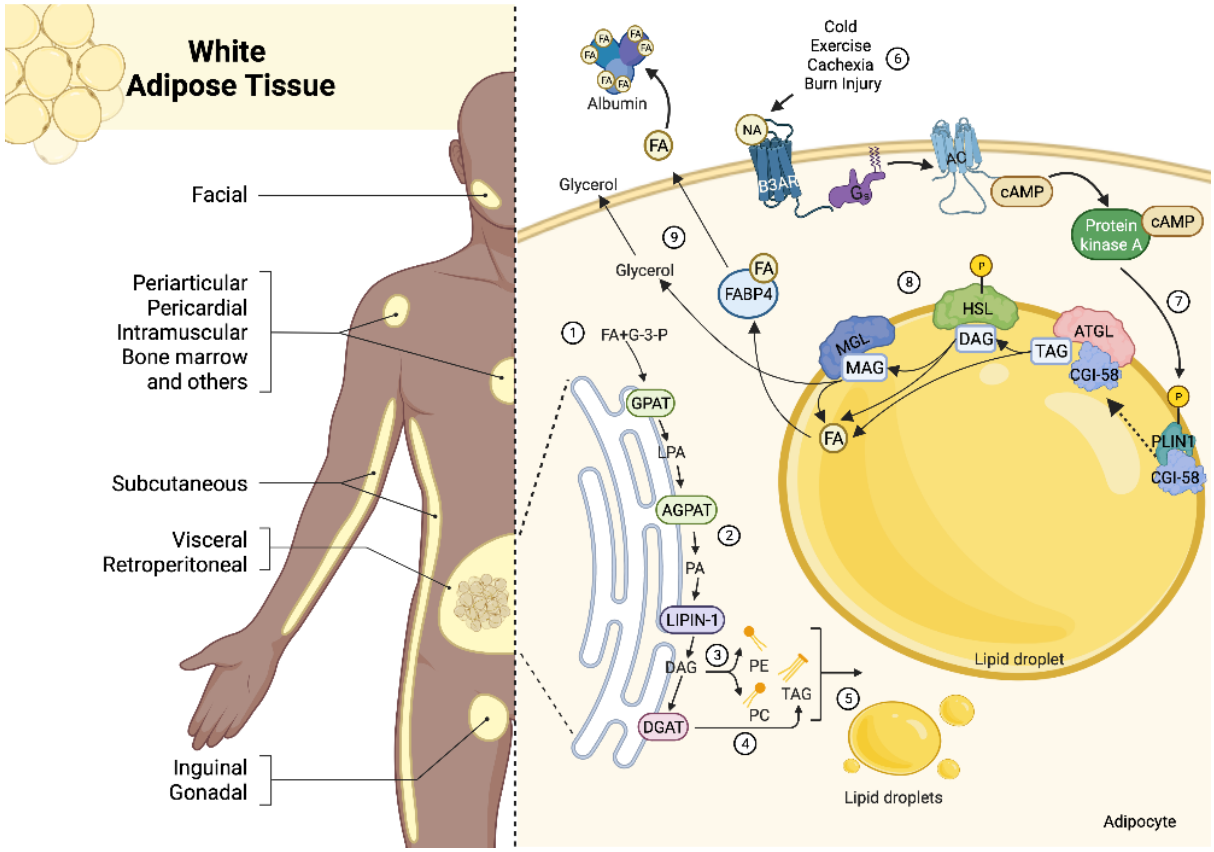

Figure 1-1 White adipose tissue distribution, and white adipose tissue plays a critical role in energy storage and lipid remodeling (Triglycerides synthesis and triglycerides hydrolysis).

1.2 Activation of adipocyte lipolysis during Cold, Fasting, and Exercise.

Cold exposure is an acute activator of energy expenditure, which constitutes a fundamental interaction between adipose tissues and the liver, forming a well-established model of intercommunication. The sensory response to cold through neural pathways triggers the activation of adipose triglyceride lipase (ATGL), leading to the breakdown of adipose tissue lipids into free fatty acids (FFAs) that serve as fuel for non-shivering thermogenesis (Yu, Lewin et al. 2002, Simcox, Geoghegan et al. 2017). Simultaneously, cold exposure fosters the initiation of the browning process, resulting in a significant upregulation of thermogenesis-related genes expression such as UCP1, PGC1α, and others. Findings from prior studies involving mice have demonstrated that the absence of ATGL in white adipocytes is necessary fold cold adaption in the fasting state, however, loss of ATGL in brown adipocytes does not impair cold adaptation (Schreiber, Diwoky et al. 2017, Shin, Ma et al. 2017). This study highlights that white adipose tissue is critical in providing energy for thermogenesis. Moreover, when subjected to cold conditions, the liver assumes a crucial role in generating acyl-carnitine as an additional source of fuel. Previous investigations have highlighted that the deficiency of hepatic HNF4α or PPARα in mice can lead to an increased vulnerability to cold sensitivity (Simcox, Geoghegan et al. 2017, Fougerat, Schoiswohl et al. 2022).

Exercise represents another physiological challenge of acute energy expenditure. Similar to exposure to cold temperatures, physical activity has the capacity to enhance the breakdown of fats and carbohydrates in beiging and brown adipose tissue and stimulate the expression of genes such as UCP1 and PGC1α. Concurrently, exercise promotes the browning of white and beige adipose tissue, but its impact on brown adipose tissue remains unclear (Martin, Chung and Koehler 2020). The intricate molecular mechanisms underpinning the effects of exercise training

on non-alcoholic fatty liver disease (NAFLD) treatment are not yet fully elucidated. Nonetheless, multiple investigations have indicated that exercise can diminish levels of fat accumulation and oxidative stress in the liver, while also mitigating processes of lipogenesis and inflammation (Farzanegi, Dana et al. 2019, Azzu, Vacca et al. 2020). Through the mobilization of fats in adipose tissue, exercise activates receptors such as PPAR and HNF, thereby augmenting lipid metabolism. Moreover, there is a substantial elevation in the processes of β-oxidation and the tricarboxylic acid (TCA) cycle within skeletal muscle. As a collective consequence, energy expenditure by the muscle and liver can effectively counteract lipid buildup within these organs (Keating, Hackett et al. 2015, Martin, Chung and Koehler 2020).

Fasting has emerged as a novel lifestyle approach aimed at extending both lifespan and overall health by mitigating oxidative and metabolic stresses, cardiovascular risks, obesity, and NAFLD. Fundamentally, fasting causes a shift from glucose metabolism to the utilization of fats and ketones, concurrently dampening the activation of mTOR-mediated nutrient signaling pathways (Wilhelmi de Toledo, Grundler et al. 2020). Even brief periods of fasting can induce the liberation of fats from adipose tissue, allowing these lipids to flux into various organs, including the liver and muscles. This influx can sometimes lead to lipid accumulation in the liver. Nevertheless, with glucose fasting, the predominant energy source transitions to fats and ketones (Watanabe, Tozzi et al. 2020). Furthermore, fasting escalates the process of autophagy within the liver, facilitating the breakdown of proteins, glycogen, lipids, as well as damaged organelles like mitochondria and excess endoplasmic reticulum (ER) (Qian, Chao et al. 2021). However, recent research also proposes that both fasting and subsequent refeeding disproportionately amplify the expression of genes linked to lipogenesis in adipose tissue and the liver (Tang, Tang et al. 2017).

1.3 Adipose tissue lipolysis releases the signals and source of lipids for hepatic lipid remodeling.

Adipose tissue lipolysis mainly releases FFAs and glycerol to the circulation system. The intracellular FFA and glycerol levels increase with stimulation to the AR-PKA-lipase axis in adipocytes. Also, the different FFAs, glycerol, and FA derivatives (branch chain FAs, phospholipids, and acyl-carnitine) are released to the circulation system(Hilton, Karpe and Pinnick 2015, Simcox, Geoghegan et al. 2017). The composition of the secretome are still unclear; the releasing could be the FFAs gradian concentration, and it also might be transported by specific channels or associate carriers (like FABPs) (Kuryszko, Slawuta and Sapikowski 2016, Villeneuve, Bassaganyas et al. 2018). In the meantime, with meta inflammation, it is not well known whether adipokines and cytokines from adipose tissue, such as TNF-a, IL-6, and IL-8, might be released to contribute to NAFLD development(Pirzgalska, Seixas et al. 2017, Azzu, Vacca et al. 2020). For the released FFAs, palmitic acid (C16:0), oleic acid (C18:1), and linoleic acid (C18:2) are the most abundant fatty acids (REF). Normally, the long-chain fatty acids (LCFAs, 12-20 carbons) would have a relatively higher concentration (10 to 1000 uM). And the very long chain fatty acids (VLCFAs, over 20 carbons) would be less. Under normal conditions, FFAs from adipose tissue lipolysis are critical energy substrates for the liver. Responding to acute stimulation, such as, cold exposure, fasting, and drug treatment, the lipids would overload the liver (REF). During the lipolysis, Free fatty acids in-taken by the liver would be used for different purposes, such as being catabolized by carnitine palmitoyltransferase1 a/b (CPT1a/b) to acyl-carnitine, TG synthesis, and lipid droplets biosynthesis, and going into the nucleas to activate transcription factors (TFs, like PPARs, HNF4a)(Simcox, Geoghegan et al. 2017, Fougerat, Schoiswohl et al. 2022). After the stimulation, to clear the over-accumulated hepatic

lipids, the de novo synthesis of hepatic TG can be exported out of cells by the VLDL pathway. Also, other organs play essential roles in lipid consumption or temporary accumulation, like adipose tissue, muscle, heart, bones, and so on (Arner and Rydén 2022).

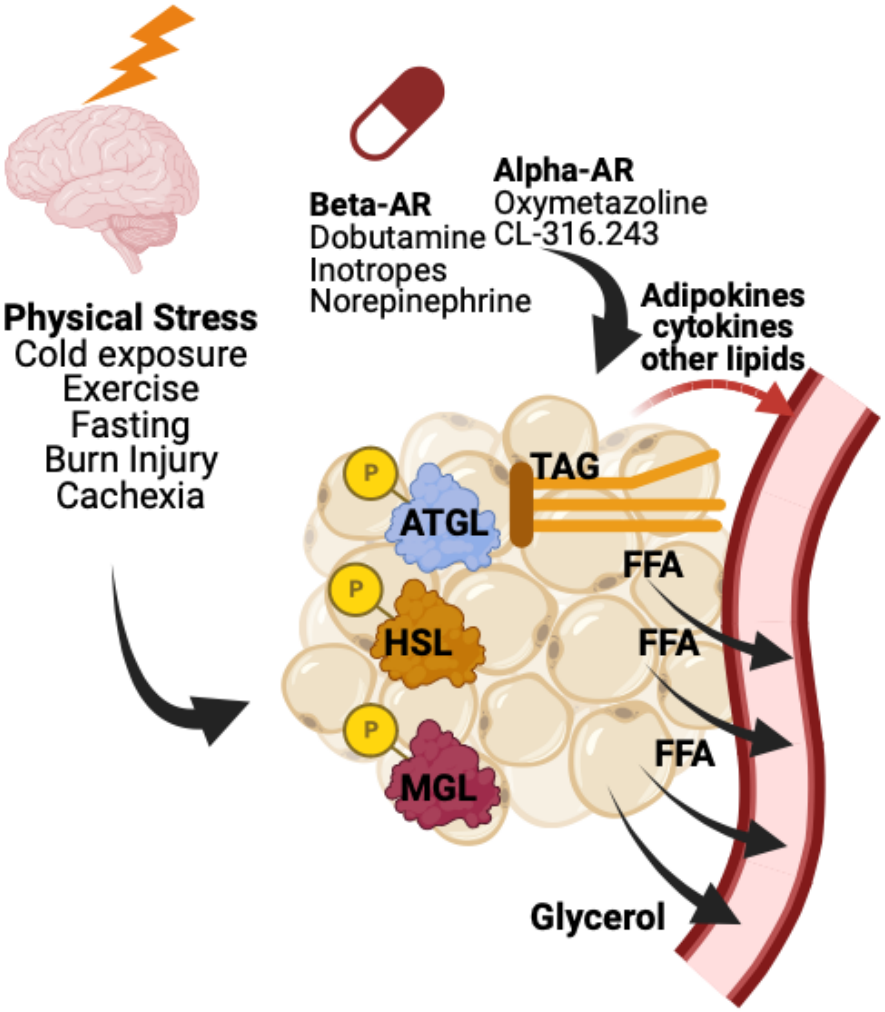

Figure 1-2 Adipose tissue lipolysis activation and molecular mechanism abstract.

1.4 Cellular organelles in hepatocytes and response to adipocyte lipolysis.

Adipocyte lipolysis increases free fatty acids (FFAs) and glycerol in the blood, providing signals to the liver to adjust its metabolism (Heine, Fischer et al. 2018, Zhang, Williams et al. 2023). In hepatocytes, FFAs can cross the plasma member by FFAs channel, then enter the mitochondria and be used for energy production through beta-oxidation. In the mitochondria of

hepatocytes, FFAs can be oxidized through the process of beta-oxidation to generate energy in the form of ATP. However, when free fatty acids (FFAs) rise in the liver rise (Overload), they can accumulate in the mitochondria and overwhelm the capacity for beta-oxidation (Caturano, Acierno et al. 2021, Petrescu, Vlaicu et al. 2022). This can lead to impaired oxidative metabolism and decreased energy production, which can ultimately result in liver dysfunction and other related health problems. Additionally, FFAs can also stimulate the production of glucose through gluconeogenesis and increase ketone body production. The glycerol produced from adipose tissue lipolysis can also contribute to glucose production.

The endoplasmic reticulum (ER) and Golgi apparatus, as well as mitochondria, are involved in these metabolic adjustments in hepatocytes. The ER and Golgi are involved in the production and modification of metabolic enzymes, while the mitochondria are the site of beta-oxidation and energy production. Also, the endoplasmic reticulum (ER) lumen is the starting point for lipid droplet synthesis. The ER membrane-bound enzymes, such as diacylglycerol acyltransferase (DGAT) and acyl-CoA cholesterol acyltransferase (ACAT), are responsible for synthesizing triacylglycerols (TGs) from fatty acids and glycerol-3-phosphate (Monetti, Levin et al. 2007). Some of these FFAs that are not immediately used for energy production can be stored in the liver in the form of triglycerides (TG) within cytosolic lipid droplets (LD) (Wang, Liu et al. 2021). The newly de novo synthesized TGs are then incorporated into the growing lipid droplet, leading to lipid droplet formation and expansion. The lipid droplets are composed of a hydrophobic core of TGs surrounded by a monolayer of phospholipids, cholesterol, and peripheral proteins, called lipid droplet-associated proteins (LDAPs).

Lipid overloading would cause lipid droplet hypertrophy. LD hypertrophy refers to an increase in the size of lipid droplets within cells, often because of excess accumulation of lipids

such as triglycerides. Lipid droplet hypertrophy can increase the risk of oxidative stress due to the accumulation of lipids within cells. The lipids can become oxidized, generating reactive oxygen species (ROS), which can cause DNA damage. Additionally, the increase in lipid droplets can cause a decrease in the size and function of mitochondria, which are important for cellular energy production. This can lead to a state of mitochondria disorder and decreased energy production, further exacerbating the oxidative stress in the cells (Gluchowski, Becuwe et al. 2017, Schulze, Drižytė et al. 2017, Seebacher, Zeigerer et al. 2020).

Lysosomes are cellular organelles in hepatocytes that are involved in the degradation and recycling of cellular waste and foreign substances. They contain a variety of hydrolases and enzymes that break down different types of molecules, including lipids and amino acids. Lysosomes can also play a role in lipid metabolism by acting as a site for lipid degradation and removal of excess lipids from the cell. In hepatocytes, lysosomes can take up FFAs released from adipose tissue lipolysis and degrade them for energy production or further storage (Martinez-Lopez and Singh 2015, Carotti, Aquilano et al. 2020). The lysosomes action in the hepatocytes helps to regulate the level of FFAs in the liver and maintain energy balance.

The peroxisome serves as one of the key cellular components involved in processes such as cholesterol metabolism, synthesis of bile acids, and the breakdown of fatty acids. Specifically, peroxisomes play a crucial role in the metabolism of long chain and very long chain fatty acids (LCFA and VLCFA) through α- and β-oxidation pathways (Stradomska, Syczewska et al. 2020). Within this context, peroxisomal β-oxidation relies on the enzyme acyl-CoA oxidase 1 (ACOX1), which acts as a limited step in the generation of acyl-CoA molecules (Ding, Sun et al. 2021). Notably, in the liver, the peroxisomal enzyme EHHADH assumes a critical role in the tricarboxylic acid (TCA) cycle, functioning as both an Enoyl-CoA Hydratase and a 3-

Hydroxyacyl CoA Dehydrogenase (Zhao, Xu et al. 2010). In the process of lipolysis within adipose tissue, the activation of Pparα stimulates the transcription of key peroxisomal oxidation genes such as ACOX1 and EHHADH, among others (Huang, Yang et al. 2022). This orchestrated activation enhances the breakdown of fatty acids within peroxisomes, contributing to the overall metabolic processes associated with lipid metabolism.

1.5 Transcription regulation and transcription factors activation process

Hepatic transcription regulation is the most common regulation in responding to adipose tissue lipolysis, particularly responding to the stress of FFAs. The transcription could be regulated by transcription factors, co-transcription factors, histone modifications, and RNA polymerases.

1.5.1 Transcription factors.

For transcription factors regulation, FFA-regulated transcription factors are critical transcriptional regulation in hepatocytes, including PPAR (α, β, γ1, and γ2), HNF4 (α and γ), retinoid X-receptor (RXR) α, and liver X receptor (LXR) (α and β)(Dixon, Nardo et al. 2021, Welch, Billon et al. 2022) .

PPARα (Peroxisome Proliferator-Activated Receptor alpha) is one of the most dominant metabolic transcription factors and has been the most well-studied. PPARα contains a free fatty acid binding domain, which can be activated directly by the cellular FFA concentration, so that the FFAs from the adipose tissue lipolysis can activate PPARα directly. PPARα has been reported that it would be essential for responding to fasting and cold exposure (Fougerat, Schoiswohl et al. 2022). When PPARα is lacking in the liver, the normal regulation of fatty acid oxidation and glucose metabolism would be disrupted, leading to an impairment in energy balance. This can lead to an increase in the accumulation of lipids, decreased energy production,

and an increase in oxidative stress in liver cells. Additionally, a lack of PPARα can also lead to changes in the expression of genes involved in lipogenesis and insulin resistance, further exacerbating the metabolic problems in the liver. In the PPAR pathway, PPARα regulates a variety of genes involved in lipid metabolism, including those involved in the uptake and transport of fatty acids, fatty acid oxidation enzymes, and genes involved in lipoprotein metabolism(Fougerat, Schoiswohl et al. 2022). For example, PPARα activation increases the expression of the fatty acid translocase CD36 and the fatty acid transport protein (FATP), which increases the uptake of fatty acids into cells. It also increases the expression of acyl-CoA oxidase (ACOX), carnitine palmitoyltransferase (CPT1a/b, CPT2), and other enzymes involved in beta-oxidation. Additionally, PPARα activation decreases the expression of genes involved in lipogenesis, such as fatty acid synthase, and reduces the formation of triglycerides(Brocker, Yue et al. 2017, Li, Jin et al. 2021). Except for PPARα, the other FFA-binding nuclear receptors, like HNF4a, RXR, and LXR, also perform critical roles in responding to lipid loading stress (Zhou, Febbraio et al. 2008, Kasano-Camones, Takizawa et al. 2023). Normally, the functions of these transcription factors are complementary or associated.

HNF4 (*Hepatocyte Nuclear Factor 4*α and γ) is another classical FFAs binding transcription factor. It is involved in the regulation of many genes involved in various metabolic processes, including glucose and lipid metabolism, bile acid synthesis, thermogenesis and drug metabolism. It regulates the expression of genes involved in fatty acid and cholesterol synthesis, as well as genes involved in fatty acid oxidation and lipoprotein metabolism (Hunter, Poolman et al. 2022, Kasano-Camones, Takizawa et al. 2023, Thymiakou, Tzardi and Kardassis 2023). HNF4α activates the expression of genes involved in the fatty acid synthesis, such as acetyl-CoA carboxylase (ACC) and fatty acid synthase (FAS), which catalyze the conversion of acetyl-CoA

into fatty acids. It also activates the expression of genes involved in cholesterol synthesis, such as HMG-CoA reductase, which catalyzes the conversion of HMG-CoA to mevalonate, a precursor for cholesterol synthesis (Kasano-Camones, Takizawa et al. 2023). On the other hand, HNF4α also activates the expression of genes involved in fatty acid oxidation, such as carnitine palmitoyltransferase I (CPT-1) and acyl-CoA oxidase (ACOX1), which catalyze the transport of fatty acids into the mitochondria and their subsequent oxidation(Simcox, Geoghegan et al. 2017). HNF4α also regulates the expression of genes involved in lipoprotein metabolism, such as apolipoprotein A-IV (APOA4), which is involved in the transport of lipids in the bloodstream(Simcox, Geoghegan et al. 2017). Dysregulation of HNF4α activity can lead to various metabolic disorders, including dyslipidemia, insulin resistance, and non-alcoholic fatty liver disease (NAFLD). HNF4α is, therefore, a potential target for the treatment of metabolic disorders associated with lipid metabolism dysfunction.

LXR (Liver X receptor(α and β)) is a nuclear hormone receptor, the activation of LXR can also promote lipid metabolism, such as, lipogenesis and lipid transport. (Dixon, Nardo et al. 2021). It can induce the expression of genes involved in fatty acid uptake and storage, such as CD36 and SREBP-1c, which can increase the hepatic accumulation of triglycerides and promote the development of fatty liver disease (Zhou, Febbraio et al. 2008, Chen, Zhang et al. 2011). Here, unsaturated fatty acids from adipose tissue lipolysis would lower SREBP-1c mRNA levels in part by antagonizing the actions of LXR (Ou, Tu et al. 2001).

RXRa (Retinoid X-receptor α), is a member of the retinoid X receptor (RXR) subfamily of nuclear receptors, which plays a crucial role in regulating lipid metabolism in the liver. It forms heterodimers with several other nuclear receptors, including peroxisome proliferator-activated

receptors (PPARs) and liver X receptors (LXRs), to regulate the expression of genes involved in lipid metabolism (Zhou, Febbraio et al. 2008, Li, Jin et al. 2021).

Transcription factors also can be activated or inhibited by phosphorylation, which can change their function or localization within the cell. Phosphorylation can also regulate the interaction of transcription factors with other proteins and with the DNA itself (Schrem, Klempnauer and Borlak 2002). In this way, phosphorylation can play a critical role in modulating the activity of transcription factors and the regulation of gene expression. There are various signaling pathways that can lead to the phosphorylation of transcription factors in response to different stimulation, including hormones, growth factors, and other signaling molecules related to lipid metabolism. The kinases (for example, PKA and AMPK) responsible for phosphorylating transcription factors can be activated by these stimuli and then phosphorylate specific sites on the transcription factor, leading to its activation or inhibition (McGee and Hargreaves 2008, Hirota and Fukamizu 2010, Muise, Guan et al. 2019). In this way, the phosphorylation status of transcription factors can act as a switch to control the expression of specific genes and play a role in cellular responses to various signals. The transcription factors include Sterol regulatory element-binding proteins (SREBPs), Carbohydrate response element binding proteins (ChREBPs), FOXO (Forkhead box O) proteins, CREB (cAMP response element-binding protein), ETS complex proteins, and so on (Iizuka and Horikawa 2008, Hirota and Fukamizu 2010, Shao and Espenshade 2012, Rui 2014, Dong 2017, Pan, Zhang et al. 2017).

Transcription factors that are regulated by Kinase ERN1(also called IRE1), PERK, and ATF6 are involved in Endoplasmic reticulum (ER) stress. ER stress is triggered by the unfolded protein response (UPR) and serves as a defensive mechanism to reduce protein load while also playing a critical role in metabolic regulation (Kaneko, Imaizumi et al. 2017). Within the ER

stress process, specific actions are taken by ERN1, ATF6, and PERK. ERN1 (IRE1) controls XBP1 mRNA precursor splicing ATF6 regulates its own protein folding. PERK regulates the transcription of ATF4. These transcription factors (XBP1, ATF6, and ATF4) subsequently regulate the expression of downstream genes involved in lipid metabolism, apoptosis, and autophagy (Avril, Vauleon and Chevet 2017, Kaneko, Imaizumi et al. 2017)。

1.5.2 Transcriptional coregulators

Transcriptional coregulators can modulate the activity of transcription factors by directly binding to them (but not having to bind to DNA), altering their DNA binding affinity, or altering their activity through post-translational modifications such as phosphorylation. The co-transcription factors include PGC1a/b, SRC1, CBP, MED1, and other co-factors (Kim, Sweeney et al. 2007, Besse-Patin, Jeromson et al. 2019).

PGC1α (peroxisome proliferator-activated receptor gamma coactivator 1-alpha, coded by PPARGC1A): PGC1α is a transcriptional coactivator that interacts with a variety of transcription factors, including PPARs, HNF4a, and GR, to regulate the expression of genes involved in mitochondrial biogenesis, oxidative metabolism, and gluconeogenesis (Besse-Patin, Jeromson et al. 2019).

SRC1 (steroid receptor coactivator 1): SRC-1 is a coactivator of nuclear receptors, including estrogen receptor that regulates the expression of genes involved in lipid metabolism and glucose homeostasis (Louet, Chopra et al. 2010) (Martínez-Jiménez, Gómez-Lechón et al. 2006). CBP (CREB-binding protein) is a coactivator that interacts with a variety of transcription factors, including CREB, to regulate gene expression. CBP is involved in the regulation of glucose metabolism, and its loss in the liver can lead to insulin resistance. MED1 (Mediator complex subunit 1) is a subunit of the Mediator complex, which is a coactivator of RNA

polymerase II. MED1 interacts with a variety of transcription factors, including PPARs, to regulate the expression of genes involved in lipid metabolism and glucose homeostasis. (Bai, Jia et al. 2011)

In addition, some of the transcription factors we mentioned in the previous contents can also perform as co-transcription factors to regulate the other transcription factors, such as HNF4a and GR (Weikum, Knuesel et al. 2017).

1.5.3 Histone modifications

Histone modifiers play a crucial role in regulating liver lipid sensing and metabolism. For example, histone acetyltransferases (HATs) and histone deacetylases (HDACs) regulate gene expression by modifying the acetylation status of histones, which in turn affects chromatin structure and accessibility of transcription factors to DNA (Mandrekar 2011, Van Beneden, Mannaerts et al. 2013). Furthermore, histone methylation, catalyzed by histone methyltransferases (HMTs), is another important histone modification that regulates liver lipid metabolism. For instance, the HMTs and SUV39H1 have been implicated in regulating hepatic lipid metabolism by repressing the expression of lipogenic genes, such as FASN and ACC1 (Robin, Fritsch et al. 2007, Kondo, Shen et al. 2008).

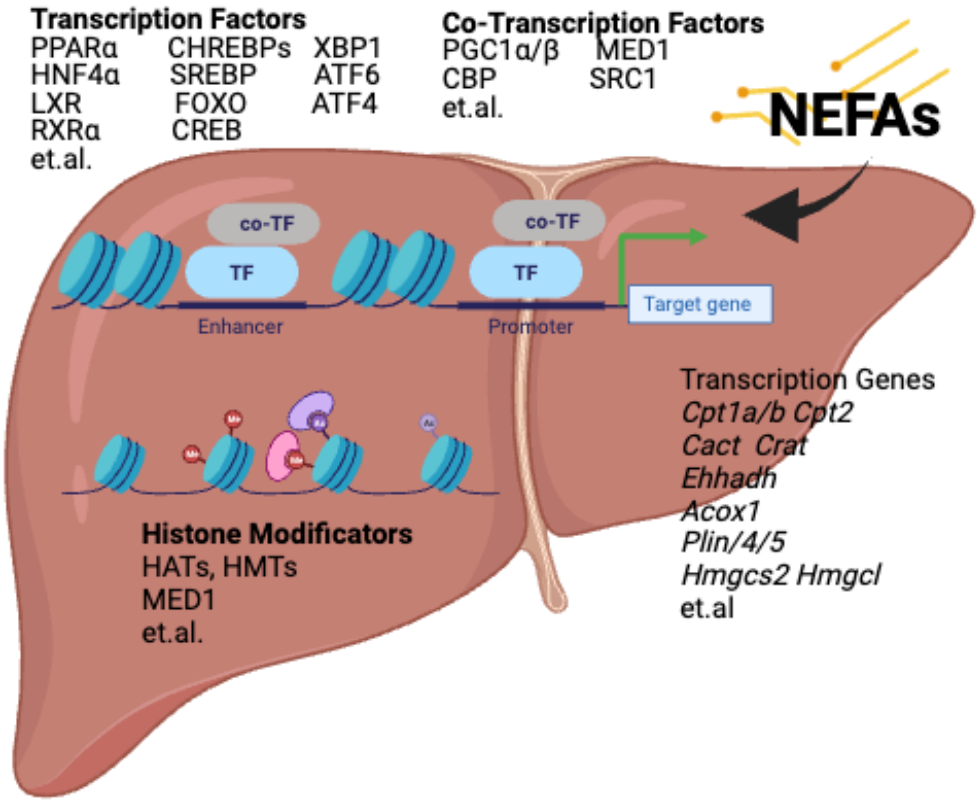

Figure 1-3 Abstract of hepatic transcription regulation responding to free fatty acids (or NEFAs) sensing. The Transcription regulation includes transcription factors activation/inactivation, Co-transcription factors activation/inactivation, and histone modifications.

1.6 Summary

Non-alcoholic fatty liver disease (NAFLD) is a condition where excess fat accumulates in the liver, not caused by excessive alcohol consumption. Obesity is a significant risk factor for NAFLD, as it can lead to insulin resistance and increased inflammation in the liver. Hence, adipose tissue lipolysis, the breakdown of fat stored in adipose tissue, releases fatty acids and signaling molecules that can contribute to hepatic lipid remodeling, a process where the liver remodels its lipid composition to adapt to changing metabolic demands. Excessive adipose tissue lipolysis can contribute to the development of NAFLD and other metabolic disorders.

Understanding the regulation of adipose tissue lipolysis and hepatic liver remodeling would benefit the therapy for NAFLD and other metabolic diseases.

Chapter Two

Acute adipocyte lipolysis and dynamic lipid remodeling of the liver lipidome

Adipose tissue is the site of long-term energy storage. During the fasting state, exercise, and cold exposure, the white adipose tissue mobilizes energy for peripheral tissues through lipolysis. The mobilization of lipids from white adipose tissue to the liver can lead to excess triglyceride accumulation and fatty liver disease. Although the white adipose tissue is known to release free fatty acids, a comprehensive analysis of lipids mobilized from white adipocytes *in vivo* has not been completed. In these studies, we provide a comprehensive quantitative analysis of the adipocyte secreted lipidome and show that there is inter-organ crosstalk with liver. Our analysis identifies multiple lipid classes released by adipocytes in response to activation of lipolysis. Time-dependent analysis of the serum lipidome, showed that free fatty acids increase within 30 minutes of beta-3-adrenergic receptor activation, and subsequently decrease, followed by a rise in serum triglycerides, liver triglycerides, and several ceramide species. The triglyceride composition of liver is enriched for linoleic acid despite higher concentrations of palmitate in the blood. To further validate that these findings were a specific consequence of lipolysis, we generated mice with conditional deletion of ATGL exclusively in adipocytes. This loss of *in vivo* adipocyte lipolysis prevented the rise in serum free fatty acids and hepatic triglycerides. Furthermore, conditioned media from adipocytes promotes lipid remodeling in hepatocytes with concomitant changes in genes/pathways mediating lipid utilization. Together these data highlight critical role of adipocyte lipolysis in inter-organ crosstalk between adipocytes and liver.

2.1 Introduction

Adipocyte lipolysis plays a critical role in the metabolic transition between the fed and fasted state, exercise, thermogenesis, and cancer cachexia (Daas, Rizeq and Nasrallah 2019, De Carvalho, Justice et al. 2019) (Han, Jiao et al. 2017, Schreiber, Diwoky et al. 2017, Shin, Ma et al. 2017, Simcox, Geoghegan et al. 2017, Lynes, Shamsi et al. 2018, Goncalves, Lu et al. 2019). Furthermore, adipocyte lipolysis is regulated by numerous pharmacological agents including anti-inflammatories, psychiatric medications, insulin, rosiglitazone, and glucocorticoids(Zhao, Wu et al. 2020). Several studies have examined the composition of adipose tissue or the adipocyte secretome(McTernan, Harte et al. 2002, Fain, Cheema et al. 2008, Albaugh, Judson et al. 2011). The adipocyte secretome includes lipids, proteins, hormones, RNAs and other bioactive factors (Lynes, Shamsi et al. 2018) (Schreiber, Diwoky et al. 2017, Simcox, Geoghegan et al. 2017, Villeneuve, Bassaganyas et al. 2018, Tran, Brown et al. 2020). Metabolites can act as metabolic precursors or as signaling molecules that provide important paracrine and endocrine communication during metabolic transitions. FFAs can provide substrate or act as signals to regulate lipid remodeling in multiple organs (Schreiber, Diwoky et al. 2017, Lynes, Shamsi et al. 2018, Jain, Özgümüş et al. 2020, Sakers, De Siqueira et al. 2022). Although fatty acids have been implicated as signaling molecules, a comprehensive quantitative assessment and compositional analysis of products of lipolysis has not been determined. Furthermore, both the time dependent changes in plasma lipids and lipid remodeling of the liver have not been assessed. During adipocyte lipolysis, a lipidome from a short time or single stimulation to adipocyte lipolysis might differ from other long-term physiological treatments or long-term adipocyte lipolysis stimulation (Schreiber, Diwoky et al. 2017). Therefore, revealing

the signals or substrate from lipolysis would contribute to defining how WAT-derived lipids change over time and the impact on hepatic lipids.

Physiological adaptations to conditions such as cold exposure or exercise, stimulate adipocyte lipolysis through release of norepinephrine (NE) by the sympathetic nervous system (Blondin and Haman, 2018; Lange et al., 2021). NE promotes the activation of b1, b2 and b3 adrenergic receptors (ARs) that are found on the plasma membrane of adipocytes. While the b1AR and b2AR are expressed in multiple tissues, the b3-AR have limited expression, which is confined to white and brown adipocytes. Small molecules such as CL-316,243 (CL) can be used to mimic lipolysis by activating b3ARs. Long-term treatment with CL promotes remodeling of both brown adipose tissue and white adipose tissue browning (Danysz, Han et al. 2018, Medak, McKie et al. 2022). There are several enzymes involved in the complete hydrolysis of triglycerides (Morak, Schmidinger et al. 2012, Møller, Pedersen et al. 2015, Marzolla, Feraco et al. 2020). The first step is completed by Adipose tissue Triglyceride Lipase (ATGL), which hydrolyzes triglycerides on the lipid droplet surface to generate an acyl chain and diacylglycerol (Lass, Zimmermann et al. 2011). Conditional deletion of ATGL in adipocytes prevents a rise in blood FFAs in response to CL-316,243 (Schoiswohl, Stefanovic-Racic et al. 2015, Shin, Ma et al. 2017).

There is evidence to suggest that lipid mediators promote chronic liver disease, such as Nonalcoholic fatty liver disease (NAFLD), Nonalcoholic steatohepatitis (NASH), and Hepatocellular carcinoma (HCC) (Parker, Kim and Gao 2018, Azzu, Vacca et al. 2020, Zhao, Zhao et al. 2020, Hall, Chiarugi et al. 2021).Use of stable isotope tracers suggest that NAFLD and obese patients have a greater amount of FFA release from adipose tissue into plasma, contributing to lipid accumulation in the liver (Fabbrini, Mohammed et al. 2008, Rosso,

Kazankov et al. 2019, Sekizkardes, Chung et al. 2020). Adipocyte lipolysis releases a myriad of lipid species that could impact hepatic lipid remodeling and function. Given the profound impact of these processes on human health and disease, there a tremendous need for a more granular and the context-specific understanding of adipocyte lipolysis on the serum and hepatic lipidome.

In this study, we applied quantitative lipidomic analysis to assess how lipids in circulation and the liver change over time after an acute stimulus of adipocyte lipolysis. This method provided a comprehensive coverage of over 1400 lipids species across 17 subclasses using a broadly targeted approach that provides a quantitative assessment of lipid species. With a combination of 70 lipid standards, we quantified the molar concentration of each specific lipid. Our analysis showed how dynamic changes in fatty acids impacts other lipid classes like ceramides and a variety of phospholipid species. Use of mice with conditional deletion of ATGL in adipocytes allowed us to directly interrogate how signals from adipose tissue can impact lipid remodeling in the liver. Highlighting the lipid species in serum that are a product of adipocyte lipolysis and how they drive lipid remodeling in the liver.

2.2 Targeted Quantitative Lipidomic Analysis Using LC-MS of Whole Mouse Serum after Acute Activation of Adipocyte lipolysis.

To systematically quantify lipids in serum upon activation of lipolysis, we applied a comprehensive quantitative approach to analyze lipids. Previously we completed a time course to understand how FFAs change during cold exposure in mice and found that serum FFAs peak at 30 minutes (Simcox, Geoghegan et al. 2017). Therefore, we used the 30-minute time point with a single dose of 1 mg/kg of CL-316,243 (CL), a beta3-adrenergic receptor agonist to provide a thorough quantitative analysis of both serum and hepatic lipid changes (Figure 2-1-1 and

Supplemental Figure 2-1-2D 2-1-2E). Using a LC-MS/MS approach we were able to assess the concentrations of 1450 lipids with corresponding standards that can provide a quantitative assessment of the serum lipidome (Su, Bettcher et al. 2021). Through this analysis, we identified 771 lipid species that fell under 17 lipid classes (Figure 2-1-1A). Lipids were grouped by their corresponding lipid class, which was primarily composed of triacylglycerols (TAG) and polar lipids, with fewer lipids under the category of diacylglycerol (DAG) and cholesteryl esters (CE). Polar lipids include fatty acids (FFA), Sphingomyelins (SM), ceramides (CER), and several phospholipid species (Figure 2-1-1B). All detailed specific lipids change has been shown in supplement Figure 1. We found that FFAs were the only lipids to increase in response to CL administration (Figure 2-1-1B and 2-1-1C). In contrast, we found that PI and PG decreased during this time (Figure 2-1-1C). Of the 771 lipids quantified in serum, we found 89 lipids that significantly change in response to CL (Figure 2-1-1D, 2-1-1E, and 2-1-1F). Correlation cluster analysis of serum lipids suggest that serum FFAs and serum TG are coregulated (Figure 2-1-1E). Most of these lipids were FAs with varying lengths and saturation. Notably there were a few triglyceride species that were elevated in response to CL (Figure 2-1-1F).

Further analysis showed that various FFA species were elevated in response to CL, where the most abundant were myristic acid (C14:0), palmitic acid (C16:0), palmitoleic acid (C16:0), stearic acid (C18:0), oleic acid (C18:1), Linoleic acid (C18:2), and linolenic acid (C18:3). However, several very-long-chain FAs (VLCFAs) did not change, such as Docosahexaenoic acid (C22:6), lignoceric acid (C24:0), nervonic acid (C24:1) (Figure 1G). Surprisingly, we also found the odd chain FAs, FA(15:0) and FA(17:0), increased in serum after CL administration. In contrast, we found that LPE(18:2) and LPE (16:0) decreased in serum 30 minutes after CL administration, (Supplement Figure 2-1-1).

To test whether the composition of FFAs from the adipose tissue reflected the serum levels, we applied our quantitative analysis to measure FFAs and triglycerides in inguinal white adipose tissue (iWAT) after 30 mins of CL administration (Figure 2-1-2A). We found that most free fatty acids increased in response to CL administration around two-fold. The most abundant FFA are FA(16:0), FA(18:1), and FA(18:2) (Figure 2-1-2A). However, triglyceride levels or composition were not changed after CL treatment (Figure 2-1-2B).

To assess whether other metabolic intermediates changed in serum during the time when free fatty acids peaked, we measured intermediates of fatty acid oxidation, products of glycolysis, TCA-related substrates, and amino acids by LC-MS (Supplement Figure 2-1-2A-C). We found reduced serum carnitine levels, while glycerol was elevated (Supplement Figure 2-1-2A). Notably, most amino acids decreased in serum, with the exception of Cysteine. (Supplement Figure 2-1-2C).

To understand how liver lipids changed, we applied a similar quantitative strategy after 30 minutes of CL administration. Using a $p<0.05$ threshold, we found 225 lipids that changed in the liver (Supplement Figure 2-1-2E), with 163 triglyceride species with varying acyl chains, 11 PE, 13 PC, 15 PG, 3 PI, 4 PS, 7 fatty acids, 3 DG, 3 LPC, 1 LPE, 1 SM, and 1 PA. Although serum FFAs peaked at 30 minutes, total hepatic FAs remained unchanged, except for very long chain fatty acids, which were reduced. In contrast, CL-treated mice had a small induction in TAG accumulation in the liver, although not significant (Supplement Figure 2-1-2D). A more detailed analysis showed that there were several TAG species that were elevated with CL administration, with the highest induction in palmitate and linoleate containing triglycerides.

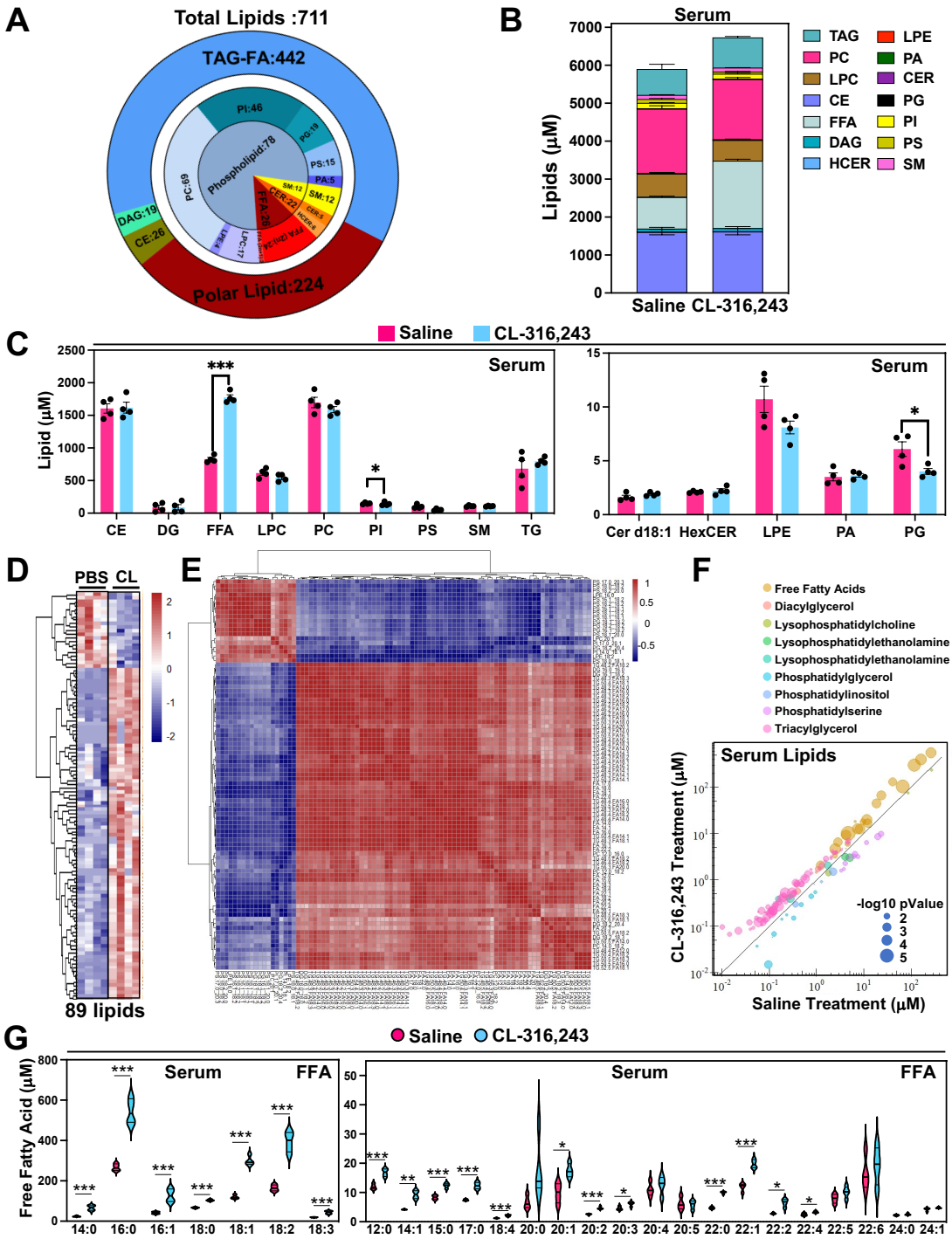

Figure 2-1-1. Quantitative lipidomic analysis of serum with acute activation of adipose tissue lipolysis. A. Graphical representation of lipids identified in mouse serum after 30 minutes of CL-316,243 administration grouped by the corresponding lipid class. B. Concentration of lipid molecular species after 30 minutes of saline or CL administration grouped by the corresponding lipid class. C. Major lipid classes in serum 30 minutes with saline or CL-316,243 administration. D. Heatmap highlighting significant lipid changes between saline of CL-316,243 administration (n=4, $p<0.05$). E. Correlation cluster of 89 significant lipids. F. Distribution of significant lipids by lipid classes, concentration and p-value. Color represents lipids classes, Y axis represents the lipid concentration

after CL treatment, X axis represents saline treatment. Dot diameter represents –log10(p-value). G. Violin plots highlighting compositional changes of serum FFA species with saline or 30 minutes of CL administration. (n=4, *: p<0.05, **: p<0.01, ***: p<0.005)

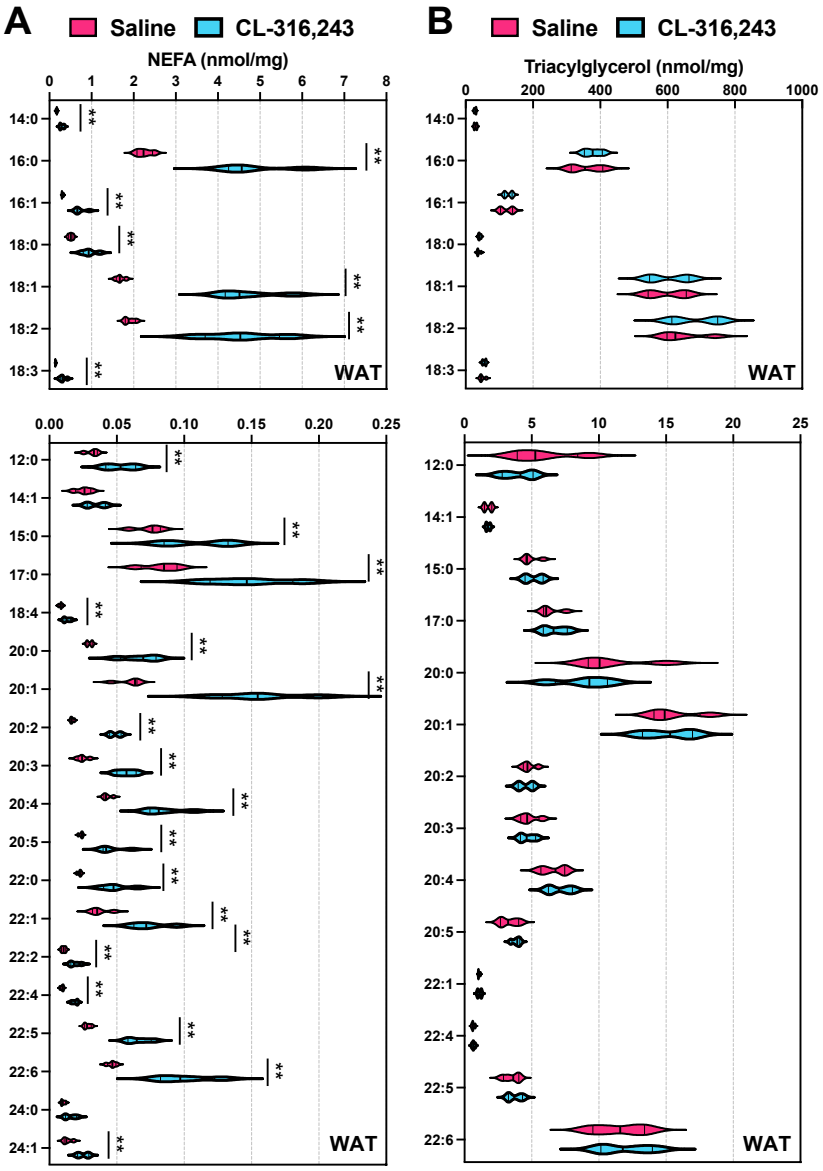

Figure 2-1-2. Quantitative analysis of fatty acid composition from WAT after acute activation of adipose tissue lipolysis. Non-esterified fatty acids (NEFA) and triacylglycerol were measured in inguinal white adipose tissue (WAT) 30 minutes after saline or 1 mg/kg CL-316,243 administration (n=4, *: p<0.05, **: p<0.01, ***: p<0.005).

2.3 Hepatic Lipid Remodeling Dynamic

A single time point only provided a snapshot of lipid changes, to explore the dynamic changes in serum, we isolated serum from mice at 15mins, 30 mins, 1hr, 2hrs, 3hrs, 5hrs, and 12hrs after the activation of lipolysis. The data showed serum FAs had been upregulated to the

peak concentration in 30 minutes and sustained at higher levels. In contrast, serum TAG concentration peaked in 1 hr. Then the TAG concentration dropped down to a lower level than the initial time point. In addition, we found that CE concentration did not change in the serum (Figure 2-2-1A).

2.3.1 Time Dependent Changes in Serum and Liver Lipids Highlight Dynamic Lipid Remodeling

To assess how liver lipids changed during this time, we completed lipidomic analysis by LC-MS for liver samples after a single dose CL injection at various time points (30mins, 1hr, 2hrs, 3hrs, 5hrs, and 12hrs). Clustered with the serum and liver lipid species data (Supplement Figure 2-2-1), serum FAs and TAGs were increased earlier than liver FAs and TAGs. Through correlation analysis, we confirmed that some of the other signal lipids, such as Ceramides (CER, both in the serum and liver), were co-regulated with serum FAs (Figure 2-2-1B). We found that hepatic TAGs, FAs, and CEs increased in livers (Figure 2-2-1C). Liver TAGs reached the highest concentration at 5hrs and remained elevated. In contrast, LPE was reduced in livers after 1hr of CL administration and remained lower throughout the experiment.

2.3.2 Adipocyte lipolysis promotes the expression of genes involved in lipid handling and hepatic lipid remodeling.

With our observation that liver triglycerides were elevated with a single dose of CL, we hypothesized that pathways involved in fatty acid oxidation, pyruvate metabolism, and lipid handling would be elevated to accommodate the influx of incoming lipids from adipose tissue. We found that genes involved in regulating pyruvate metabolism, such as Pdk4, were elevated in response to a stimulus of adipocyte lipolysis, suggesting that pyruvate oxidation is blocked in response to influx of lipids from lipolysis. Genes that encode for enzymes involved

in fatty acid oxidation, such as Ehhadh(Houten et al., 2012) and *Cpt1a* and *Cpt1b*(Simcox et al., 2017a), TAG synthesis genes *Gpat3 and Fasn* (Gao et al., 2019; Shan et al., 2010), VLDL lipoprotein gene *Apoa4*(Simcox et al., 2017a), and lipid droplet biogenesis (*Cidec*) were upregulated after CL administration compared to saline controls. However, *Dgat1, Dgat2 and Pnpla2* expression did not change with CL administration (Figure 2-2-1D).

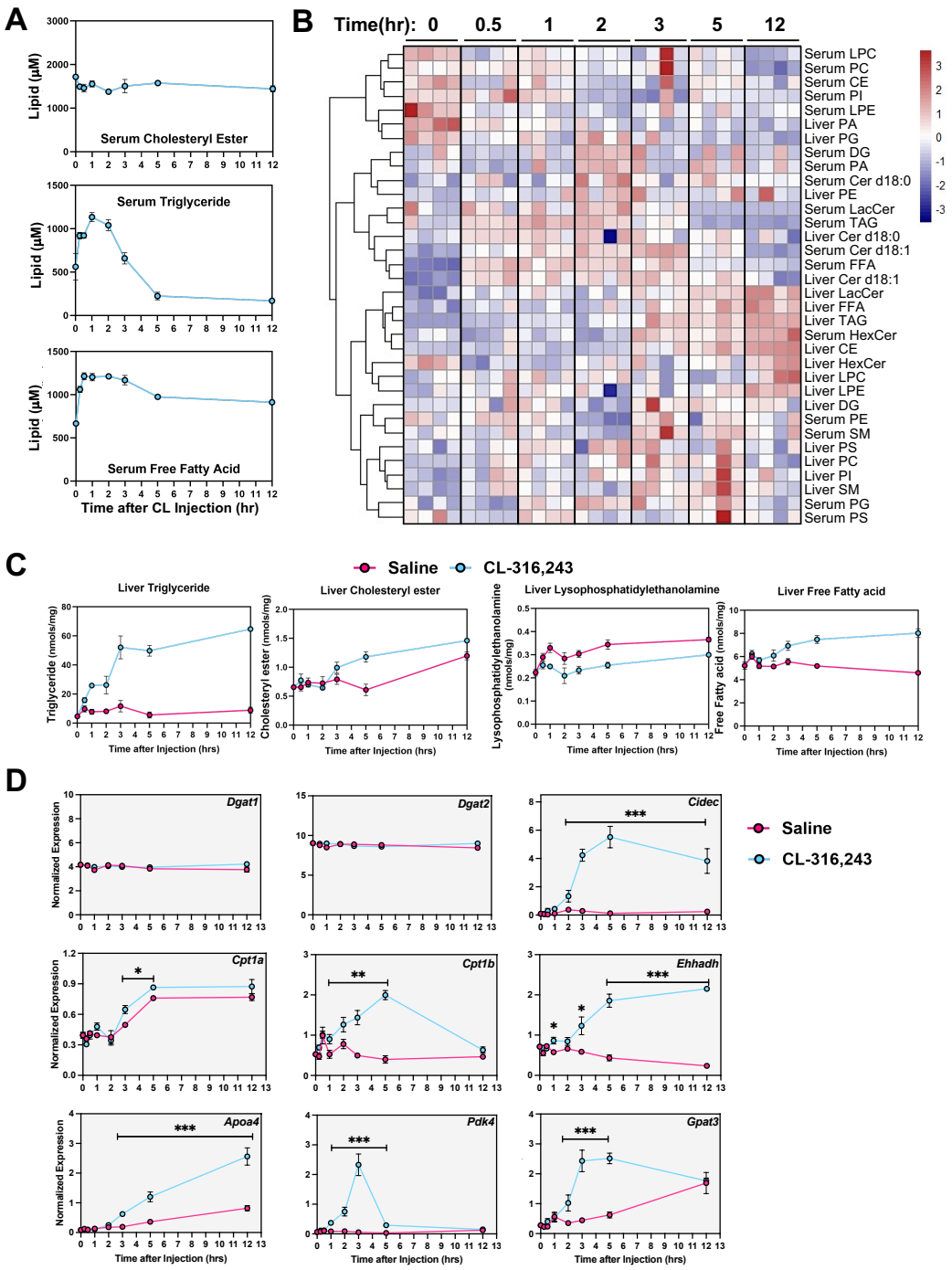

Figure 2-2-1. Time-dependent changes in serum and liver lipids after CL-316,243 administration. A. Time-dependent changes in serum cholesteryl ester (CE), triglyceride (TAG), and free fatty acids (FFA) after CL-316,243 administration. (time points 0, 0.5, 1, 2, 3, 5, 12 hours). B. Cluster analysis of major lipid classes. (time points 0, 0.5, 1, 2, 3, 5, 12 hrs). C. Liver triglycerides, cholesteryl ester, lisophosphatidylethanolamine, and free fatty acids measured after saline or CL-316,243 administration. D. Dynamic changes in hepatic genes expression with activation of adipose tissue lipolysis. Tissues were collected a designated times after a single dose of CL treatment. (n=4, *: $p<0.05$, **: $p<0.01$, ***: $p<0.005$).

Although serum FFAs peaked after 30 min and were associated with several hepatic lipid species as noted above, hepatic FFA content did not change significant following adipocytes lipolysis. However, the composition of fatty acids within hepatic TAGs did change significantly. In particular, the percentage of hepatic TAGs containing palmitoleate (16:1) and linoleate (18:2) increased substantially in response to adipocyte lipolysis. In addition, the composition of hepatic TAGs changed from early (1hr) to late (5hrs) time points. Notably, the composition of TAGs at 5 hrs was similar in serum and liver (Figure 2-2-2A). Together, these data indicate that adipocyte lipolysis enriches linoleate (18:2) in hepatic TAG following adipocyte lipolysis (Figure 2-2-2A 2-2-2C 2-2-2E). To address the extent to which acyl chains change in serum FFAs and TAGs, we plotted each lipid's time course. Surprisingly, we found that palmitate (16:0) was the dominant FFA found in mouse serum, whereas linoleate (18:2) was the most abundant esterified fatty acid within serum TAGs (Figure 2-2-2B 2-2-2E). For serum PC, palmitate acid (16:0) was still the dominant esterified fatty acid (Figure 2-2-2D). For hepatic TAGs, linoleate (18:2) was the most abundant esterified fatty acid. These data indicate that lipid remodeling occurs primarily within TAGs rather than other lipid species with the liver in the context of adipocyte lipolysis (Figure 2-2-2E 2-2-2F). To address further refine the specific TAG species (e.g. combination of three esterified fatty acids), we plotted the top ten hepatic TAG species (Figure 2-2-2G). The most abundant hepatic TAG species was TAG (52:4)-FA (18:2), which represents TAG (52:4) with at least a FA (18:2) tail.

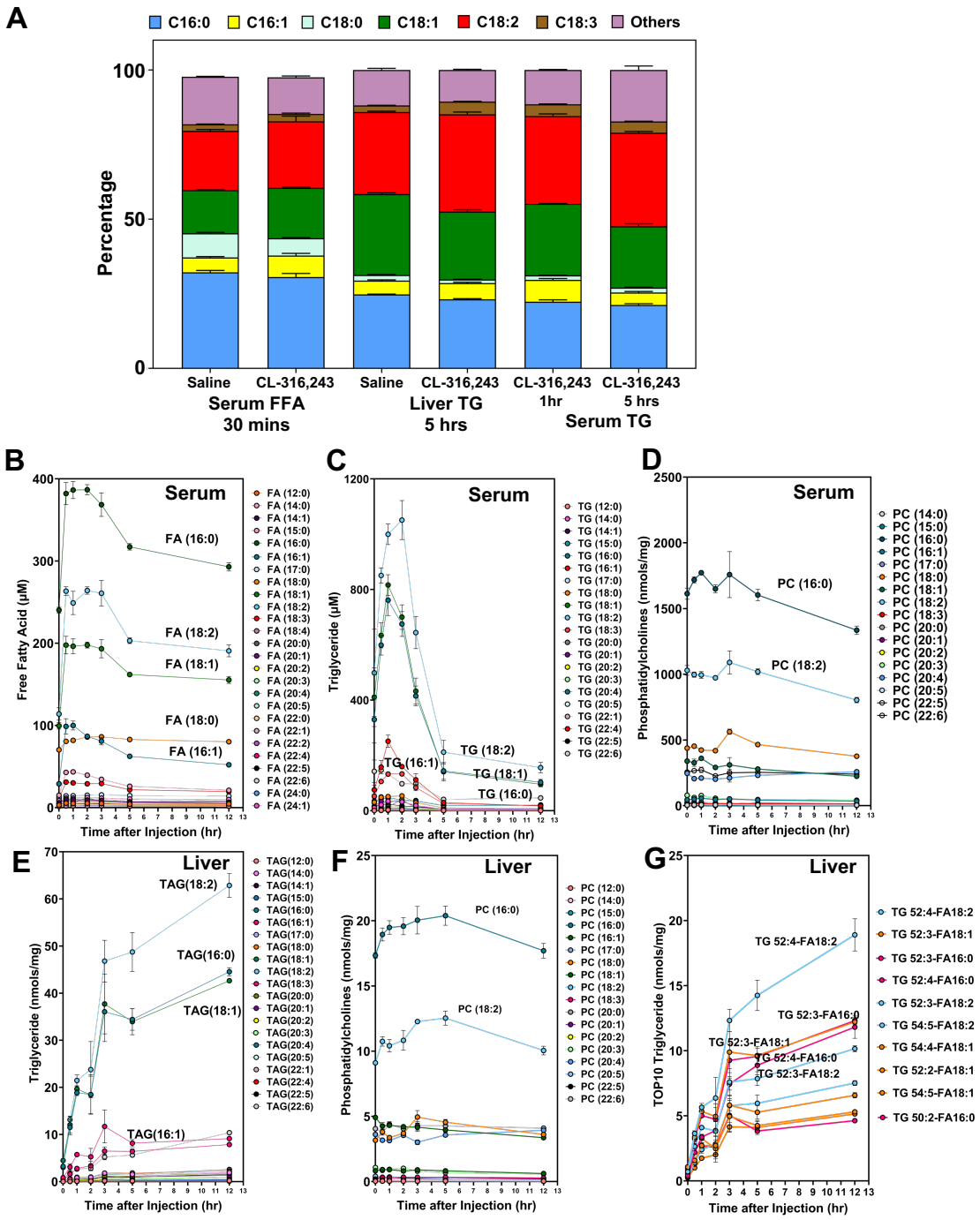

Figure 2-2-2. Fatty acid composition of serum and liver triglycerides after CL administration. A. Fatty acid composition of serum FFAs, liver triglycerides, and serum triglycerides as a percentage of total lipid class. B. Time-dependent changes in individual fatty acid species in serum after giving a single dose of 1 mg/kg of CL-316,243. C. Fatty acid composition of serum triglycerides (one of three tails) after giving a single dose of 1mg/kg CL-316,243. D. Fatty acid composition of serum phosphatidylcholines (one of three tails) after a single dose of 1mg/kg CL-316,243. E. Fatty acid composition of liver triglycerides (one of three tails) after a single dose of 1mg/kg of CL-316,243. F. Fatty acid composition of liver phosphatidylcholines after a single dose of 1mg/kg CL-316,243. G. Fatty acid composition of top10 liver TAG species. Each species has carbon number, number of double bonds, and one of the acyl chains associated with TAG species.

2.3.3 Adipocyte lipolysis increases energy expenditure and oxidation of both endogenous and dietary-derived lipids.

Our observation that TAGs containing linoleate (18:2) are enriched in the hepatic TAG pool suggests that other fatty acids (e.g. palmitate) may be preferentially hydrolyzed and/or oxidized relative to linoleate (18:2). To test this hypothesis, we measured fat oxidation in mice provided dietary source of U-13C-palmitate or U-13C-linoleate by gavage. We found that with CL treatment, there was significant reduction in products of fat oxidation from U-13C-palmitate and U-13C-linoleate as measured by 13C-CO2 release (Figure 2-2-3A and 2-2-3C). We hypothesized that this resulted from release of unlabeled fatty acids from WAT upon activation of lipolysis. To test this hypothesis, we measured the amount of 12C-CO2 release, and found that it was indeed elevated (Figure 2-2-3B and 2-2-3D). These findings would suggest that both products of lipolysis and dietary-derived fatty acids are being utilized during CL treatment. There was no significant difference in respiratory exchange ratio (RER) with CL treatment during the light phase, but CL reduced the RER in the dark phase when food was provided (Supplement Figure 2-2-2A 2-2-3B). In addition, the CL treatment induced Energy expenditure (EE) and oxygen consumption (measured by VO_2 test); the data is presented by the area under the Curve (AUC) (Figure 2-2-3E and 2-2-3F. And the time course data is shown in Supplement Figure 2-2-2C-2-2-2F. We found that fractional labeling of CO_2 relative to fractional labeling of palmitate or linoleate was similar in response to CL treatment (Figure 2-2-3F).

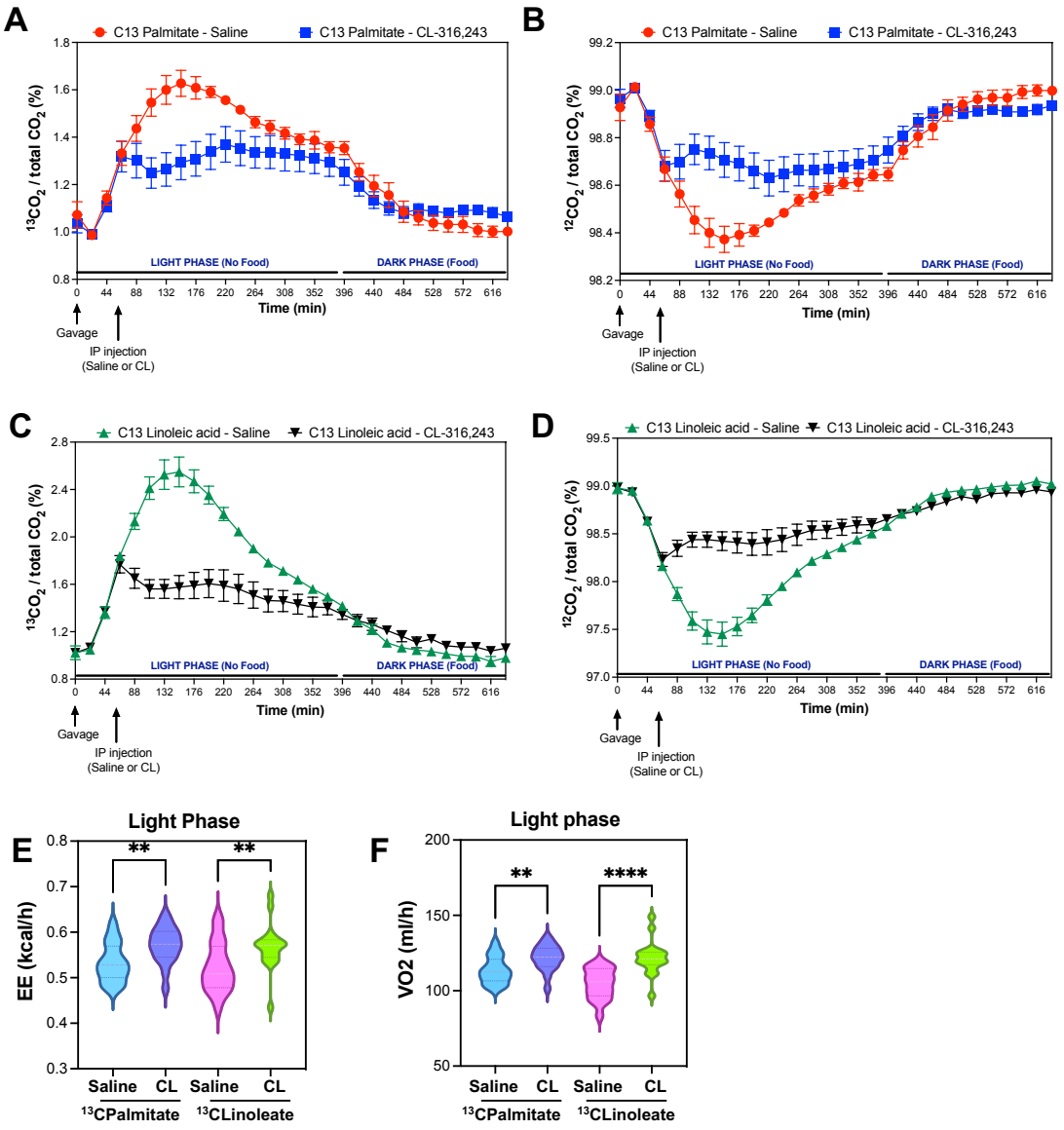

Figure 2-2-3. Dietary palmitate and linoleate utilization in response to activation of lipolysis. A. Percentage of $^{13}CO_2$ release after gavage with ^{13}C-palmitate. Mice were treated with saline or 1 mg/kg CL-316,243. B. Percentage of $^{12}CO_2$, release after gavage with ^{13}C-palmitate. C. Percentage of $^{13}CO_2$ release after gavage with ^{13}C-linoleic acid. D. Percentage of $^{12}CO_2$ release after gavage with ^{13}C-linoleic acid. E and F. Area under the Curve (AUC) of Energy Expenditure (EE) (E) or oxygen consumption (F) after saline or CL treatment in mice given ^{13}C-palmitate or ^{13}C-linoleic acid.

2.4 The Impact of Blocking adipocyte lipolysis on Hepatic lipid Remodeling

2.4.1 Blocking adipocyte lipolysis prevents hepatic lipid remodeling induced by b3-AR activation.

The ATGL enzyme (*Pnpla2*) catalyzes the first step of TAG hydrolysis, generating DAGs and FFAs (Møller et al., 2015). To address which lipid changes were directly due to adipocyte lipolysis in response to CL-316,243, we generated mice lacking ATGL in adipocytes (Figure 2-3-1A) (Morak, Schmidinger et al. 2012, Schreiber, Diwoky et al. 2017). Following CL administration (5hr), livers of control $Pnpla2^{F/F}$ mice developed a pale appearance, but not $Pnpla2^{F/F}::Adipoq^{CRE}$ mice (Figure 2-3-1B). In addition, control $Pnpla2^{F/F}$ mice had increased liver/body weight ratio in response to CL-316,243, however $Pnpla2^{F/F}::Adipoq^{CRE}$ mice did not have greater liver weight in response to CL-316,243. Loss of ATGL increased the weight of inguinal white adipose tissue (iWAT) and brown adipose tissue (BAT), but not epididymal adipose tissue (eWAT) (Figure 2-3-1C). During the acute treatment with CL, we did not find changes in body weight between $Pnpla2^{F/F}$ and $Pnpla2^{F/F}::Adipoq^{CRE}$ mice (Figure 2-3-1C). We found that serum FFAs were increased after 5 hours of CL administration in the control group ($Pnpla2^{F/F}$), while $Pnpla2^{F/F}::Adipoq^{CRE}$ lacked a similar increase (Figure 2-3-1D 2-3-2A). Similarly, lack of ATGL in adipocytes reduced serum triglycerides. In contrast, CL administration increased liver triglycerides, while $Pnpla2^{F/F}::Adipoq^{CRE}$ mice were protected (Figure 2-3-1E 2-3-2E).

To understand the impact of adipocyte lipolysis on circulating lipids, we completed lipidomic analysis of the serum after 5hrs of CL administration. In the serum we identified 583 lipids (Supplement Figure 2-3-1A). We found that several long-chain fatty acid species were significantly elevated in the $Pnpla2^{F/F}$ mice in response to CL, in contrast

Pnpla2$^{F/F}$*::Adipoq*^{CRE} mice had reduced levels of palmitate (16:0), palmitoleate (16:1), oleate (18:1), stearate (18:0), linoleate (18:2), a-linolenic acid(18:3) (Figure 2-3-2C 2-3-2D). We completed cluster analysis of 583 lipids in *Pnpla2*$^{F/F}$ and *Pnpla2*$^{F/F}$*::Adipoq*^{CRE} mice (Figure 2-3-2B). We found that 143 were significantly changed between saline and CL in control mice, however, *Pnpla2*$^{F/F}$*::Adipoq*^{CRE} mice had reduced serum levels of several triglycerides species, free fatty acids, ceramides, and LPEs (Figure 2-3-3A). Compared with the *Pnpla2*$^{F/F}$*::Adipoq*^{CRE} and *Pnpla2*$^{F/F}$ group, 37 significant lipids overlapped. However, these lipids changed in the opposite direction (Supplement Figure 6B 6C). For specific serum lipid concentrations, we plotted that data in Supplement Figure 2-3-2.

To test the impact of adipocyte lipolysis on liver lipids, we completed lipidomic analysis in control and Ko mice (*Pnpla2*). We could quantitatively assess 731 lipids that were identified in the liver (Supplement Figure 2-3-1D). In *Pnpla2*$^{F/F}$ controls, we found that CL treatment increased both liver triglycerides and FFAs (Figure 2-3-2E). In *Pnpla2*$^{F/F}$*::Adipoq*^{CRE} mice, CL did not increase liver triglycerides (Figure 2-3-2E). We completed cluster analysis based on the 731 lipids from the control group; *Pnpla2*$^{F/F}$*::Adipoq*^{CRE} did not change for these lipids (Figure 2-3-2F). There are 100 significant lipids overlapped here. However, for lipids species, hepatic TAGs decreased compared with saline treatment (Supplement Figure 2-3-1E 2-3-1F). For all specific hepatic lipid species, we plotted that data in Supplement Figure 7.

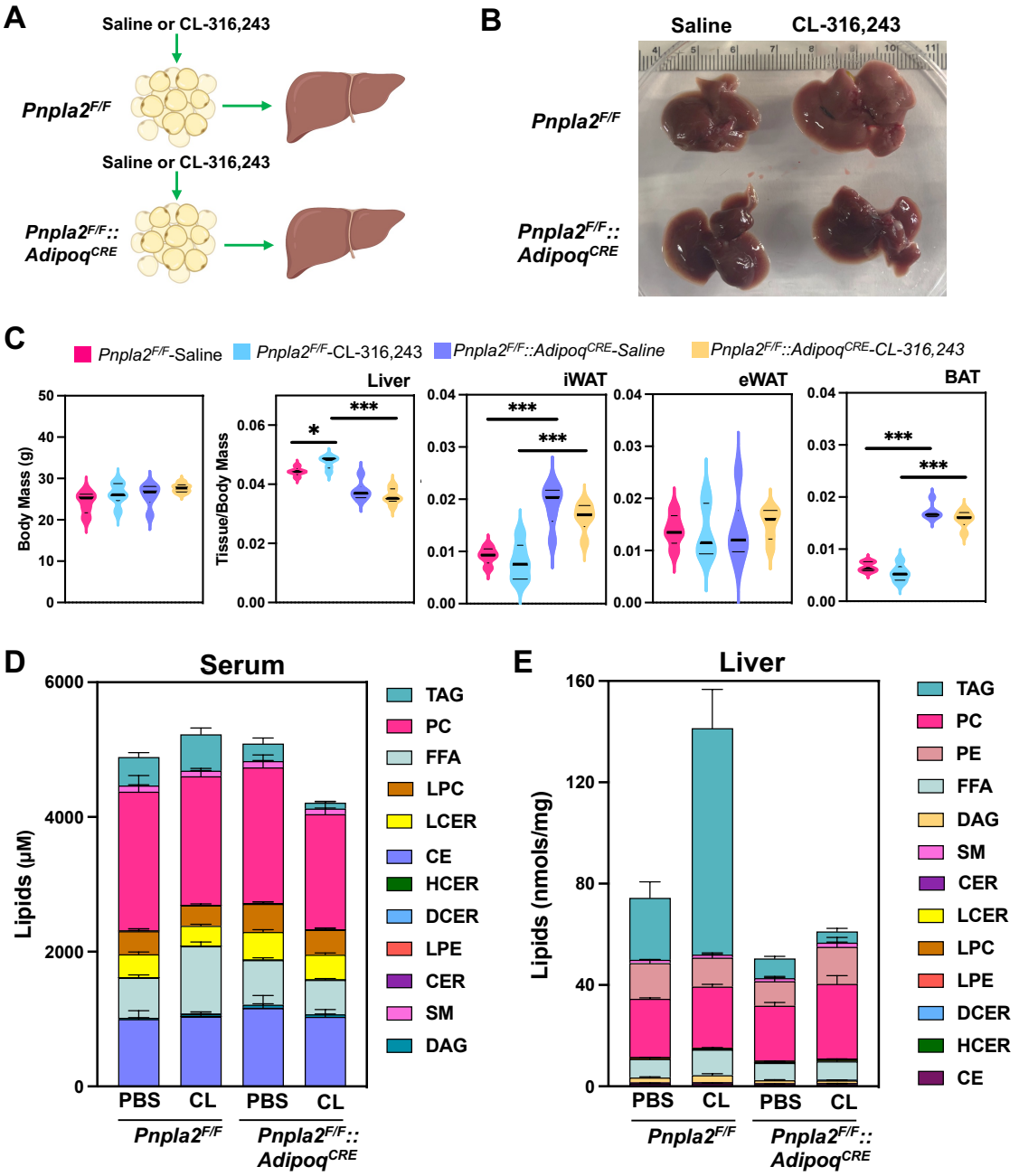

Figure 2-3-1. Targeted Lipidomic analysis of serum and liver from mice with selective deletion of ATGL in adipocytes. A. Experimental design to test the €mpact of adipose tissue lipolysis on systemic lipid metabolism and liver. *Pnpla2*$^{F/F}$ and *Pnpla2*$^{F/F}$*::Adipoq*^{CRE} mice were treated with a single dose of saline or 1 mg/kg CL-316,243. B. Morphological changes in livers after saline or CL-316,243 treatment. C. Liver, iWAT, eWAT and BAT weights corrected for body weight. D and E. Stacked graphs showing serum lipids (D) and liver lipids € from major lipid classes. (n=5-7, *: p<0.05, **: p<0.01, ***: p<0.005)

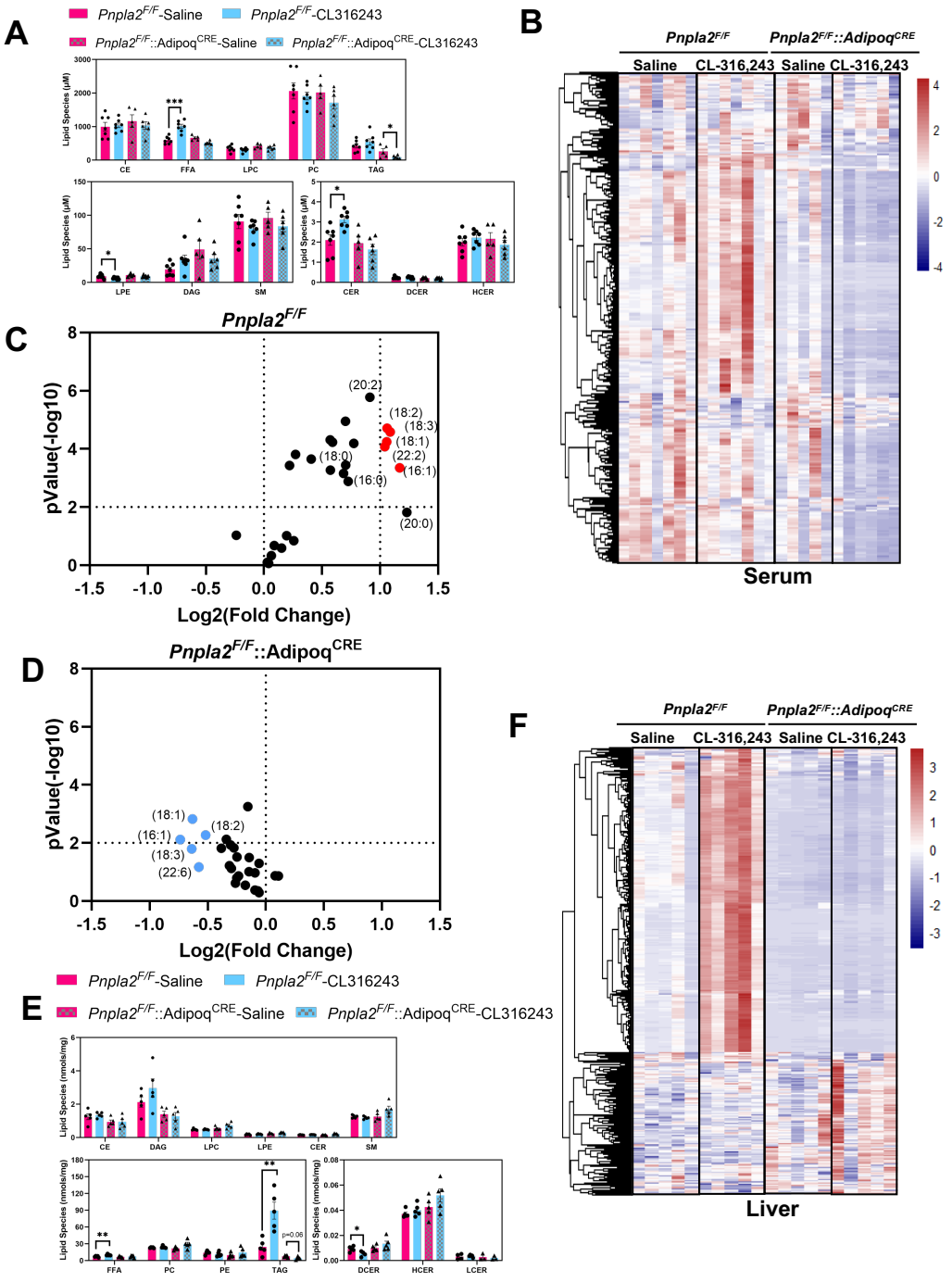

Figure 2-3-2. Inhibition of adipose tissue lipolysis prevents lipid remodeling in the liver. A. Major lipid classes in serum after 5 hours of saline or CL administration (n=5-7, *: p<0.05, **: p<0.01, ***: p<0.005). B. Heatmap for all four groups in serum lipidome. C. Volcano plot of LC-MS-based FFAs from the plasma of *Pnpla2*$^{F/F}$ group. FFAs that are increased 2-fold after CL administration and have a p-value below 0.01 are labeled in red. D. Volcano plot of LC-MS-based FFAs from the plasma of *Pnpla2*$^{F/F}$*::Adipoq*^{CRE} group. FFAs that are increased 2-fold after CL administration and have a p-value below 0.01 are labeled in red. E. Major lipid classes in liver after saline or CL administration. (n=5, *: p<0.05, **: p<0.01, ***: p<0.005). E. Heatmap for all four groups in liver lipidome. F. Heat map highlighting liver lipid changes after saline or CL administration.

2.4.2 Blocking adipocyte lipolysis attenuates triglyceride accumulation in the liver.

To understand how adipocyte lipolysis impacts serum and liver lipids, we plotted changes in lipid classes with a p-value < 0.05. We found 117 lipids induced by CL in the *Pnpla2*$^{F/F}$ group in serum and no lipids were induced by CL in *Pnpla2*$^{F/F}$*::Adipoq*^{CRE} group (Figure 2-3-3A). In the liver, we found 507 lipids increased with activation of adipocyte lipolysis in the *Pnpla2*$^{F/F}$ group and 22 lipids increased in the *Pnpla2*$^{F/F}$*::Adipoq*^{CRE} group (Figure 2-3-2F). For the serum samples, in the control group, the most abundant upregulated lipids were FAs and TAGs (Figure 2-3-3A). Also, there are a few ceramides increased, such as CER(16:0) and CER(24:1) (Figure 2-3-3A). Notably, the combination of blocking adipocyte lipolysis and CL treatment reduced serum and liver fatty acids and triglycerides in *Pnpla2*$^{F/F}$*::Adipoq*^{CRE} mice (Figure 2-3-3B). Of the 507 lipids induced in the liver, 455 triglyceride species were upregulated with CL administration. The triglyceride species had varying acyl chain length and saturation.

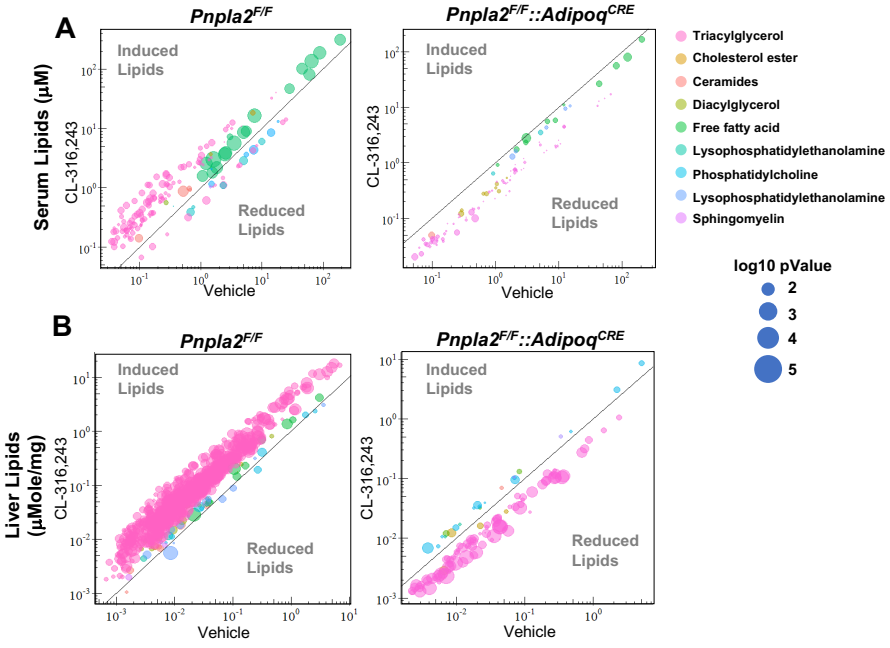

Figure 2-3-3. Quantitative changes in lipids from serum and liver in Pnpla2$^{F/F}$ and Pnpla2$^{F/F}$::Adipoq^{CRE}mice. Distribution of significant serum lipids (A) and liver lipids (B) by lipid classes. The Y-axis represents the lipid concentration after CL treatment, and X-axis represents the lipid concentration with vehicle treatment. Dot diameter represents –log10(p-value). (n=5-7).

2.5 Targeted lipidomic analysis for differentiated white adipocyte and hepatocytes in vitro

2.5.1 Targeted lipidomic analysis of lipid secretome of differentiated white adipocyte.

With multiple organs responding to the acute adipocyte lipolysis, it would be hard to analyze the exact lipid secretome from adipose tissue in vivo. We applied an in vitro approach to decipher the composition of the lipids secreted from adipocytes. We differentiated immortalized preadipocytes from iWAT of 12-week-old male mice. We treated cells with vehicle or 10nM CL for 5hrs to stimulate lipolysis and collected the conditioned medium (CM) to complete untargeted LC-MS analysis (Figure 2-4-1A). Through this analysis we found 559 unique lipid species in the media, of which 125 were increased and 225 decreased with activation of lipolysis (Figure 2-4-1B 2-4-1C). These included fatty acids of various lengths. Notably, we identified triglycerides in the media, which were decreased with activation of lipolysis.

Using a quantitative lipidomics approach, we identified 412 lipids in condition medium samples (Figure 2-4-1B 2-4-1D), 32 increased and 189 decreased (Figure 2-4-1D). Free fatty acids made up the greatest concentration in the conditioned media (Figure 2-4-1E). Notably, we also found LPCs were upregulated by CL treatment. However, PEs, LPEs, and TAGs were downregulated by CL (Figure 2-4-1E). However, it differed with all FAs upregulated in mice serum (except a few VLCFAs, Figure 2-1-1G, Supplement Figure 2-2-3); only saturated FAs increased in the condition medium (Supplement Figure 2-4-1B). The most abundant fatty acid released into the media was palmitate. Further analysis of metabolites showed that glycerol and lactate was increased in the media with CL treatment (Supplement Figure 2-4-1C-D).

Compared with in vivo experiments, we overlapped the lipid species with the condition medium, 30mins, and 5hrs serum after CL administration. For all the lipids analyzed, there are

260 lipids overlapped. For significant increased lipids, only FAs (7 FAs, FA(12:0), FA(14:0), FA(16:0), FA(16:1), FA(18:0), FA(20:0), and FA(22:0)) overlapped with the three lipidomic analysis experiments. For the decreased lipids, there were no significant overlapped lipids by three lipidomes. For other specific condition medium lipids species, we plotted that data in Supplement Figure 2-4-1.

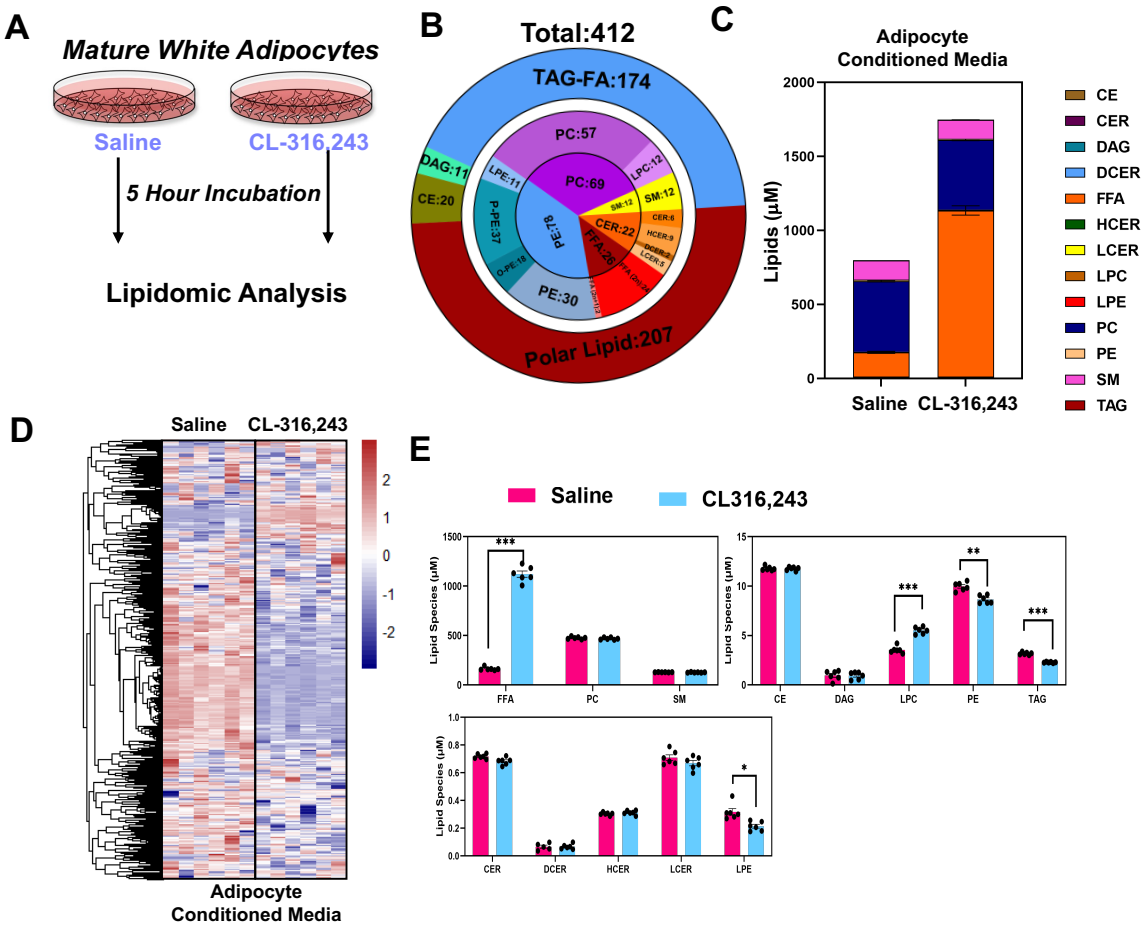

Figure 2-4-1. Quantitative lipidomic analysis of conditioned media from differentiated white adipocytes. A. The workflow for condition medium collection and LC-MS analysis. B. Pie graph representing targeted LC-MS analysis. C. The concentration of lipid molecular species of condition medium lipidome grouped by the corresponding lipid class. D. Heatmap displaying all lipid molecular species (targeted LC-MS) between CL and vehicle treatment (n=6). E. Absolute concentrations of major lipid classes identified in adipocyte conditioned media.

2.5.2 Conditioned media from activation of lipolysis leads to lipid remodeling of hepatocyte lipidome.

To test the impact of conditioned media from adipocytes treated with vehicle or CL, we collected condition medium from mature adipocytes and incubated the media from adipocytes with hepatocytes (HEPA 1-6) for 5 hours (Figure 2-4-2A). After removing condition medium, we completed targeted lipidomic analysis of hepatocytes. We identified 954 lipids in hepatocytes (Figure 2-4-2B 2-4-2C). The most significant lipids were FAs and TAGs (Figure 2-4-2D 2-4-2E), which matched with the in vivo experiments (Figure 2-2-1G). Notably, we found sphingomyelin (SM) and phospholipids occupied a large part of lipid composition, such as PC, PE, PI, and PS (Figure 2-4-2D). Except for FAs and TAGs, LPCs also increased by CL condition medium (Figure 2-4-2E). For the specific lipids species from condition medium treated hepatocytes, we plotted that data in Supplement Figure 2-4-2.

Overlapped with the three lipidomic datasets (condition medium treated hepatocytes, 5hrs CL liver, and condition medium), there are a large overlap between the three groups. However, for the statistically significant lipids, condition medium only have few FAs overlapped with the other two lipidomes, such as FA(14:0), FA(16:0), and FA(16:1). Compared with the lipidomic data from hepatocyte and 5hrs liver samples, there are 367 lipids overlapped as CL induced lipids, include most of saturated, unsaturated FAs, and TAGs (Figure 2-4-1F, Supplement Figure 2-3-2). There were no overlap as decreased lipids (Figure 2-4-2F).

To test whether there is direct communication between adipocytes and hepatocytes, we collected condition media from differentiated adipocytes and incubated conditioned media with hepatocytes and liver organoids. Fully differentiated preadipocytes We found that conditioned media isolated from CL-treated adipocytes, was able to stimulate expression of genes in

pathways involved in fat utilization (Figure 2-4-2G 2-4-2H). The CL condition medium upregulated CPT1a, PDK4, and PLIN2 expression significantly (Figure 2-4-2G). These genes are PPARα and HNF4a targets, and they play critical roles in lipids sensing, particularly for cellular FAs level increasing. To test whether these effects are a result of products of adipocyte lipolysis, we treated cells with ringer's media that never came into contact with cells. We found that CL did not directly impact gene expression in hepatocytes. In addition, hepatocyte organoids grown in 3D culture using hepatocyte progenitors, showed that condition media elevated the expression of genes involved in lipids metabolism, including CPT1a, CPT2, PGC1a, and PLIN2. Also, the pyruvate metabolism inhibiting gene PDK4 was induced (Figure 2-4-2H).

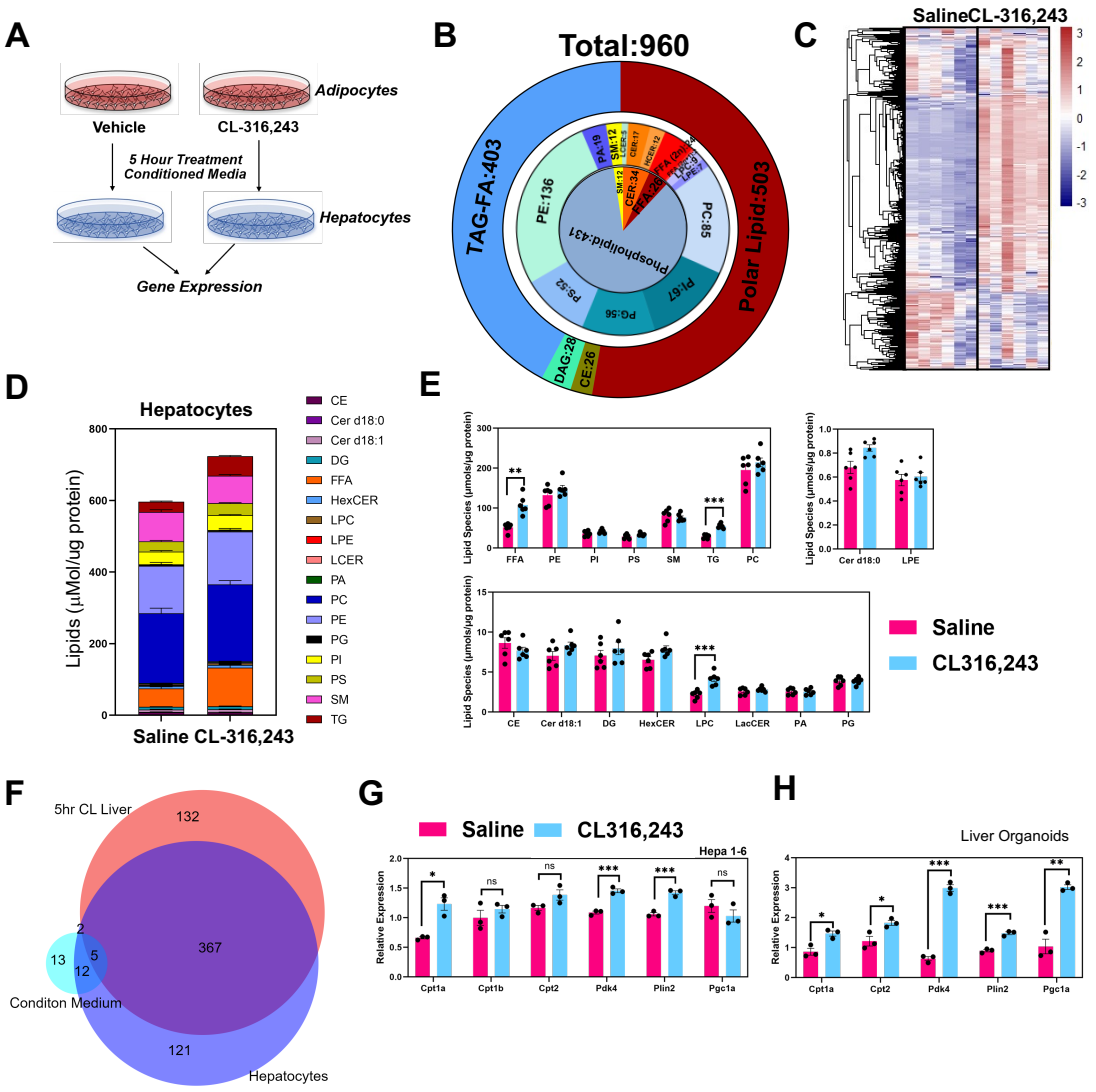

Figure 2-4-2. Lipidomic analysis of hepatocytes treated with adipocyte conditioned media. A. The workflow highlighting the production of conditioned media and the treatment of hepatocytes. B. Pie diagram highlights targeted LC-MS analysis of hepatocyte lipidomic analysis grouped by corresponding lipid class. C. Heatmap displays all lipid molecular species comparing hepatocytes treated with conditioned media from adipocytes treated with vehicle or CL-316,243 (n=6). D. Stacked bar plot with major lipid species comparing hepatocytes treated with adipocyte conditioned media. E. The major lipid classes were grouped by major molecular species. F. Overlapping of characterized lipids species, three Venn graphics present All lipid species overlapping, CL significantly induced lipids overlapping ($p<0.05$), and CL significantly repressed lipids overlapping ($p<0.05$). Red pie represents liver lipidome after 5hrs CL treatment. Blue pie represents hepatocyte lipidome after condition medium treatment. Aqua pie represents condition medium lipidome. G. Real-time PCR analysis of HEPA 1-6 cell line in response to condition media from differentiated adipocytes. H. Real-time PCR analysis of mouse liver organoids treated with adipocyte conditioned media. In all experiments, conditioned media was collected from adipocyte after 5 hour incubation with saline or CL-316,243.

2.6 Discussion

Non-alcoholic fatty liver disease (NAFLD) occurs when excess triglycerides accumulate in the liver. The acyl chains in triglycerides can originate from various sources, such as dietary intake, *de novo* fatty acid synthesis, or adipose tissue through the release of fatty acids during lipolysis. However, the specific contribution of adipose-derived fatty acids to the hepatic lipid pool is not well understood. Although adipose-derived fatty acids are thought to contribute to 70% of the triglyceride pool in human livers (Kawano and Cohen 2013), there is little known about the direct contribution of exogenous fatty acids on the liver *in vivo*. In this study we set out to develop a quantitative assessment of the time-dependent changes in serum and liver lipids after a single stimulus of adipocyte lipolysis. To our knowledge, there has been no previous *in vivo* study that has measured the dynamic changes in serum and hepatic lipids upon activation of adipocyte lipolysis. Our findings suggest that the adipose tissue drives profound changes in lipid remodeling in the liver. Interestingly there are several lipid classes where steady state levels do not change. This comprehensive analysis provides a valuable resource for understanding how dynamic changes in lipid metabolism occur.

White adipose tissue (WAT) is responsible for releasing energy to peripheral tissues *via* the activation of lipolysis. This process involves the activation of the β3-AR, a G-protein coupled receptor that signals through PKA to promote release of FFAs from WAT and induce thermogenesis in BAT. A previous study on long-term cold exposure has shown that the lipid composition of serum, WAT, and BAT changes, leading to profound changes in cardiolipin and thermogenesis (Lynes, Shamsi et al. 2018). Others have highlighted the essential role of adipocyte lipolysis in cold adaptation (Schreiber, Diwoky et al. 2017, Shin, Ma et al. 2017). However, the effects of acute cold exposure or adipocyte lipolysis on lipid composition are still

unclear. Our study aimed to investigate how the acute activation of adipocyte lipolysis impacts hepatic lipid remodeling. Our findings suggest that when adipocyte lipolysis is activated, free fatty acids increase to 1.5 mM in the serum at 30 minutes, which we found is primarily composed of palmitate (30.6%), oleate (16.9%), and linoleate (22.3%). During this time, serum triglycerides show a transient rise that mirrors the induction of free fatty acids that seems to be delayed by around 30 minutes. In contrast, triglyceride levels in the liver peak at 3 hours and are maintained elevated over 12 hours during which serum FFA and TG largely revert to normal. These effects are due to CL mediated activation of white adipocyte lipolysis, as mice lacking ATGL are protected against hepatic triglyceride accumulation.

As the liver accumulates triglycerides, we see an early rise in expression of genes involved in lipid metabolism and lipid droplet dynamics. Expression of *Gpat3* increased in the liver with activation of adipocyte lipolysis. The induction mirrored the rise in liver triglycerides up to 5hrs after the initial stimulus. There are four mammalian GPAT enzymes. GPAT1 and GPAT2 are found in the mitochondria, while GPAT3 is localized to the endoplasmic reticulum. The induction of GPAT3 provides one of the key initiation steps in triglyceride synthesis (Cao, Li et al. 2006, Yu, Loh et al. 2018). This rise in GPAT3 likely provides protection against cellular stress caused by the considerable influx of fatty acids entering from circulation. During the time course we failed to see changes in expression of DGAT enzymes, as both *Dgat1* and *Dgat2* expression were unaltered as liver triglycerides increased. Although previously it was shown that *Dgat1* expression increases with fasting, a condition where there would be activation of adipocyte lipolysis, we found that WAT-lipolysis does not drive the increase in *Dgat1* expression. Perhaps other mechanisms like hormonal regulation of *Dgat1* expression is more relevant in the fasting state. In addition, genes involved in fatty acid oxidation of long-chain fatty

acids like *Cpt1 a/b* and *Ehhadh* were also induced with the activation of adipocyte lipolysis, both reported transcriptional targets of PPARα (Pawlak, Lefebvre and Staels 2015). Another target of PPARa, Pdk4, was induced by adipocyte lipolysis. PDK4 phosphorylates pyruvate carboxylase, which has been shown to inhibit pyruvate metabolism (Qin, Lin et al. 2020, Jiang, Mo et al. 2021). The inhibition of pyruvate oxidation leads to the preferential use of fatty acids as a source of energy. Notably, Cidec, a regulator of lipid droplet remodeling is highly induced in the liver and closely follows the changes in liver triglycerides (Herrera-Marcos, Sancho-Knapik et al. 2020).

Our analysis suggests that upon activation of adipocyte lipolysis, palmitate (16:0) is the most abundant free fatty acid in the serum, and the second and third are linoleate (18:2) and oleate (18:1), respectively. However, quantitative assessment of TAG pool in serum and liver, shows that triglycerides containing linoleate (18:2) are the most abundant. Linoleic acid (18:2) is an essential polyunsaturated fatty acid that is a precursor for prostaglandins, leukotrienes, and thromboxane (Simopoulos 2008, Goncalves, Lu et al. 2019). Therefore, it's possible that hepatocytes spare the use of linoleic acid for the synthesis of these potent signaling molecules and store linoleic acid in molecular species like triglycerides to prevent their use for fatty acid oxidation. We also considered the possibility that DGAT enzymes could prefer substrate like linoleate to preferentially esterify into the triglyceride pool. However, DGAT activity assays using an *in vitro* reconstitution assay where various acyl-CoA species were tested, showed a lack of preference for linoleic acid (DeLany, Windhauser et al. 2000).Our isotope tracer studies suggest that activation of WAT lipolysis promotes the use of both dietary derived fatty acids and those that are internally stored. Notably, the basal utilization of linoleate was higher than palmitate. Consistent with these findings, isolated mitochondria from rats show higher rates of

acylcarnitine production when offered linoleate as the source of fatty acid (Reid and Husbands 1985). Alternatively, differences in basal respiration when providing palmitate or linoleate could be explained by solubility of fatty acids and their affinity for intracellular fatty acid binding proteins.

CL treatment raised liver triglyceride levels to those seen in mice challenged with high-fat diet (Schreiber, Diwoky et al. 2017, Zhu, Li et al. 2021). To confirm that these effects were due to adipocyte lipolysis, we generated mice lacking ATGL in adipose tissue (*Pnpla2*$^{F/F}$*::Adipoq*^{CRE}). This allowed us to directly test whether lipolysis from white adipose tissue was the driver of serum and hepatic lipid changes. We noted that conditional deletion of ATGL in adipocytes completely blocked the CL-induced changes in liver triglycerides, highlighting the potential to target adipocyte lipolysis to reverse hepatic steatosis. Notably, CL treated *Pnpla2*$^{F/F}$*::Adipoq*^{CRE} mice showed a greater reduction in liver triglycerides than saline control, an outcome that is likely due to the activation of BAT thermogenesis (Huijsman, van de Par et al. 2009, Morak, Schmidinger et al. 2012). Thus, the inhibition of adipocyte lipolysis and activation of thermogenesis has profound effects on liver triglycerides and preventing hepatic steatosis.

Our studies suggest that there is direct communication between adipocytes and hepatocytes. In our study we used an *in vitro* system to understand how adipocyte-derived lipids impact hepatocyte lipids. In addition to even chain fatty acids, like FA(14:0), FA(16:0), FA(16:1), and FA(18:0), FA(18:1), FA(18:2), FA(18:3), we identified odd chain fatty acids in the serum and conditioned media, including FA(15:0), and FA(17:0). Normally, straight odd chain FAs are only synthesized in plants and only exist at a low level in mammals (Jenkins, West and Koulman 2015). However, in culture the relative levels of odd-chain fatty acids were proportionally higher

compared to even-chain fatty acids. We suspect that FA(15:0) and FA(17:0) are derived from branched-chain fatty acids through branch chain amino acid metabolism (Green, Wallace et al. 2016, Wallace, Green et al. 2018). These studies suggest that *de novo* fatty acid synthesis *in vitro* primarily drives the synthesis of odd chain fatty acids. Thus, the composition of fatty acids *in vitro* in adipocytes, may not reflect the composition *in vivo*.

We noted significant changes in other lipid classes, we found that LPE is consistently downregulated *in vitro* and *in vivo* after CL administration. LPE is a rare phospholipid found in cell membranes. LPE also plays a role in cell-cell signaling and enzyme activation, such as MAPK pathway and calcium channel activation (Nishina, Kimura et al. 2006, Lee, Park and Im 2017). The reduction of serum LPE might be a potential mechanism to balance calcium levels in different organs in responding to adipocyte lipolysis. With a reduction of LPE in serum, the activity of calcium channels might be reduced by lower phosphorylation of MAPK. Ceramides also showed dynamic changes with activation of adipocyte lipolysis. Liver ceramides (Cer d18:0, Cer d18:1) and serum ceramides (Cer d18:0, Cer d18:1) both increase acutely with the rise in serum free fatty acids. While liver and serum HexCer cluster together with liver FFA and Liver TG. These observations would suggest that ceramide accumulation is likely driven from excess adipocyte lipolysis. Perhaps a compensatory mechanism to deal with fatty acid overload. Ceramides are linked with NASH (Kakazu, Mauer et al. 2016, Nikolova-Karakashian 2018) and insulin resistance (Pagadala, Kasumov et al. 2012), conditions where one might expect to see nutrient overload (Summers, Chaurasia and Holland 2019). Thus, adipocyte lipolysis is sufficient in driving induction of both serum and liver ceramides.

In summary, we provide a detailed analysis of both the serum and liver lipidome in response to activation of adipocyte lipolysis. Here we demonstrated that the lipids from adipose tissue

could remodel the hepatic lipids directly and indirectly. Acute activation of lipolysis led to a dramatic rise in serum lipids, most of which were fatty acids and ceramide species. These studies provide a framework to understand the lipid signaling that drives regulation of lipid metabolism in the liver and the genes involved in lipid remodeling.

*This Chapter has been published on Journal of Lipid Research (2023) as “Sicheng Zhang, Claudio Villanueva et al. Acute activation of adipocyte lipolysis reveals dynamic lipid remodeling of the hepatic lipidome.” (Zhang, Williams et al. 2023)

Chapter Three

Adipose-Liver Crosstalk Signaling Promotes GR-Plin5 Axis to Regulate Ketogenesis

Hepatic transcriptional regulation is a pivotal mechanism in response to adipose tissue lipolysis. We employed bioinformatics analysis to forecast potential transcription factors within the liver that react to adipose tissue lipolysis. In addition to well-established transcription factors such as PPARα, HNF4α RXR, and LXR, our investigation unveiled the hepatic glucocorticoid receptor (GR) as a potential novel transcription factor playing a crucial role in lipid metabolism. During adipose tissue lipolysis, GR translocation can be triggered by the hypothalamic-pituitary-adrenal (HPA) axis. Furthermore, we observed that acute adipose tissue lipolysis induced by CL substantially promotes ketogenesis. Notably, the absence of hepatic GR inhibits the CL-induced ketogenesis process. Additionally, our findings suggest that hepatic GR may directly regulate hepatic Plin5 expression as a downstream target, and the absence of hepatic GR also diminishes CL-induced ketogenesis. In summary, our study demonstrates that adipose tissue lipolysis activates hepatic GR to orchestrate a cascade of lipid metabolism processes. The hepatic GR-Plin5 axis emerges as a pivotal pathway in ketogenesis.

3.1 Introduction

The liver has developed different ways to sense and respond to signals from adipose tissue lipolysis and other sources of lipids. Transcriptional regulation is one of the important mechanisms by which the liver adapts to changes in lipid availability and metabolism. Several transcription factors have been identified that play important roles in regulating hepatic lipid metabolism, including peroxisome proliferator-activated receptors (PPARs), liver X receptors (LXRs), and sterol regulatory element-binding proteins (SREBPs). In addition to these transcription factors, other signaling pathways and transcriptional regulators also play important roles in regulating hepatic lipid metabolism (Rando, Tan et al. 2016, Fougerat, Schoiswohl et al. 2022). For example, the insulin signaling pathway regulates the expression of genes involved in glucose and lipid metabolism, while the AMP-activated protein kinase (AMPK) pathway is a key regulator of cellular energy homeostasis (Enevoldsen, Polak et al. 2007, Kim, Tang et al. 2016).

In this study, by using tissue-specific knock-out mouse models, we investigated the mechanism of how adipose tissue lipolysis affects hepatic lipid remodeling. The activation of the glucocorticoid receptor (GR) by fatty acids during adipose tissue lipolysis through the hypothalamic-pituitary-adrenal (HPA) axis is an intriguing finding (Liang, Zhong et al. 2014). It suggests that the HPA axis and GR signaling are involved in the regulation of lipid metabolism in response to adipose tissue lipolysis. Furthermore, our study identified a role for GR in regulating the coat protein perilipin 5 (PLIN5) on lipid droplets. This finding highlights a potential mechanism by which GR influences hepatic lipid metabolism during acute adipose tissue lipolysis. The involvement of the GR-PLIN5 axis in regulating ketogenesis is particularly interesting and suggests a potential link between adipose tissue lipolysis and ketogenesis in the liver. While the exact mechanism is not yet clear, our findings have important implications for

understanding metabolic disorders and studying the physiological processes associated with acute lipid flux. This research may provide insights that could be beneficial for developing therapeutic strategies for metabolic disorders and furthering our understanding of the physiological responses to acute changes in lipid metabolism. It would be exciting to see further studies uncovering the detailed mechanisms and exploring the potential therapeutic applications of targeting the GR-PLIN5 axis in metabolic disorders and acute lipid flux physiology.

3.2 Glucocorticoid receptor pathway activation during adipose tissue lipolysis.

CL-316,243 (CL) is the beta-3-adronergic receptor (B3AR) agonist, which can activate the B3AR to promote the lipase phosphorylation through the cAMP-PKA pathway. Here, CL treatment to mice would be a good module for us to mimic the lipolysis stimulation in vivo and in vitro. Since Beta-3-receptor is expressed in adipose, but not in liver (Fougerat, Schoiswohl et al. 2022). CL would not have influence on the liver directly.

3.2.1 Glucocorticoid receptor pathway might be activated during adipose tissue lipolysis.

The key process for adipose tissue lipolysis is consecutive hydrolysis of triglycerides (TGs) and the formation of free fatty acids (FAs) and glycerol by adipose lipase (ATGL, HSL, and MGL). Adipose triglyceride lipase (ATGL, coded by Pnpla2) is the rate-limiting enzyme that catabolizes TGs to diglycerides (DGs) and FAs. Here, we applied Adipose ATGL knock-out mice (AAKO, *Pnpla2*$^{F/F}$:: *Adipoq*^{CRE}) treated with CL or saline (Figure 3-1-1A). The control group (*Pnpla2*$^{F/F}$) can respond to CL to release the FAs, glycerol, and other lipids into the circulation system to affect multiple organs including the liver. Lacking ATGL in adipose tissue could cause the deficiency of adipose tissue lipolysis and lipids releasing (Schoiswohl, Stefanovic-Racic et al. 2015) (Fougerat, Schoiswohl et al. 2022).

Our RNA-seq analysis after 5 hours of CL or saline administration in the liver samples has provided valuable insights into the gene expression changes associated with adipose tissue lipolysis. In the control group (*Pnpla2*$^{F/F}$), you observed significant upregulation of 1739 genes and downregulation of 1470 genes upon CL administration. However, in the AAKO group (*Pnpla2*$^{F/F}$:: *Adipoq*^{CRE}), where ATGL is lacking in adipose tissue, the number of differentially expressed genes was reduced, with only 203 genes upregulated and 332 genes downregulated (Figure 3-1-1B). To validate the gene expression changes in different lipid metabolic pathways, you performed rt-PCR analysis. In the control group, CL administration resulted in the upregulation of PPARα-target genes (ApoA4 and Pdk4), as well as genes involved in fatty acid oxidation (Cpt1a/b and Ehhadh), hepatic lipid droplet coating (Plin2, Plin4, Plin5, and Cidec), and ketogenesis (Hmgcs2, Hmgcl, Bdh1, and Slc16A6). The Enrichment analysis shown that CL potentially induced several metabolic pathway, incudes lipids metabolism, fructose metabolism, amino acids metabolism, and nucleotides metabolism (Figure S3-1-1E S3-1-1F). However, in the AAKO group, these CL-induced gene inductions were not observed (Figure Sl1A-C). To identify potential regulators in the liver during adipose tissue lipolysis, you utilized the upstream regulator analysis (URA) tool in the Ingenuity Pathway Analysis (IPA). ln the control group, we identified 224 regulators that were activated by CL administration. These included well-known transcription factors (TFs) associated with classical lipid metabolism (such as Pparα and Hnf4α), anti-oxidation (Tp53 and Nrf2), endoplasmic reticulum stress (Xpb1, ATF4, and ATF4, leads by IRE1 (Tsuru, Imai et al. 2016)), and lipogenesis (Srebp1 and Mixipl) (Figure 3-1-1C). However, in the AAKO group, only 46 pathways were significant, indicating a differential regulatory response compared to the control group (Figure 3-1-1D). There were 13 overlapping pathways

between the two genotypes, while 211 pathways were uniquely regulated in response to adipose tissue lipolysis (Figure 3-1-1E).

Our findings regarding the unexpected activation of the glucocorticoid receptor (GR) in the liver during adipose tissue lipolysis are indeed intriguing (Figure 3-1-1C 3-1-1E). The GR is a hormone-dependent transcription factor that is involved in various metabolic processes, including glucose metabolism, lipid metabolism, and inflammation. Its activation in the context of lipid sensing and metabolism adds another layer of complexity to the regulatory network(Præstholm, Correia et al. 2021) (Bose, Hutson and Harris 2016). It is interesting that the expression of Nr3c1 (GR) was repressed by the lipolysis-inducing compound (CL) in the control group, but there was no change in the adipose tissue-specific knock-out (AAKO) group (Figure 3-1-1F). Furthermore, in the control group, the expression of GR target genes such as G6Pc, Pck1, Insig2a, Fgf21, Igfbp1, Nfkbia, and Dusp1 was induced by CL, while in the AAKO group, there was either no effect or an opposite trend (Figure 3-1-1F 3-1-1G). We compared the CL induced and repressed genes with a GRKO CHIP sequence project(Præstholm, Correia et al. 2021). We also found GR might associate with other lipid sensing transcription factors, such as Ppara and Hnf4a (Figure S3-1-1D). These observations suggest that GR may play a role in mediating the effects of adipose tissue lipolysis on gene expression in the liver. While some of the GR target genes overlap with those regulated by other transcription factors such as PPARα and HNF4α, it is still highly possible that GR activation is specifically involved in the response to adipose tissue lipolysis.

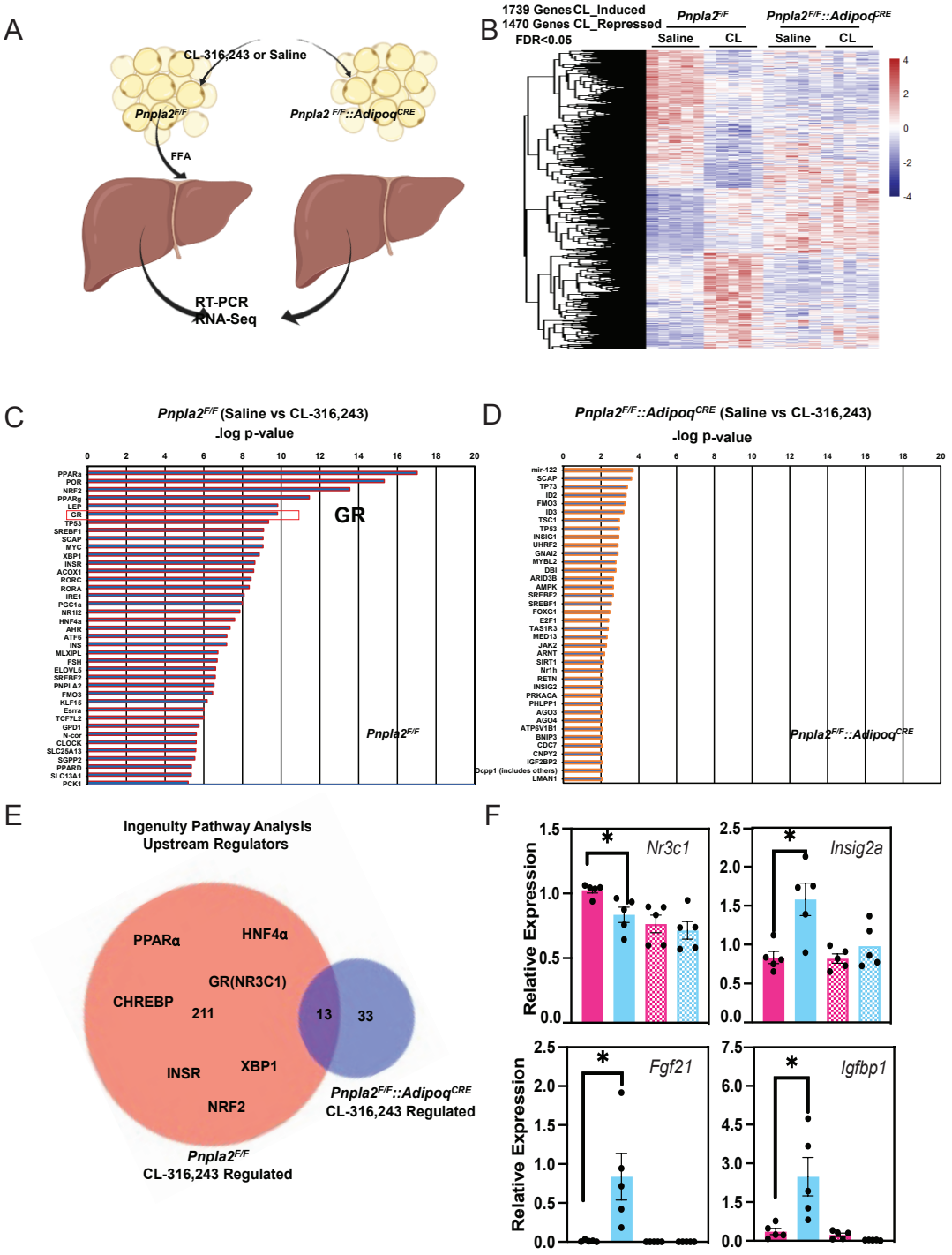

Figure 3-1-1 An analysis of liver transcriptions in mice with targeted removal of ATGL in adipocytes revealed that GR, or Glucocorticoid Receptor, shows promise as a potential regulator in the liver's response to the breakdown of fats in adipose tissue. A. Abstract graphics of the impact of adipose tissue lipolysis to the liver. Control (*Pnpla2*$^{F/F}$) and AAKO(*Pnpla2*$^{F/F}$*::Adipoq*^{CRE}) mice were treated with a single dose of saline or 1 mg/kg CL-316,243. B. RNA-seq Clustering the gene expression by the control group and observed the different patterns in the gene expression of

the AAKO group (qValue < 0.05, n=5). C. Ingenuity Pathway Analysis (IPA) analysis for the CL induced control groups to identify potential upstream regulators including transcription factors (TFs) and any gene or small molecule that has been observed experimentally to affect gene expression. D. IPA analysis for CL induced AAKO groups. E. Overlapping the IPA lists by control groups and AAKO groups. F. RT-PCR to quantify the gene expression of GR targets expression, including *Insig2a, Igfbp1*, and *Fgf21*. (*: $p<0.05$, **: $p< 0.01$, ***: $p<0.005$, ****: $p<0.001$, n=5).

3.2.2 Glucocorticoid receptor deficiency causes hepatic lipid accumulation in vitro.

We conducted an in vitro study using an adipocyte-hepatocyte co-culture model to investigate the impact of specific transcription factors identified in our RNA-seq analysis. In our experimental setup, mature adipocytes were treated with either ringer buffer added PBS or CL-316,243 for a duration of 5 hours. The conditioned medium from these adipocytes was collected and stored at -80 degrees Celsius. We generated mutant AML12 hepatocytes using CRISPR SaCAS9, with scramble sgRNA serving as the control group. The mutant hepatocytes were then treated with the conditioned medium obtained from the adipocytes. To assess lipid accumulation, we utilized BODIPY staining to visualize lipid droplets in the hepatocytes (Figure 3-1-2A). We expected that higher GFP signaling would correspond to increased lipid (triglyceride) accumulation. In this study, we generated mutant hepatocyte cell lines with mutations in the Pparα, Myc, Rorc, and GR genes. Each gene had two different sgRNAs used as duplicate controls. However, the three mutant genes, aside from GR, did not exhibit a significant effect on lipid droplet accumulation (Figure S3-1-2A-C). We confirmed the GR mutation through western blot analysis, using beta-Actin as a loading control (Figure 3-1-2B). Under cell imaging, we observed that the GR mutant hepatocytes (Nr3c1_sgRNA1 and Nr3c1_sg2) accumulated more lipid droplets. Notably, even under treatment with saline-conditioned medium, the GR mutant hepatocytes already displayed increased lipid droplet formation. The conditioned medium from CL-treated adipocytes, which contains more lipids released from mature adipocytes, induced lipid droplet accumulation in the control group (Scr sgRNA). Intriguingly, the hepatocytes with

GR mutations exhibited a significantly higher lipid droplet formation when exposed to the CL-conditioned medium (Figure 3-1-2C). To investigate the underlying mechanism responsible for the lipid accumulation associated with GR deficiency, we performed RNA-seq analysis on the hepatocytes treated with the CL-conditioned medium (SCR_CL, Nr3c1sg1_CL, Nr3C1sg2_CL, n=3). We identified 1928 genes that were significantly differentially expressed compared to the control group (Scr_sgRNA) (Figure 3-1-2D). Among the overlapped genes between Nr3c1sg1 and sg2, 1067 were upregulated, while 852 were downregulated (Figure 3-1-2E). Gene enrichment analysis revealed that while the oxidative phosphorylation pathway might be upregulated, the FoxO signaling pathway was significantly suppressed (Figure 3-1-2F). The deficiency of GR in hepatocytes may hinder lipid oxidation, leading to lipid accumulation. Therefore, we decided to further explore the metabolic functions of hepatic GR in vivo.

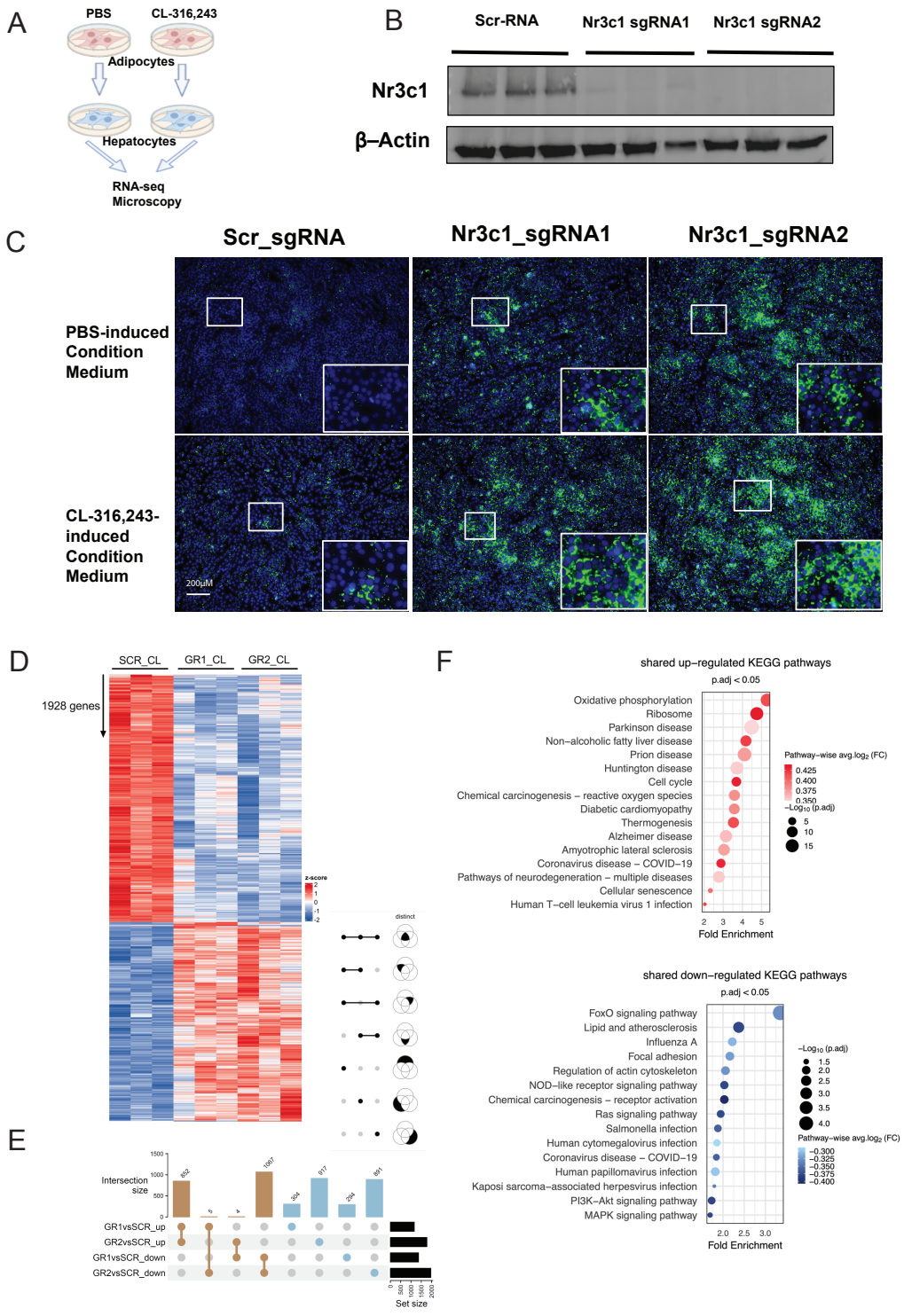

Figure 3-1-2**. In vitro model for identifying GR function responding to adipose tissue secretum.** A. The workflow for condition medium collection and GR mutated hepatocytes (AML12) treated with condition medium. B. Western blot to verify the CRISPR-SaCas9 knock-out *Nr3c1* (GR) in hepatocytes. (n=3). C. Imaging to assess the accumulation of lipids in hepatocytes after treating them with conditioned medium for 6 hours (Green: BPDIPY, Blue: DAPI, n=3). D. RNA-seq analysis to investigate the effects of CL-induced conditioned medium on

hepatocytes with GR mutations (qValue < 0.05, n=3). E. Number of gene upregulated or down regulated. F. Gene set enrichment analysis (GSEA) was conducted on the RNA-seq data. Upregulated pathways are indicated in red, while downregulated pathways are represented in blue.

3.3 Adipose tissue lipolysis activates hepatic GR through HPA axis.

We hypothesize that the glucocorticoid receptor (GR) is activated during adipose tissue lipolysis. While it has been shown that several target genes are induced by CL treatment, the exact mechanism of GR activation remains unclear (Figure 1F 1G). The primary mouse GR agonist is corticosterone (cortisol in humans) (Walker 2006). Corticosterone release is typically dependent on the hypothalamic-pituitary-adrenal (HPA) axis (Liang, Zhong et al. 2014), To investigate this, we measured the levels of corticosterone and adrenocorticotropic hormone (ACTH) in the serum of B57C6 mice after a single dose of CL injection. Corticosterone levels were measured at 1 hour and 5 hours after administration. We observed a three-fold increase in corticosterone levels in the CL group compared to the saline group after one hour. Although corticosterone levels dropped at the 5-hour time point, they remained higher in the CL group compared to the saline group (Figure 3-2A). Furthermore, we measured the levels of ACTH, an upstream signal in the HPA axis, at 0.5 hours, 3 hours, and 5 hours. The CL group exhibited higher ACTH levels compared to the saline group (Figure 3-2B).

To investigate the effects of adipose tissue lipolysis on the HPA axis, we utilized an AAKO (*Pnpla2*$^{F/F}$:: *Adipoq*^{CRE}) model and a control group (*Pnpla2*$^{F/F}$). After 1 hour of treatment, the ACTH and corticosterone levels induced by CL were higher in the control group compared to the AAKO group (Figure 3-2C, 3-2D). Additionally, we examined the translocation of GR protein in C57B6 mice after 3 hours of CL administration. Given the signaling delay, we expected this time point to be appropriate for assessing protein levels. We observed that the levels of GR in the cytoplasm and total lysates remained unchanged, but the CL group exhibited increased nuclear GR levels (Figure 3-2E). As a single dose of CL treatment induces acute time-sensitive reactions,

we conducted a time course analysis to measure the expression of target genes. The expression of Nr3c1 (GR) was downregulated (Figure 3-2F). Most of the GR target genes, such as G6pc, Pck1, Dusp1, and Nfkbia, were upregulated (Figure 3-2F), while some targets, like Scara5 and Per1, did not show any significant changes (Figure S3-2).

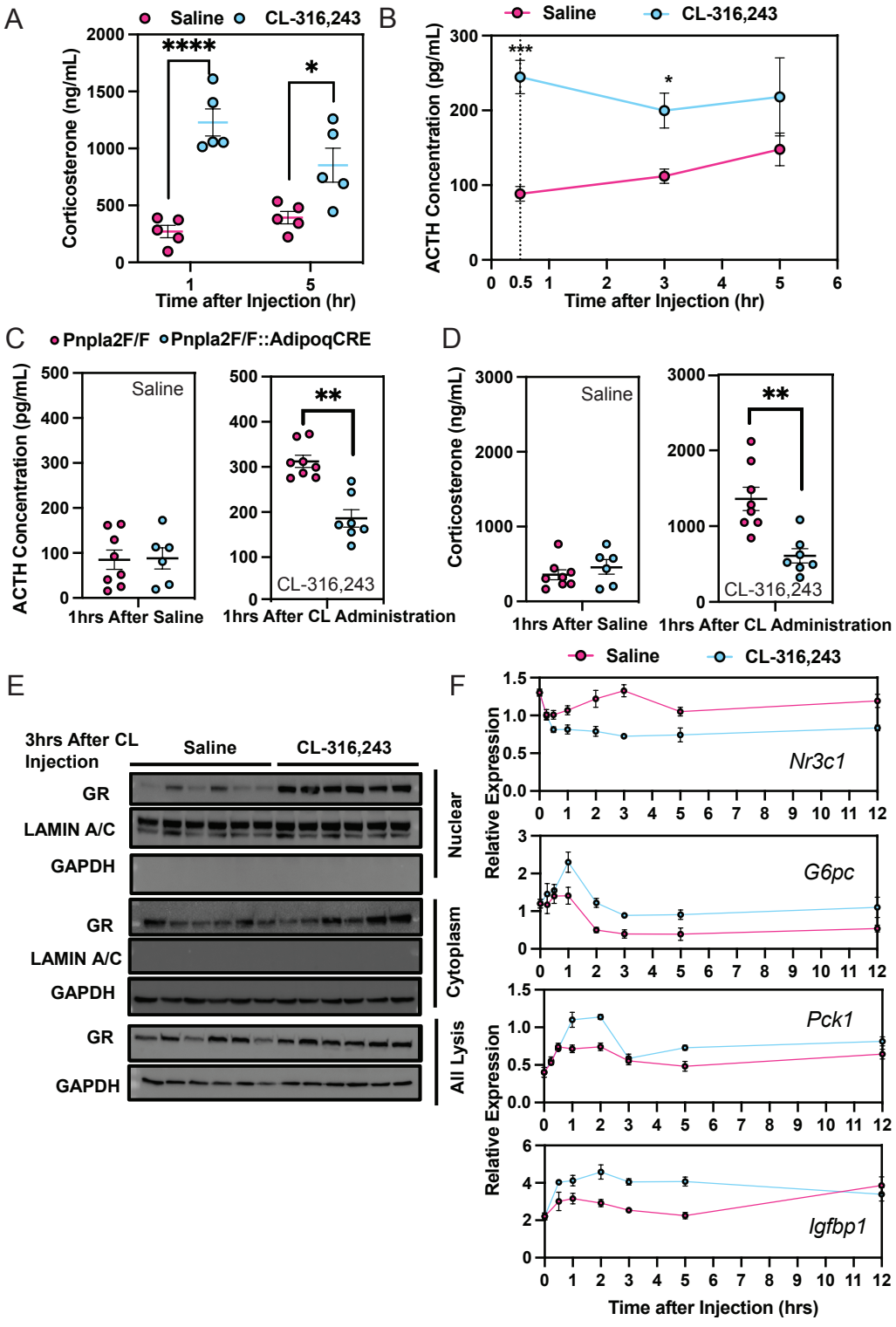

Figure 3-2. GR was activated after CL administration. A. Mouse GR ligand corticosterone measurement after 1- and 5-hours CL administration. B. ACTH measurement after 0.5-, 3- and 5-hours CL administration. (*: p<0.05, **: p< 0.01, ***: p<0.005, ****: p<0.001, n=5). C. ACTH measurement after 1-hour CL or saline administration in AAKO mice group and control group (n=6-8). D. ACTH measurement after 1-hour CL or saline administration in AAKO

mice group and control group(n=6-8). E. Western blot to quantify the GR translocation in nuclear, cytoplasm, and all lysis (n=6). F. Time course for *Nr3c1* (code for GR) and GR targeted genes (n=4).

3.4 Hepatic GR is essential regulators responding to Adipose tissue lipolysis.

3.4.1 Hepatic GR deficiency results in aberrant gene expression in the liver in response to adipose tissue lipolysis.

To investigate the role of hepatic GR during the liver's response to adipose tissue lipolysis, we employed the AAV2/8-TBG-Cre system in *Nr3c1*$^{F/F}$ mice to generate liver-specific knockout mice (Figure 3-3-1A). The advantage of this system is that AAV injection after one week allows us to obtain liver-specific GR knockout mice (GRLKO), thereby limiting the effects on GRLKO mice before CL treatment. Also, there was no significant difference with mice body weight, organs weight, and AST&ALT level between control and knockout mice (Figure S3-3-1B-D). The knockout in the liver was confirmed through western blot and rt-PCR analyses (Figure 3-3-1A, 3-3-1C). We examined the gene expression related to carnitine metabolism, lipid droplet coating, and ketogenesis (Figure 3-3-1D-F). Interestingly, we observed that Cpt1a expression was unaffected by GRLKO. However, the induction of Cact and Cpt1b by CL treatment was hindered in GRLKO mice. Additionally, GRLKO mice exhibited elevated expression of Ehhadh, a gene associated with peroxisomal beta-oxidation, upon CL exposure (Figure 3-3-1D). Notably, we found that the expression of perilipin coating genes, Plin4 and Plin5, important for lipid droplets, was impaired in GRLKO mice, while Plin2 was upregulated (Figure 3-3-1D). Moreover, key genes involved in ketogenesis during CL treatment, except for Hmgcs2, were unaffected by GRLKO (Figure 3-3-1F).

To gain a comprehensive understanding of the broader effects of lacking GR in the liver, we performed RNA-seq analysis of the liver transcriptome in four groups of mice: control groups (*Nr3c1*$^{F/F}$ with AAV-TBG-Null, treated with saline and CL) and GRLKO groups (*Nr3c1*$^{F/F}$ with

AAV-TBG-Cre, treated with saline and CL). Using a threshold (Fdr < 0.05, log2FC > 0.5) based on the control group, we identified 553 upregulated genes and 801 downregulated genes after 3 hours of CL administration. However, the gene expression patterns were different in the GRLKO groups. Based on these patterns, we clustered the genes into six groups and performed gene enrichment analysis to predict their functions (details shown in Figure 3-3-1B). Cluster 3 consisted of genes that were induced by CL treatment in the control group but showed little or no induction in the GRLKO groups. Functional pathways associated with these genes included triglyceride biosynthetic process, acyl-CoA metabolic process, fatty acid beta oxidation, and more (Figure 3-3-1B). By comparing the induced and repressed genes in GRLKO (under CL treatment) with a previous GRKO CHIP-seq project (Præstholm, Correia et al. 2021), we identified enriched motifs that overlapped with GRLKO. Notably, GR may interact with lipid-sensing transcription factors such as Ppara and Hnf4a. Additionally, general transcription factors like Cebp may be associated with GR function (Figure 3-3-1G). Under saline treatment, there were fewer motif enrichments, but similar motifs such as Ppara, Hnf4a, and Cebp were still present (Figure S3-3-1A).

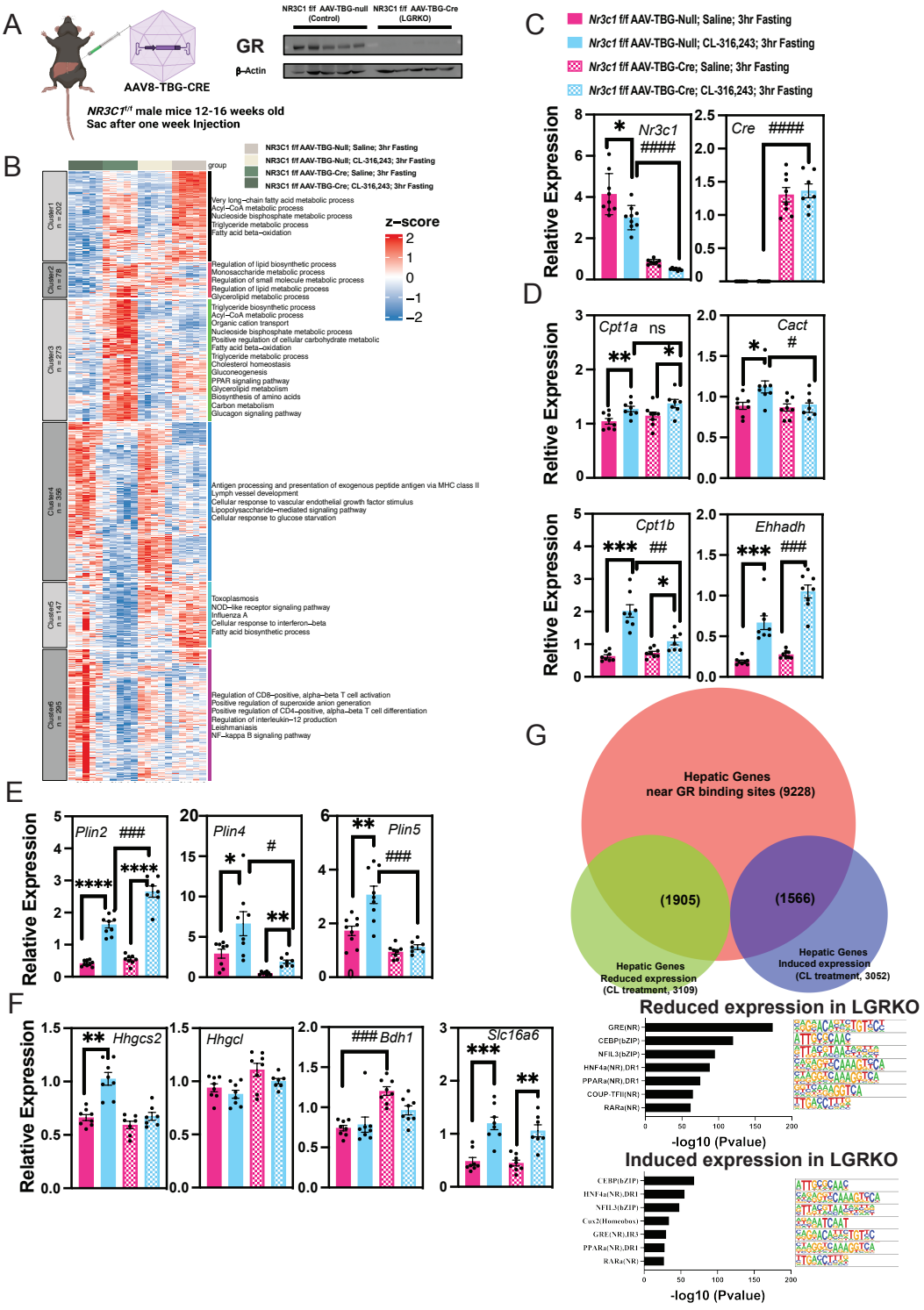

Figure 3-3-1. **Hepatic GR deficiency mice in response to adipose tissue lipolysis.** A. AAV-TBG-Cre:: *Nr3c1*$^{F/F}$ mice system to generate liver-specific GR knockout mice. The GR knock-out was verified by western blot. B. RT-PCR quantify the Gene expression of Nr3c1 and Cre. C. Fatty acid oxidation related gene expression. D. Perilipin gene expression. E Ketogenesis gene expression. (Control groups CL vs Saline, *: p<0.05, **: p< 0.01, ***: p<0.005, ****: p<0.001; GRLKO CL vs Control CL, #: p<0.05, ##:

p< 0.01, ###: p<0.005, ####: p<0.001, n=7-9). F. RNA-seq Clustering the gene expression by the control group and observed the different patterns in the gene expression of the GRLKO group (qValue < 0.05, n=5). Significant GSEA pathways were listed based on 6 clusters gene set. G. Hepatic genes near GR binding sites overlapped with hepatic gene GRLKO reduced and induced expression (CL treatment), the overlapped motifs were analyzed by Homer-motif analysis.

3.4.2 Hepatic GR deficiency impedes adipose tissue lipolysis induced ketogenesis and triglyceride metabolism.

We conducted a time course experiment to investigate the effects of a single dose of CL injection on acute adipose tissue lipolysis. Specifically, we focused on GRLKO mice and performed various measurements at different time points (1hr, 3hr, and 5hr) after CL administration. With a time course, there was still no significant body weight and organ weight change between control and knockout mice (Figure S3-3-2A). Our objective was to assess ketogenesis and triglyceride accumulation levels in the serum and liver samples (Figure 3-3-2A). The Knock-out verification is depicted in Figure 3-3-2B. Previous findings indicated that CL could enhance the serum ketone levels, likely due to its influence on ketone metabolism, a unique fatty oxidation process occurring in the liver. Consequently, we examined the levels of serum beta-hydroxybutyrate (a ketone body diagnostic marker) and serum/liver triglycerides. Notably, the control group exhibited an increase in serum beta-hydroxybutyrate following CL administration. However, in the GRLKO group, CL failed to induce an upregulation of beta-hydroxybutyrate (Figure 3-3-2C). At the 3hr time point, we observed significantly higher levels of serum triglycerides in the GRLKO group. Additionally, the liver exhibited lower triglyceride accumulation compared to the control group (Figure 3-3-2C). Furthermore, the GRLKO group displayed an upregulation of the VLDL marker gene ApoA4. We also noted an upregulation of Pdk4, an enzyme responsible for inhibiting pyruvate oxidation, which is typically upregulated during fatty acid accumulation (Zhao, Tran et al. 2020). This upregulation of Pdk4 was observed

due to the GR deficiency in the liver (Figure 3-3-2B). Furthermore, Gpat3, one of the markers for triglyceride synthesis, was acutely induced in the GRLKO mice (Figure 3-3-2B). For transcription regulators, the expression of Pgc1α was decreased and Pparγ increased (Figure S3-3-2B). For oxidation gene, the Cpt1b was downregulated and Ehhadh was upregulated (Figure S3-3-2C). Considering the collective evidence, we propose that GR deficiency hinders fatty acid oxidation. It is plausible that certain downstream targets of GR play a crucial role in regulating ketogenesis and maintaining triglyceride homeostasis.

Returning to our previous RNA-seq analysis of GRLKO mice, we specifically examined cluster 3 (Figure 3-3-1B, Figure 3-3-2D). Our investigation revealed that the expression of Plin4 and Plin5 genes was induced by CL treatment in the control group. However, in the GRLKO group, the expression of Plin4 and Plin5 was hindered. Analyzing the GR CHIP-seq data on the genome browser (Præstholm, Correia et al. 2021), we identified at least three significant binding peaks of the GR near or between the Plin4 and Plin5 genomic regions. These peaks were primarily located in the intron area, suggesting that they may serve as enhancers for GR binding, thereby regulating the transcription of Plin4 and Plin5 (Figure 3-3-2E). To further validate these findings, we performed RT-PCR to measure the gene expression of Plin4 and Plin5 in the liver. In the absence of hepatic GR, we observed a complete lack of Plin4 expression and delayed expression of Plin5. Additionally, we conducted western blot analysis to verify the protein level of Plin5 (Unfortunately, an appropriate Plin4 antibody was not available) (Figure 3-3-2F).

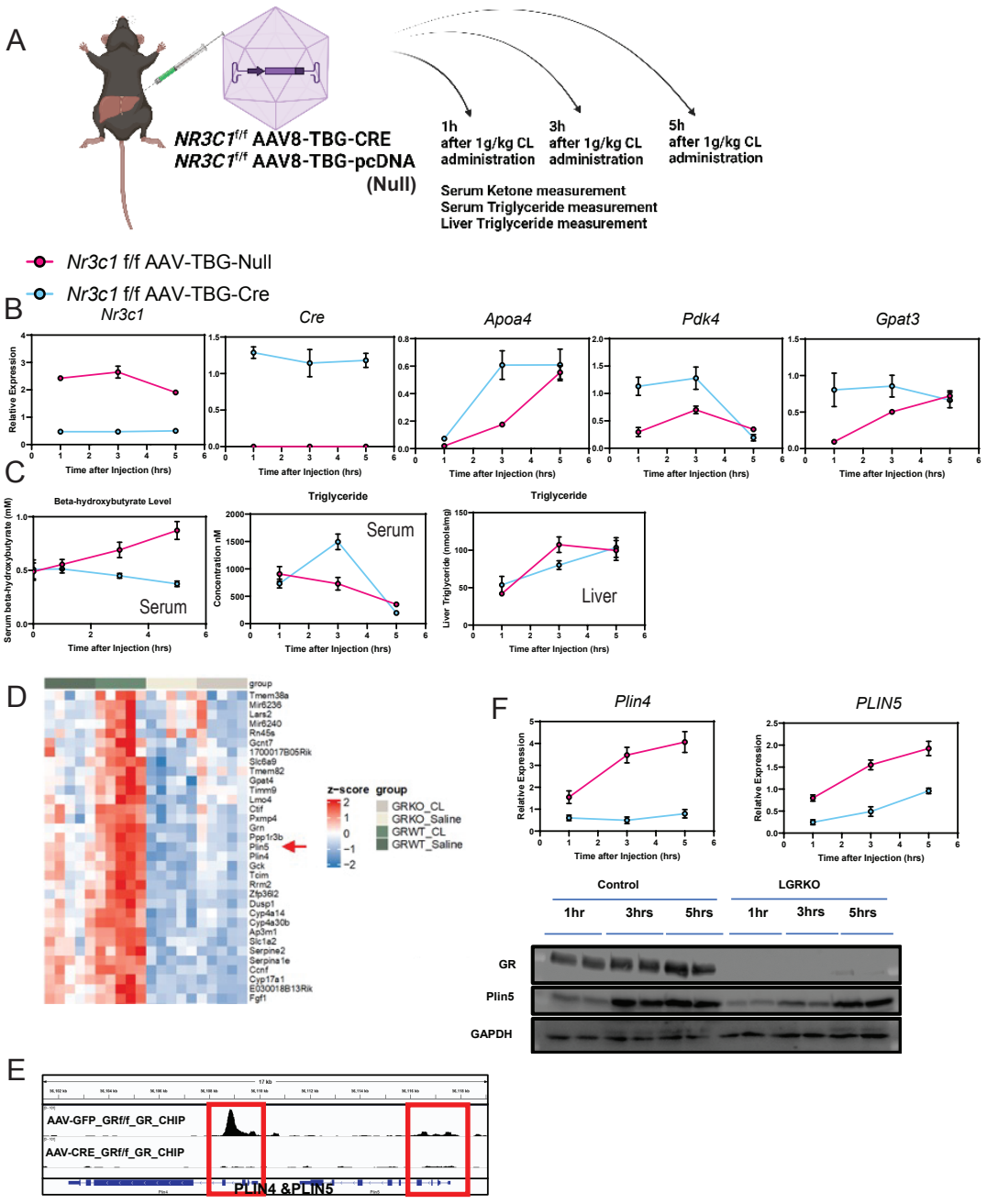

Figure 3-3-2. Time course for gene expression and ketogenesis from hepatic GR deficiency liver in response to adipose tissue lipolysis. A. AAV-TBG-Cre:: *Nr3c1*$^{F/F}$ mice system for CL time course. B. Time course for gene expression of *Nr3c1,*and *Cre*. C. Time course for serum beta-hydroxybutyrate, serum triglycerides, and liver triglycerides (1, 3, and 5 hours). D. Time course for related metabolic marker genes expression (*Apoa4, Pdk4*, and *Gpat3*). E. We focused on Cluster 3 from the GRLKO RNA-seq data and observed that the expression of Plin 4 and Plin 5 was downregulated by GRLKO. F. The GR-CHIP-Seq data was presented using the IGV browser, providing insights into the genomic binding sites of GR. G. Expression of *Plin4* and *Plin5*. Western blot for quantification of *Plin5* protein level (n=5-7).

3.4.3 The absence of hepatic GR hinders the induction of ketogenesis by dexamethasone.

Dexamethasone (Dex) is a synthetic corticosteroid medication categorized as a glucocorticoid. Previous studies, including our own data, have demonstrated that appropriate Dex treatment can induce ketogenesis (Loft, Schmidt et al. 2022)(Figure S3-3-3). In this study, we administered a dosage of 1uM/Kg Dex to GRLKO mice and measured beta-hydroxybutyrate levels at 1hr, 3hr, and 5hr time points. Our findings revealed that in the control group, ketone bodies significantly increased at 3hr and 5hr after Dex administration. However, in the GRLKO mice, there was no significant response in terms of ketogenesis following Dex treatment (Figure 3-3-3A). We also evaluated the gene expression of ketogenesis-related genes and perilipin genes. The genes involved in the ketogenesis pathway did not show significant changes with Dex treatment or in the presence of GR liver deficiency (Figure 3-3-3B).

Furthermore, most of the GR targets, including G6Pc, Pck1, Igfbp1, Scara1, and Dusp1, exhibited upregulation in response to Dex treatment but failed to respond in the GRLKO group (Figure 3-3-3C, 3-3-3D). Interestingly, the expression of perilipin genes followed a consistent trend with GRLKO mice treated with CL. Dex treatment induced the expression of Plin4 and Plin5 while inhibiting the expression of Plin2. However, in the absence of GR in the liver, the expression of Plin4 and Plin5 was significantly reduced, while Plin2 expression remained unchanged (Figure 3-3-3E). These findings prompt inquiries into the role of Plin5 in the liver and suggest a potential association between Plin5 expression and hepatic ketogenesis dependent on GR activity.

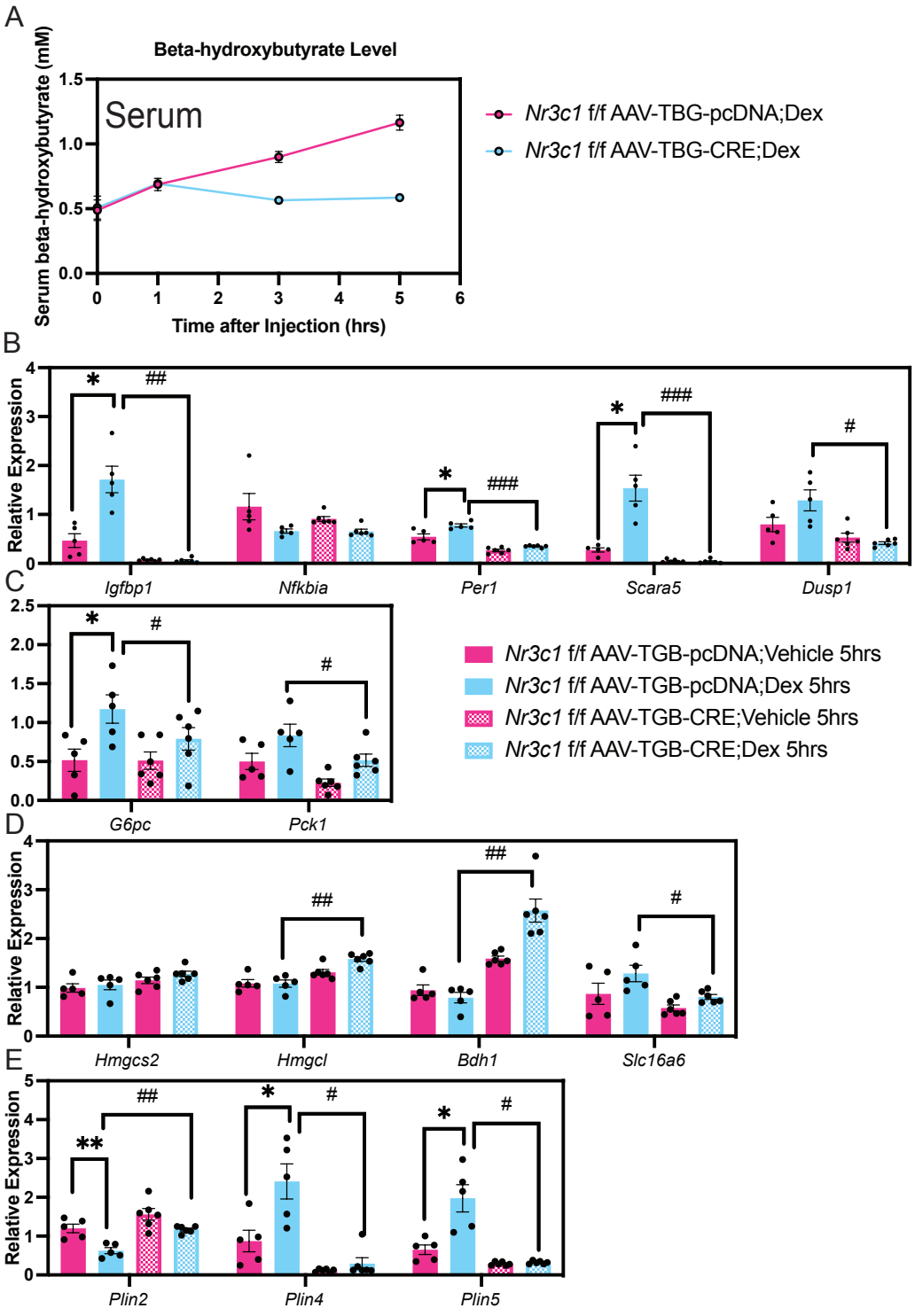

Figure 3-3-3. Hepatic GR deficiency in response to Dexamethasone treatment. A. Time course measurement for serum beta-hydroxybutyrate. B. C. GR targeted gene expression measurement after Dex 5 hours treatment. D. Ketogenesis pathway genes expression after 5 hours Dex treatment. E. Perilipin expression after hours Dex treatment. (Control groups CL vs Saline, *: p<0.05, **: p< 0.01, ***: p<0.005, ****: p<0.001; GRLKO CL vs Control CL, #: p<0.05, ##: p< 0.01, ###: p<0.005, ####: p<0.001 n=5-6).

3.5 Hepatic Plin5 deficiency hampers the initiation of ketogenesis during adipose tissue lipolysis.

From our previous time course experiment involving CL treatment on wild type B57C6 male mice, we made notable observations. Specifically, we found that CL administration induces the expression of Plin2, Plin4, and Plin5, while Plin3 (Plin1 has no expression in hepatocytes) remained unaffected. The induction of Plin2 occurred early, reaching its peak at 3 hours and declining thereafter. On the other hand, both Plin4 and Plin5 exhibited consistent expression levels from 1 to 12 hours (Figure 3-4A). To investigate the role of Plin5 in the liver, we employed CRISPR SaCas9 targeting Plin5 using three different guide RNAs (sgRNAs) to generate liver-specific Plin5-mutated mice (PLIN5LKO). The HLF promoter was used to ensure that SaCas9 was expressed exclusively in the liver. The SaCas9 and Plin5sgRNA were delivered using AAV2/8, which was injected into B57C6 male mice one week prior to the experiment (Figure 3-4B). The liver-specific knockout was confirmed by western blot analysis (Figure 3-4C). To begin, we administered Dex to both the PLIN5LKO (hepatic Plin5-deficient) and control group mice. Interestingly, we observed that the PLIN5LKO mice displayed a diminished response in ketogenesis compared to the control group following Dex treatment (Figure 3-4D). Similarly, when subjected to CL treatment to induce adipose tissue lipolysis, the PLIN5LKO mice exhibited impaired ketogenesis compared to the control group (Figure 3-4E).

Additionally, we conducted substrate metabolism analysis by isolating liver mitochondria and performing a seahorse assay using pyruvate and palmitoyl-carnitine as substrates. Interestingly, we observed an increased capacity for pyruvate oxidation in PLIN5LKO mice, while palmitoyl-carnitine oxidation remained unaffected (Figure 3-4F). We also investigated the expression of pyruvate metabolic genes and discovered that Pdk4 (pyruvate dehydrogenase kinase 4, an

inhibitor of pyruvate oxidation) was downregulated in PLIN5LKO mice, whereas Mpc1/2 (Mitochondrial pyruvate carrier 1/2) were upregulated (Figure 3-4G). This finding suggests that in the absence of Plin5, the mice compensate by increasing pyruvate oxidation as a complementary metabolic pathway.

Lastly, we quantified the levels of liver triglycerides (TAG) and free fatty acids (FFA). The absence of hepatic Plin5 appeared to impede fat oxidation, resulting in increased TAG accumulation in the liver during acute adipose tissue lipolysis. However, we did not observe significant accumulation of FFAs (Figure 3-4H). These alterations were specific to the condition of adipose tissue lipolysis and did not impact the basal levels of TAG and FFA.

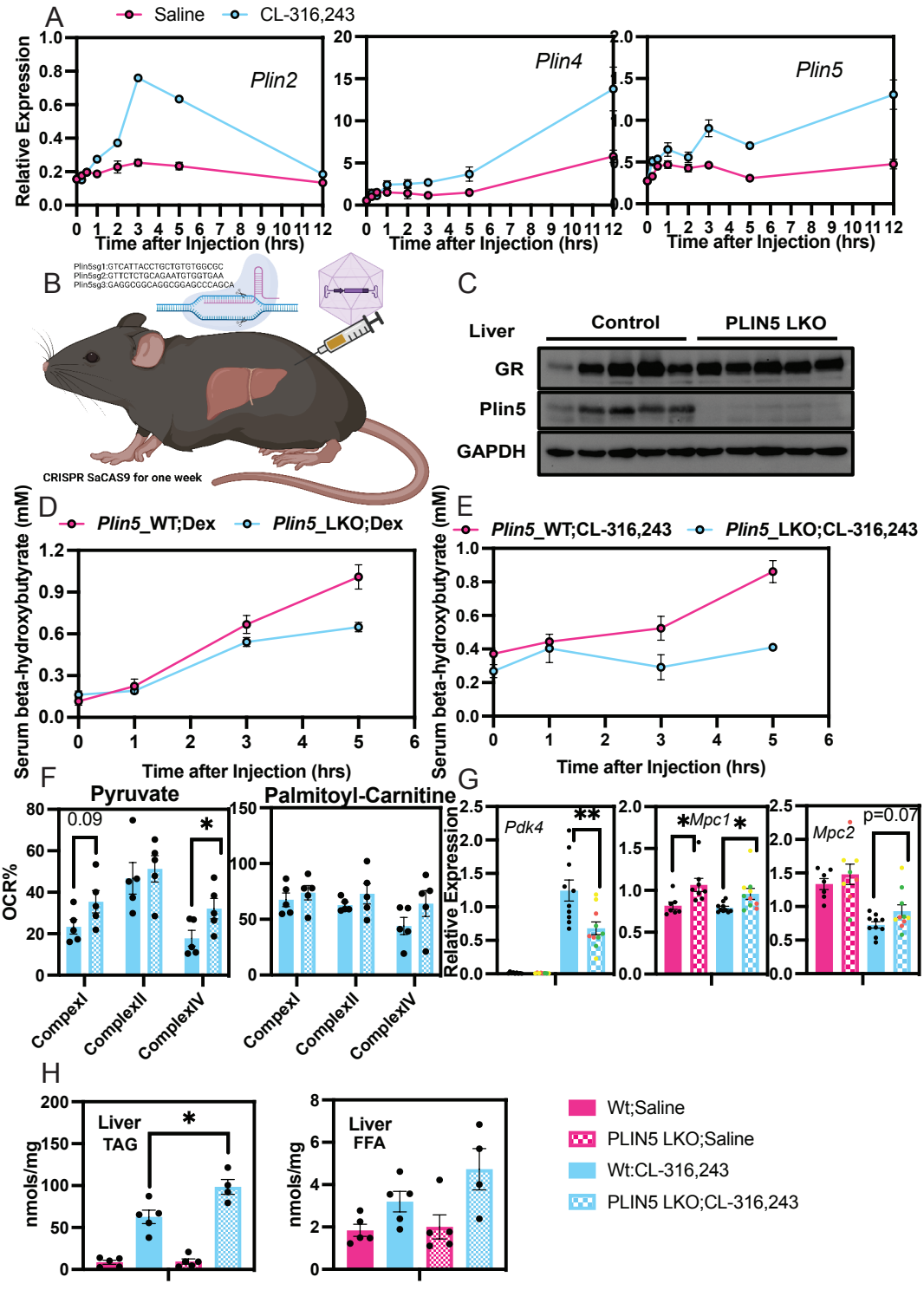

Figure 3-4. H**epatic Plin5 deficiency mice in response to adipose tissue lipolysis.** A. Time course for perilipin expression after CL administration (*Plin2, Plin4*, and *Pin5*). B. CRSPR SaCAS9 for *Plin5* liver specific knock out. C. Western blot verified the Plin5 Knock-out in the liver (n=5). D. E. Time course for beta-hydroxybutyrate measurement after Dex or CL administration (n=5). F. Isolated mitochondria from PLIN5LKO mice liver for seahorse, pyruvate or palmityl-carnitine was the substrates (*: p<0.05, **: p< 0.01, ***: p<0.005, ****: p<0.001,

n=5). G. Gene expression related to pyruvate oxidation (n=8-10). H. LC-MS quantified hepatic triglyceride and free fatty acid in the liver with PLIN5LKO and control mice. (n=4-5).

3.6 Discussion

Numerous studies conducted in both mice and humans have investigated the mechanism underlying the communication between adipose tissue and the liver (Blüher 2013) (Latteri, Sofia et al. 2023). These studies have revealed that disruptions in the interaction between these two organs can lead to disturbances in energy homeostasis (Seebacher, Zeigerer et al. 2020). Adipose tissue lipolysis serves as a fundamental process for regulating lipid remodeling in various organs, including the liver, where it exerts a significant impact (Sakers, De Siqueira et al. 2022). The prevailing understanding is that adipose tissue lipolysis provides hepatocytes with free fatty acids, which serve as a source of energy or are stored within the liver. Acute adipose tissue lipolysis occurs during periods of fasting, cold exposure, and exercise, and it can lead to an excessive accumulation of lipids in the liver. This lipid overload triggers a pronounced increase in beta-oxidation, ketogenesis, very low-density lipoprotein (VLDL) production, and triglyceride accumulation within hepatocytes. In essence, the process of acute adipose tissue lipolysis not only fails to supply lipids as substrates for the liver but also triggers regulatory signals that impact hepatic transcription. Our analysis of RNA-seq and rt-PCR data reveals substantial changes in transcription levels (see Figure 3-1-1 and 3-3-1). Acute adipose tissue lipolysis prominently enhances the expression of genes associated with carnitine metabolism, beta-oxidation, ketogenesis, lipid droplet coating, very low-density lipoprotein (VLDL) production, pyruvate metabolism, and glucose metabolism (see Figure 3-1-1 and 3-3-1).

To regulate the Gene expression, transcription factors (TFs) would be critical to initiate the transcription. The common view is that Pparα and Hnf4α could be regulated by their free fatty acids (FFAs) ligands (Fougerat, Schoiswohl et al. 2022) (Simcox, Geoghegan et al. 2017).

However, in the CL treatment RNA-seq IPA analysis, several unexpected TFs would be interested. The glucocorticoid receptor (GR) is the TFs expressed in most of organs, but how GR is activated and what the role GR plays in the liver are not clear (Akalestou, Genser and Rutter 2020) (Rahimi, Rajpal and Ismail-Beigi 2020). In this study, Our Adipose ATGL knock-out mice (AAKO, *Pnpla2*$^{F/F}$:: *Adipoq*^{CRE}) could be an appropriate control for rule out the unrelated to adipose tissue lipolysis pathways lead by CL. The AAKO group also endnotes that hepatic GR was activated only in adipose tissue lipolysis.

The activation of the hypothalamic-pituitary-adrenal (HPA) axis is a well-explored mechanism for agonist (cortisol or corticosterone) releasing driving glucocorticoid receptor (GR) activation (Xiong and Zhang 2013). However, the role of FFAs-FGF21 in driving the HPA axis has only been investigated in the context of adipose tissue lipolysis induced by fasting up to 6 hours, as studied by previous study (Liang, Zhong et al. 2014). The precise function of acute adipose tissue lipolysis remains unclear. In this study, we propose a similar model: FFAs released during acute adipose tissue lipolysis may stimulate the activation of FFAs ligands TFs (possibly Pparα), leading to the transcription of FGF21 within a short time frame (around 30 minutes after CL administration). Interestingly, FGF21 expression may persist for several hours afterward. These findings suggest the involvement of an Adipose-hypothalamic-pituitary-adrenal (AHPA) axis in driving hepatic glucocorticoid receptor (GR) regulation. We anticipate that during adipose tissue lipolysis, GR may exhibit distinct metabolic and anti-inflammatory functions. Furthermore, through epigenetic analysis, we identified significant peaks with glucocorticoid response element (GRE) motifs at upstream and intron positions. GR can serve multiple roles as a promoter, enhancer, or suppressor, thereby exerting both up regulatory and downregulatory effects on gene expression. Our gene expression analysis using GRLKO mice revealed that hepatic GR is critical

in regulating the expression of carnitine metabolism-related genes Cpt1b and Cact. Additionally, GR likely plays a vital role in ketogenesis and lipid droplet remodeling during acute adipose tissue lipolysis. Notably, ketogenesis and lipid droplet remodeling appear to be interconnected. We found that treatment with CL-316,243 or the GR agonist Dex increased ketogenesis. However, the absence of hepatic GR hindered this induction of ketogenesis (see Figure 3-3-2C and 3-3-3A). Dex treatment significantly induced the expression of Perilipin4 and Perilipin5, while reducing the expression of Perilipin2 (see Figure 3-3-3E). Conversely, the absence of GR yielded opposite results. Interestingly, after a single CL injection, Perilipin2 exhibited a different trend compared to Perilipin4 and Perilipin5 (see Figure 3-4A). Perilipin2 and Perilipin4/5 likely play distinct roles in lipid droplet coating, which in turn may directly impact ketogenesis and other metabolic processes. Notably, significant peaks in the GR-chromatin immunoprecipitation (ChIP) data were observed between GR and Perilipin4/5, along with several peaks upstream of Perilipin5 (see Figure 3-3-2F). We speculate that GR may play a crucial role in facilitating the opening of double-stranded DNA for subsequent TF binding.

We anticipate that perilipin5 is one of the downstream targets of GR involved in regulating hepatic ketogenesis and promoting this metabolic process. However, despite examining liver samples from Plin5-LKO mice using electron microscopy imaging, we did not observe any significant differences in lipid droplet contraction with mitochondria. Interestingly, there was still an accumulation of triglycerides in the liver (Figure 3-4H). Perilipin5 is known for its role in phosphorylating Atgl and interacting with Atgl-related proteins (Granneman, Moore et al. 2011) (MacPherson, Ramos et al. 2013) (Zhang, Xu et al. 2022). Therefore, we suspect that the loss of perilipin5 may hinder the function of Atgl within lipid droplets, resulting in reduced hydrolysis of hepatic triglycerides.

In conclusion, adipose tissue lipolysis plays a crucial role in regulating hepatic energy homeostasis. The involvement of the Adipose-hypothalamic-pituitary-adrenal (AHPA) axis in driving the hepatic GR-Plin5 axis appears to be an important pathway in regulating ketogenesis. Further research is required to fully explore the potential of adipose tissue lipolysis and hepatic GR study as a novel strategy for addressing conditions such as obesity, fatty liver disease, and other energy expenditure therapies. These areas hold promise for the development of innovative approaches in the field.

Chapter Four

Adipose-Liver Crosstalk Signaling Triggers Hepatic Chromatin Remodeling, Activating Elk4 to Modulate Glucose Metabolism

ATAC-seq serves as a powerful instrument for examining chromatin remodeling. As discussed in the preceding section, both chromatin accessibility and chromatin modifications are pivotal for regulating transcription. In this study, we conducted ATAC-seq analysis on liver tissue from mice treated with CL for 5 hours. This analysis unveiled several novel transcription factors that could potentially impact hepatic metabolism. Among these candidates, Elk4 emerged as a promising candidate for influencing glucose metabolism, although the precise mechanism remains elusive.

4.1 Introduction

Chromatin modification plays a crucial and intricate role in controlling transcription within eukaryotic organisms. These modifications encompass processes such as histone methylation, acetylation, demethylation, deacetylation, and adjustments in chromatin accessibility. Histones, acting as structural proteins within nucleosomes, are pivotal for packaging or releasing DNA from chromatin (Kouzarides 2007, Hu and Tee 2017). The tightening or loosening of the packed chromatin intricately influences transcription by modulating chromatin accessibility. Three primary states broadly characterize the distribution of chromatin dynamics across the genome: closed, permissive, and open chromatin. Closed chromatin regions typically exhibit minimal transcription activity. In contrast, permissive chromatin allows transcription factors to initiate sequence-specific accessibility changes, leading to the establishment of an open chromatin conformation that facilitates binding of RNA polymerase II and other transcription factors. Consequently, DNA sequences originating from permissive chromatin could potentially represent transcriptional regulators that are either activated or suppressed under specific conditions (Klemm, Shipony and Greenleaf 2019).

Various effective techniques are available for detecting chromatin accessibility, including DNAse-seq, ATAC-seq, Mnase-seq, and NOMe-seq(Buenrostro, Wu et al. 2015, Li, Schulz et al. 2019, Grandi, Modi et al. 2022). In our investigation, we employed ATAC-seq (Assay for Transposase Accessible Chromatin) to capture changes in hepatic chromatin accessibility following 5 hours of CL treatment. As a comparative measure, we also utilized the AAKO ($Pnpla2^{F/F}$:: $Adipoq^{CRE}$) mice group, previously mentioned in our prior studies.

Our study revealed a significant number of peaks located in potential promoter, enhancer, and suppressor regions induced by CL treatment. Conversely, the AAKO group exhibited an

opposing outcome, providing further confirmation of altered hepatic chromatin accessibility during adipose tissue lipolysis. Employing motif analysis, we identified numerous potential transcription factors induced by CL treatment. Among these, Elk4 emerged as a promising candidate for investigating its impact on metabolic regulation within the liver. Elk4, a component of the ETF complex, has been recognized as an oncogene regulating cell growth and cycling (Adler, Braun et al. 2012). However, limited research has explored Elk4's role in metabolism, particularly within the context of hepatic function.

Our discoveries propose a potential role for ELK4 in regulating carbohydrate metabolism, potentially through its ability to stimulate PDK4 expression, thus inhibiting pyruvate production (Pettersen, Tusubira et al. 2019). Furthermore, our observations revealed that mice lacking hepatic Elk4 exhibited increased insulin sensitivity. To fully comprehend the mechanisms responsible for this phenotype, further comprehensive research is essential.

4.2 ATAC-Seq reveals that adipose tissue lipolysis promotes hepatic chromatin accessibility.

The assay for transposase-accessible chromatin with sequencing (ATAC-Seq) is a method for determining chromatin accessibility. The advantage of ATAC-seq would be more accurate (catch narrow fragments, around 150bp per enzyme DNA binding), less noise signals, and one step assay (Li, Schulz et al. 2019).

Here, we treated control group ATGL transgene ($Pnpla2^{F/F}$) and AAKO group ATGL adipose tissue specific knock out ($Pnpla2^{F/F}::Adipoq^{CRE}$) mice with a single dose CL-316,243, and we harvested the liver samples after 5hr CL administration. Then, we take the liver sample to isolate the nuclei to prepare ATAC library. Finally, we processed the sequencing and downstream analysis (Figure 4-1-1A).

4.2.1 Quantification of ATAC-Seq result reveals the impact of adipose tissue lipolysis on regulating hepatic chromatin accessibility.

Four samples were employed in each of the four experimental groups for the ATAC-seq analysis. Principal Component Analysis (PCA) demonstrated a high level of consistency with minimal variability among the samples (Figure 4-1-1B). When considering the global ATAC signals, there were no significant differences observed between the four groups (Figure 4-1-1C). However, in terms of average signals near the Transcription Start Site (TSS) positions, the control group exhibited a higher ATAC signal in response to CL treatment, while the AAKO group with CL treatment displayed the lowest signal (Figure 4-1-1D). A heightened signal near the TSS suggests increased transcriptional activity, as exemplified by the Pdk4 gene (Figure 4-1-1E). As previously discussed, Pdk4 transcription was upregulated in the control group following CL treatment, whereas the AAKO group exhibited the opposite trend.

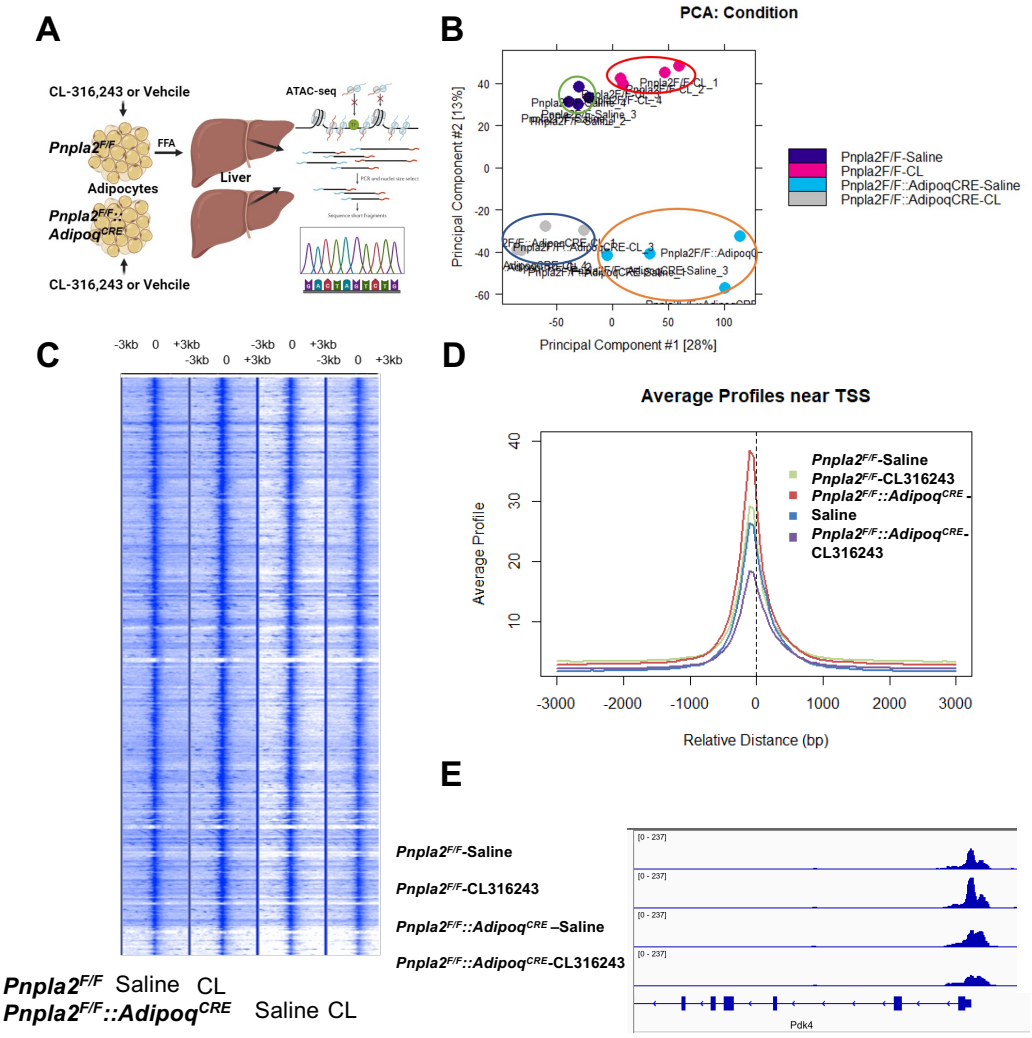

Figure 4-1-1 ATAC-Seq reveals that adipose tissue lipolysis promotes hepatic chromatin accessibility. A. Abstract of Experiment design. B. Principal Component Analysis (PCA) of the ATAC-sequencing samples. C. ATAC peaks signaling location close to the global genes Transcription Start Sit (TSS +/- 3Kbps) with four groups of samples. D. Average profiles near TSS with the ATAC peaks signaling with four groups of samples. E. ATAC peak signaling closes to PDK4 TSS on genome browser. (n=4)

4.2.2 Adipose tissue lipolysis remodels hepatic chromatin accessibility exposing new binding sites of transcription factors.

In our global genome analysis, we observed that promoters occupy only about 2.5% of the entire DNA sequence, downstream regions approximately 2.5%, and coding exons roughly 2.0%. In contrast, more than 90% of the genome comprises intronic and distal intergenic regions.

Utilizing ATAC-seq analysis, we detected approximately 40,000 to 50,000 peaks individually in the four sample groups, based on a threshold (FDR <0.05). The distribution of peaks across all four groups remained largely consistent, with intronic and distal intergenic regions remaining the predominant areas in the DNA sequence. However, with ATAC selection, the captured sequences exhibited a significantly higher percentage of promoter regions, accounting for approximately 15% of the genome (Figure 4-1-2A, 4-1-2B).

When examining the statistics for ATAC peaks in the control groups, we identified 3,679 peaks induced by CL treatment and 2,942 peaks repressed by CL (Figure 4-1-2A). Surprisingly, in the distribution of CL-induced peaks, 47.8% of the DNA sequences were located in promoter areas, while the reduced peaks did not display this distribution (Figure 4-1-2A). Similarly, in the AAKO group, we found 4,274 CL-induced peaks and 2,815 CL-repressed peaks. However, the CL-repressed peaks contained 39.2% promoter sequences (Figure 4-1-2B).

We performed motif analysis using the significantly upregulated or downregulated peaks in the control and AAKO groups through Homer motif enrichment analysis (Barta 2011). We ranked the motifs based on their representation of transcription factors by -log10Pvalue. In the CL-induced peaks, we observed significant enrichment of transcription factors such as Sp1, Nfy, Klf4, and ETS complex factors (Figure 4-1-2C). Conversely, in the CL-repressed peaks, we identified motifs associated with Irf, Yy1, Nur77, and other transcription factors (Figure 4-1-2C). Notably, in the AAKO group, the motif enrichment results exhibited an opposing trend, with YY1 as the top upregulated motif, and Sp1 and Nfy as the top downregulated motifs (Figure 4-1-2D).

A ***Pnpla2*$^{F/F}$ Groups ATAC Peaks Distribution**

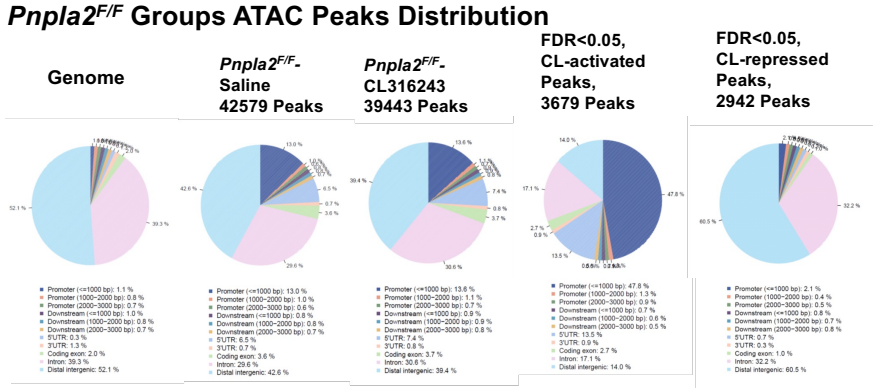

B ***Pnpla2*$^{F/F}$ *::Adipoq*^{CRE} **Groups ATAC Peaks Distribution**

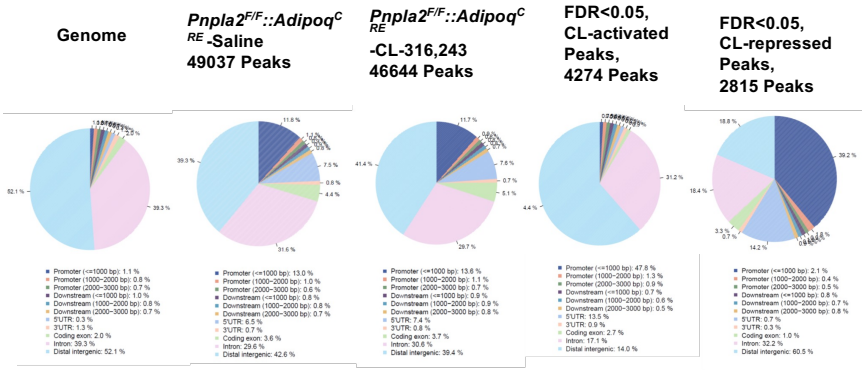

C ***Pnpla2*$^{F/F}$ ATAC Peaks Motifs Enrichment**

Upregulated Peaks

Motif	Name	P-value
	Sp1(Zf)	1e-165
	NFY(CCAAT)	1e-123
	Klf4(Zf)	1e-43
	Elk4(ETS)	1e-41
	Elk1(ETS)	1e-41
	NRF1(NRF)	1e-37
	ELF1(ETS)	1e-35
	E2F4(E2F)	1e-30
	Maz(Zf)	1e-20
	CEBP(bZIP)	1e-19
	Fli1(ETS)	1e-17
	HIF-1b(HLH)	1e-16
	E2F6(E2F)	1e-15
	c-Myc(bHLH)	1e-13
	bHLHE40(bHLH)	1e-13
	GABPA(ETS)	1e-13
	E2F1	1e-13

Downregulated Peaks

Motif	Name	P-value
	T1ISRE(IRF)	1e-665
	HRE(HSF)/HSF1	1e-106
	Nur77(NR)	1e-105
	Oct2(POU)	1e-66
	YY1(Zf)	1e-61
	CArG(MADS)	1e-44
	PRDM14(Zf)	1e-37
	STAT1(Stat)	1e-36
	Mef2a(MADS)	1e-33
	Oct4(POU)	1e-26
	ISRE(IRF)	1e-22
	Elk1(ETS)	1e-16
	Stat3(Stat)	1e-10

D ***Pnpla2*$^{F/F}$*::Adipoq*^{CRE} **ATAC Peaks Motifs Enrichment**

Upregulated Peaks

Motif	Name	P-value
	YY1(Zf)	1e-349
	HRE(HSF)/HSF1	1e-243
	Oct2(POU)	1e-178
	PRDM14(Zf)	1e-147
	Oct4(POU)	1e-77
	Rfx1(HTH)	1e-68
	Elk1(ETS)	1e-66
	Hoxc9	1e-58
	ELF5(ETS)	1e-43
	CArG(MADS)	1e-42
	Hnf1	1e-39
	MafK(bZIP)	1e-38
	Pit1+1bp	1e-30
	Pdx1	1e-23
	NeuroD1	1e-16

Downregulated Peaks

Motif	Name	P-value
	Sp1(Zf)	1e-151
	NFY(CCAAT)	1e-55
	Klf4(Zf)	1e-45
	Elk4(ETS)	1e-40
	Elk1(ETS)	1e-39
	ELF1(ETS)	1e-36
	E2F4(E2F)	1e-27
	ETS(ETS)	1e-26
	CEBP(bZIP)	1e-21
	Maz(Zf)	1e-20
	GABPA(ETS)	1e-19
	NRF1(NRF)	1e-17
	ETV1(ETS)	1e-16
	NRF(NRF)	1e-16
	Atf1(bZIP)	1e-16
	Fli1(ETS)	1e-15

Figure 4-1-2 Downstream analysis of ATAC-seq, Peaks Distribution and Homer Motif Enrichment. A. ATAC peaks distribution in control groups (*Pnpla2*$^{F/F}$). B. ATAC peaks distribution in the AAKO groups (*Pnpla2*$^{F/F}$:: *Adipoq*^{CRE}). C. Homer Motif Enrichment by CL induced or repressed peaks in control groups (*Pnpla2*$^{F/F}$). D. Homer Motif Enrichment by CL induced or repressed peaks in the AAKO groups (*Pnpla2*$^{F/F}$:: *Adipoq*^{CRE}).

4.3 Adipose tissue lipolysis elevates Elk4 binding sites in the liver, and hepatic Elk4 might be critical in glucose metabolism.

From the motif enrichment analysis, Elk4 emerged as a potential candidate transcription factor that could be activated by adipose tissue lipolysis. While Elk4 is primarily known as an oncogene that promotes cancer cell proliferation, its role in metabolic regulation remains relatively unexplored (Shin, He et al. 2013). Elk4 is a DNA-binding protein belonging to the ETS complex and is highly expressed in the liver (Adler, Braun et al. 2012). We cross-referenced the genes associated with Elk4 ATAC peaks induced by CL treatment with the lists of genes induced and repressed by CL treatment in RNA-seq. We identified 150 genes with induced Elk4 peaks and 65 genes with repressed Elk4 peaks (Figure 4-2A). Gene enrichment analysis indicated that the 150 genes with induced Elk4 peaks may be related to processes such as endoplasmic reticulum (ER) function, non-alcoholic fatty liver disease (NAFLD), thermogenesis, and autophagy (Figure 4-2A).

To investigate the role of hepatic Elk4 during adipose tissue lipolysis, we utilized HLP-CRISPR-CAS9 delivered by AAV8 to create liver-specific Elk4 knock-out mice (Figure 4-2B). However, following a 5-hour CL treatment, the Elk4 liver knock-out (LKO) mice did not exhibit significant changes in body weight or organ weight. Additionally, the gene expression levels of very-low-density lipoproteins (VLDL) or Perilipins remained unchanged. Nonetheless, we observed that hepatic Pdk4 expression was not upregulated as in the control group (Figure 4-2C). There was also an ATAC peak near the Pdk4 promoter, suggesting the possibility of direct regulation by Elk4.

Given Pdk4's function, we hypothesized that Elk4 might play a role in glucose metabolism (Pettersen, Tusubira et al. 2019). We conducted glucose tolerance tests (GTT), insulin tolerance

tests (ITT), and pyruvate tolerance tests (PTT) on Elk4 LKO mice and controls. Additionally, we subjected the mice to an 8-week high-fat diet (HFD) to assess Elk4's impact on glucose metabolism in obesity. However, we did not observe any significant phenotypic differences in obese mice, except that Elk4 LKO mice displayed increased sensitivity to insulin prior to HFD initiation (Figure 4-2D).

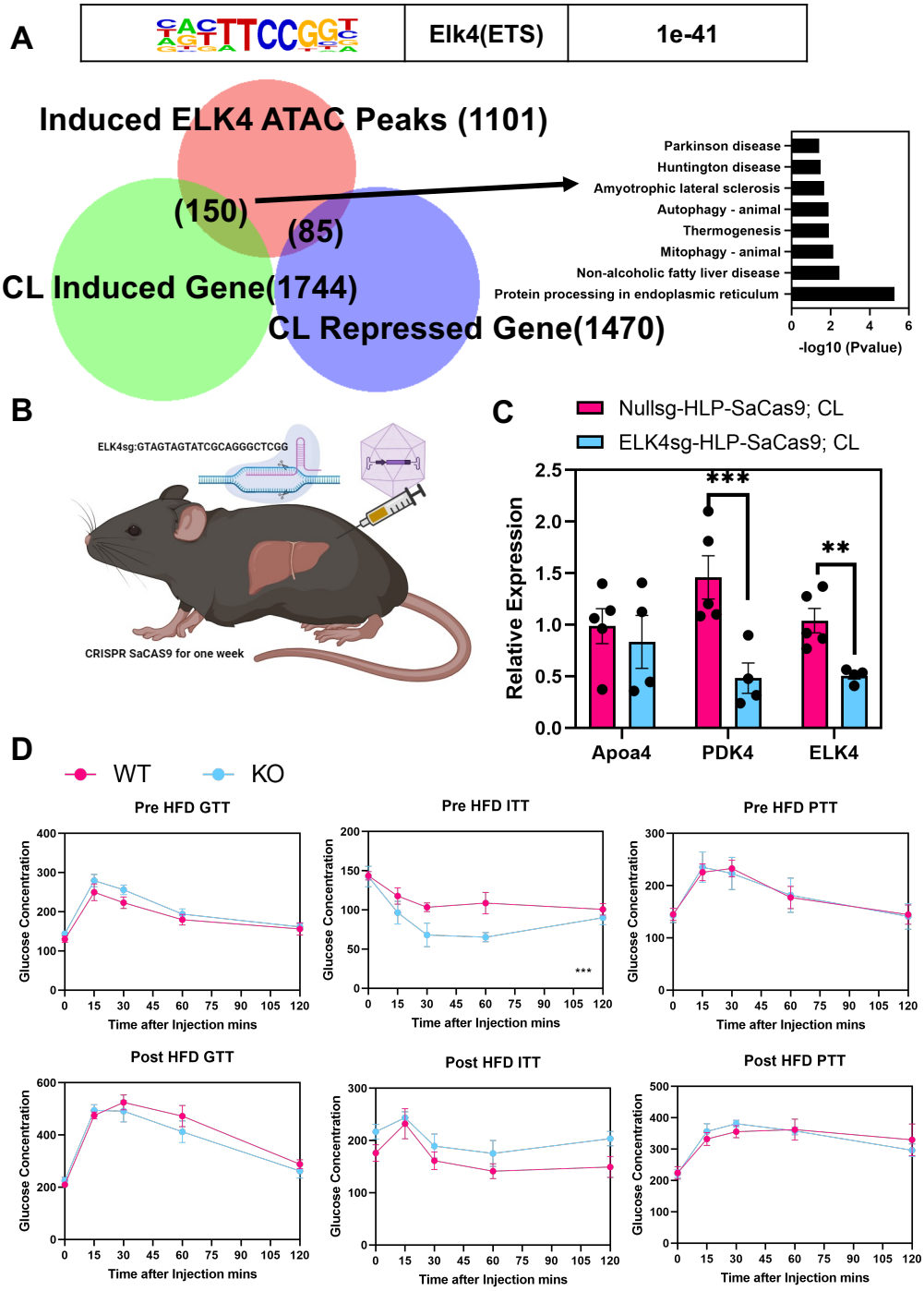

Figure 4-2 Conduct a brief assessment of the metabolic function of hepatic Elk4. A. CL induced ATAC peak list overlap with RNA-seq result, Gene pathway enrichment for the overlap between CL induced ATAC peaks and CL induced genes. B. CRISPR CAS9 model for generating liver specific Elk4 knock-out mice. C. Gene expression of ApoA4, Pdk4, and Elk4 after 5 hours CL administration. D. Pre and after 8 weeks HFD with Glucose Tolerance Test (GTT), Insulin Tolerance Test (ITT), and pyruvate Tolerance Test (PTT). (n=4-5)

4.4 Discussion

ATAC-seq proves to be a robust tool for quantifying chromatin accessibility, allowing us to investigate transcriptional regulation under various conditions. Compared to other assays, ATAC-seq effectively reduces noise signals and simplifies promoter mapping (Li, Schulz et al. 2019, Grandi, Modi et al. 2022). Nevertheless, there remain limitations in both the sequencing and bioinformatic analysis aspects, such as challenges in tracking chromatin modification dynamics, handling frozen tissue artifacts, predicting motifs, and deciphering unknown motifs.

In this study, we observed that CL distinctly altered chromatin accessibility in both the control and AAKO groups, exhibiting different trends. CL increased chromatin accessibility at promoter locations in the control group, aligning with the upregulated RNA expression following CL administration.

Motif enrichment analysis revealed that the upregulated motifs in the control group included Sp1, Nfy, Klf4, ETS complex factors, Nrf1, and Cebp, while the downregulated motifs contained Nur77, Yy1, and Irf1. Conversely, the AAKO group exhibited an opposite trend. Sp1 and Nfy are recognized as regulators initiating transcription, often functioning in concert. However, the mechanisms underlying the activation of Sp1 and Nfy during adipose tissue lipolysis remain unknown (Reed, Charos et al. 2008, Ventura, Revert et al. 2022). Yy1, a classic oncogene capable of forming "yin-yang" dimers to modulate RNA transcription, has previously been shown to inhibit Pgc1a/b expression, repressing lipid metabolism (Li, Kasim et al. 2019, Pan, Diamanti et al. 2021). Several other transcription factors in the list may also be involved in transcriptional regulation, although we will not delve into each of them in detail.

In our study, Elk4, a novel transcription factor with unclear functions and activation mechanisms, was found to directly regulate Pdk4 expression during adipose tissue lipolysis.

Given Pdk4's role in inhibiting pyruvate metabolism, hepatic Elk4 may play a role in regulating glucose metabolism. Regrettably, we did not observe any significant changes apart from increased insulin sensitivity due to hepatic Elk4 deficiency. However, this insulin sensitivity did not persist in obese mice after an 8-week high-fat diet (HFD).

Conclusions and Outlook

In our study, we provided a concise overview of the intricate interplay between adipose tissue and the liver in the regulation of adipose tissue lipolysis and its impact on hepatic lipid remodeling. Adipose tissue plays a pivotal role in maintaining energy balance within the body (Sakers, De Siqueira et al. 2022). Essentially, it functions as a reservoir for storing energy, with a particular emphasis on brown adipose tissue's involvement in non-shivering thermogenesis. The process of adipose tissue lipolysis holds a key position in remodeling the distribution of lipids across various organs, with the liver being a prominent player in this metabolic process. Consequently, an excessive accumulation of lipids in adipose tissue, commonly associated with obesity, becomes closely linked to liver-related diseases. Furthermore, adipose tissue lipolysis exerts a far-reaching influence on the overall utilization of energy resources (Sakers, De Siqueira et al. 2022). Our study, drawing from both prior research and our own findings, underscores how adipose tissue lipolysis indirectly impacts other aspects of energy metabolism, such as fatty acids, ketone, triglycerides, cholesterol, glucose, pyruvate, and fructose metabolism.

The central reaction governing adipose tissue lipolysis revolves around the hydrolysis of triglycerides. This intricate process is orchestrated by a cascade of genes, ATGL, HSL, and MGL. These three distinct lipases collectively execute the hydrolysis of the first, second, and third C-O bonds of triglycerides (Møller, Pedersen et al. 2015). Notably, ATGL assumes a dominant role in this triglyceride hydrolysis cascade, exerting its influence over the entire adipose tissue lipolysis process. Disrupting the presence of ATGL in adipose tissue leads to a complete cessation of adipose tissue lipolysis. Intriguingly, while the absence of ATGL does not prove lethal in mice and does not result in significant changes in overall body weight, it does trigger noteworthy alterations in organ weights and metabolic function. Specifically, the liver

exhibits a pronounced reduction in size and weight compared to that of a normal mouse, while adipose tissue undergoes expansion (Kim, Tang et al. 2016) (Schreiber, Diwoky et al. 2017)(Figure 2-3). Furthermore, ATGL-deficient mice display heightened sensitivity to cold, fasting, and insulin. Our research findings underscore the crucial role of ATGL in enabling acute adipose tissue lipolysis responses to various stimulation, including drug treatments and physical challenges. Beyond its role in adipose tissue, ATGL also assumes critical functions in other organs; for instance, the absence of ATGL in the heart can precipitate heart failure, emphasizing the wide-ranging impact of this gene in maintaining metabolic equilibrium (Schreiber, Diwoky et al. 2017).

Adipose tissue lipolysis is a fundamental physiological process responsible for regulating the distribution of lipids in the body. Under normal circumstances, it plays a pivotal role in maintaining lipid homeostasis. However, acute adipose tissue lipolysis necessitates the activation of adrenergic receptors, indicating that it is a more controlled and precise response to specific stimulation. This acute lipolysis can be triggered by various factors, including physiological challenges and medical interventions. Physiological challenges, such as fasting, exercise, exposure to cold temperatures, severe burn injury, and the development of cancer cachexia, can all act as stimulation for adrenergic receptor activation, thereby promoting acute adipose tissue lipolysis (Daas, Rizeq and Nasrallah 2019) (Keating, Hackett et al. 2015, Shin, Ma et al. 2017, Martin, Chung and Koehler 2020, Wilhelmi de Toledo, Grundler et al. 2020). Additionally, pharmacological approaches can be employed to stimulate adrenergic receptors artificially. For instance, compounds like CL-316,243 (artificial beta-3-AR agonist) can be administered as drugs to induce this response. The significance of acute adipose tissue lipolysis lies in its critical role in the body's stress response mechanisms. When activated, it results in a rapid release of lipids into

the circulation system. This acute lipid flux serves multiple functions, including supporting higher energy expenditure. For example, it can contribute to thermogenesis, fueling the body's ability to generate heat in response to cold exposure or exercise. Furthermore, it plays a crucial role in the context of cancer cachexia, where the body experiences significant weight loss and muscle wasting. However, it's important to note that while acute lipolysis has its benefits, it can also have adverse effects. Excessive acute lipolysis can place additional stress on the liver. This can lead to increased production of reactive oxygen species (ROS), which can potentially damage liver cells (Cichoż-Lach and Michalak 2014, Ipsen, Lykkesfeldt and Tveden-Nyborg 2018). Moreover, the excessive release of lipids into circulation can result in the accumulation of triglycerides, resembling the conditions seen in fatty liver disease (Ipsen, Lykkesfeldt and Tveden-Nyborg 2018, Geng, Faber et al. 2021). In summary, acute adipose tissue lipolysis is a finely tuned physiological response that plays a vital role in lipid metabolism and energy regulation. It is activated in response to various stimuli, both natural and artificial, and has important implications for energy expenditure, stress response, and metabolic health. However, its modulation must be carefully balanced to avoid potential detrimental effects on the liver and overall lipid homeostasis.

The secretome of adipose tissue lipolysis, our investigation primarily focused on the analysis of the lipidome and metabolites. The lipids involved in adipose tissue lipolysis is remarkably diverse, encompassing a vast array of over a thousand distinct species. Among these, palmitate acid (C:16), oleate acid (C18:1), and linoleate acid (C18:2) emerge as the dominant lipid species, constituting a substantial proportion, ranging from 70% to 90%, of the overall lipid composition (Chapter 2, Figure 2-1,2-2). In our study, we made a noteworthy discovery concerning linoleate acids, which appeared to possess a unique characteristic. These particular

lipid species exhibited a pronounced preference for triglyceride accumulation, particularly during instances of acute adipose tissue lipolysis. This underscores their pivotal role in lipid metabolism and storage dynamics within the adipose tissue microenvironment. Furthermore, our investigations also led us to identify odd-chain free fatty acids, specifically (C15:0) and (C17:0), as unique lipid entities (Figure 2-1,2-2,2-3). These intriguing lipids may also possess branch-chain attributes, adding to their distinctive biochemical profile (Green, Wallace et al. 2016, Wallace, Green et al. 2018). While our primary focus was on lipid dynamics, it's imperative to acknowledge that adipose tissue is a multifaceted source of biologically active molecules. In parallel with lipid release, this tissue also releases proteins, peptides, and hormones, contributing to its extensive role in regulating metabolic processes and physiological responses. Moreover, the activation of brown adipose tissue and other organs can have a profound impact on systemic metabolic processes. This includes heightened glucose consumption, utilization of glucose substrates, and increased amino acid turnover (MacPherson, Dragos et al. 2016, Heine, Fischer et al. 2018). These dynamic interactions underscore the intricate interplay between adipose tissue and various metabolic pathways, shedding light on the broader systemic effects of adipose tissue lipolysis and its significance in overall metabolic homeostasis (Ahmadian, Wang and Sul 2010).

In response to adipose tissue lipolysis, hepatocytes play a crucial role in orchestrating the regulation of transcription and post-transcriptional processes. In our earlier discussion, we extensively summarized the intricate mechanisms involved in transcriptional regulation. Furthermore, numerous previous studies have highlighted the pivotal roles of Ppara and Hnf4a as the dominant transcription factors responsible for sensing acute lipid flux (Brocker, Yue et al. 2017, Simcox, Geoghegan et al. 2017, Fougerat, Schoiswohl et al. 2022, Kasano-Camones, Takizawa et al. 2023). However, it is worth noting that indirect regulatory pathways remain an

expansive area for investigation. In this study, our recent findings shown the involvement of the Hypothalamic-Pituitary-Adrenal (HPA) axis in regulating the Glucocorticoid Receptor (GR), which in turn, influences ketogenesis and various other lipid metabolism processes. Notably, this regulatory cascade may be initiated by Fgf21, a factor originating from Ppara-driven transcriptional regulation (Liang, Zhong et al. 2014). Importantly, the liver itself serves as a dynamic source of signals, including hormones, proteins, and small molecules, further adding complexity to the regulatory network instigated by adipose tissue lipolysis. In summary, the interplay between hepatocytes, transcription factors, the HPA axis, and liver-derived signals in response to adipose tissue lipolysis is a multifaceted process that offers exciting avenues for exploration and a deeper understanding of lipid metabolism regulation.

Obesity, fatty liver disease, and type 2 diabetes represent pressing global health challenges. Conducting a detailed exploration of the intricate communication pathways between adipose tissue and the liver holds the key to enhancing our understanding of the regulatory mechanisms and disease development processes involved. At its core, the genesis of these health issues often stems from the excessive accumulation of lipids within various organs, thereby contributing to the development of obesity. Importantly, these lipids are not inert; they can be dynamically released from adipose tissue into the liver (Mohajan and Mohajan 2023). Simultaneously, the liver itself can generate and releasing triglycerides through de novo lipogenesis into the circulatory system. This dual lipid trafficking mechanism underscores the interconnectedness of adipose tissue and liver functions, and it plays a crucial role in the pathogenesis of both obesity and fatty liver disease (Azzu, Vacca et al. 2020, Petrescu, Vlaicu et al. 2022). Moreover, deviations from normal adipose tissue and liver function have far-reaching consequences, extending beyond obesity and fatty liver disease. These abnormalities are closely associated with

insulin sensitivity, and in more severe cases, can lead to the development of type 2 diabetes (Smith and Adams 2011). Also, the regulation of liver function through adipose tissue lipolysis is influenced by a range of physical challenges, including activities such as exercise, fasting, and exposure to cold temperatures. These physical challenges or related medicine also hold significant potential in shaping effective strategies for combating obesity. Therefore, a comprehensive exploration of the intricate interplay between adipose tissue and liver function in clinical settings becomes imperative. Such research will not only shed light on the complexities of these global health concerns but also offer valuable insights into potential therapeutic interventions and preventive strategies. In addition, adipose tissue lipolysis targets drug might be applied for obesity, fatty liver disease, and type 2 diabetes therapy.

In this study, we utilized RNA-seq, ATAC-seq, and several downstream bioinformatics data analysis tools. First of all, the sequencing tools and analytic tools are robust for exploring the potential targets gene or regulators, which regulate the cells or organs phenotypes. We believe there would be more powerful tools in the future, and the bioinformatics would also help people to understand the life science better (Grandi, Modi et al. 2022). Also, with more study on life science, it would be benefit on clinic application. In the other hand, in this study, we provided a large amount of sequencing data from the liver after CL administration. These data could also be helpful for further study on adipose tissue lipolysis regulating liver metabolism.

In this study, we used RNA-seq, ATAC-seq, and several of downstream bioinformatics data analysis tools. Our primary objective is that sequencing tools and analytic tools are robust for exploring the potential targets gene or regulators. These elements might play a pivotal role in the phenotypic traits of cells and organs. It is essential to note that the field of bioinformatics is continually evolving, and we expect the emergence of even more potent tools in the future. This

ongoing progress in bioinformatics promises to enhance our understanding of the intricacies of life sciences, allowing us to unravel the mysteries of biological systems with increasing precision. Moreover, as our knowledge deepens through further studies in the realm of life sciences, it also might be applied in clinical settings, ultimately benefitting healthcare practices. In the context of our current study, we have made available a substantial repository of sequencing data acquired from the liver following CL administration. These datasets hold significant potential, not only for our own research but also for future investigations into the regulation of liver metabolism and adipose tissue lipolysis.

Limitation of the Study

In our study, we analyzed the composition of adipose tissue lipolysis lipidome and hepatic lipidome. However, even we used the same breeding, and started all experiments at 9 am PST, the various mouse culture and breeding condition and the different time zone for the experiments would be big effects to make the variability compared with other experiments. Also, we only study the crosstalk between adipose tissue and liver, but the adipose tissue lipolysis would affect the other organs, like heart, muscle, brain, and bones.

In addition, the mice model ATGL adipose tissue specific knock out ($Pnpla2^{F/F}::Adipoq^{CRE}$) would cause Atgl gene lacking in all adipose tissue, includes iWAT, eWAT, and BAT. As we expect that the main lipids source might WAT (Shin, Ma et al. 2017), but there is no an appropriate WAT specific knock-out system without BAT knock-out. We are not sure what the BAT ATGL function in adipose tissue lipolysis system.

The AHPA-axis and GR-Plin5 axis model provide an explanation for a portion of the metabolic regulation that occurs between adipose tissue and the liver. However, it is important to acknowledge that other tissues or organs could also be involved in this process and may be affected by acute adipose tissue lipolysis or CL treatment. Additionally, it is worth noting that we used bulk tissue for RNA-seq analysis, which might result in the inclusion of gene expression from liver macrophages, rather than solely hepatocytes. Although our AAV liver-specific knockout specifically targeted hepatocytes, liver macrophages might still play a role in regulating lipid flux within hepatocytes (Guilliams and Scott 2022). Further investigations are needed to better understand the contributions of different cell types within the liver in the context of lipid regulation.

Methods

Animals and treatment

C57BL6J mice were acquired from the Jackson Laboratory (Bar,Harbor, ME, 000664). *Pnpla2*$^{F/F}$ (Jackson Laboratory, 024278) were crossed with *Adipoq*^{CRE} mice (Jackson Laboratory, 028020). All animals were housed in a room with controlled temperature (20-24°C), a 12 hrs light dark cycle, and free access to food and water. All mice used for experiment were male mice. For CL-316,243 treatment, the mice were treated with a single dose of 1mg/kg CL-316,243 by intraperitoneal injection. After injection, the mice were provided water but no food. Mice had free access to food prior to CL-316,243 administration.

ATGL transgene (*Pnpla2*$^{F/F}$) were acquired from the Jackson Laboratory (Bar,Harbor, ME, Catlog: 024278 and 000664). ATGL adipose tissue specific knock out (*Pnpla2*$^{F/F}$*::Adipoq*^{CRE}) were cross *Pnpla2*$^{F/F}$ with *Adipoq*^{CRE} mice (Catlog: 028020).

GR transgene (*Nr3c1*$^{F/F}$) mice were acquired from the Jackson Laboratory (Bar,Harbor, ME, Catlog: 021021). GR liver specific knock out (*Nr3c1*$^{F/F}$) mice were treated with AAV2/8 packed with TBG-Cre, control mice were treated with TBG-pcDNA (the 5x11E GCs AAV was injected one week before the experiment). All animals were housed and treated same with ATGL transgene mice.

Plin5 liver specific knock out mice were generated by B57C6 mice (Catlog: 000664) with treated with AAV2/8 packed with PLIN5sgRNA-HLP-SaCas9 (the 5x11E GCs AAV was injected one week before the experiment), control mice were treated with SCRsgRNA-HLP-SaCas9. All animals were housed and treated same with ATGL transgene mice.

CL-316,243 Administration

Administration of CL-316,243 (1mg/kg body weight; Catlog: C5976-5MG Sigma Aldrich) or a vehicle control of sterile PBS pH 7.5 was performed by intraperitoneal injection.

Tissue Culture

Pre-adipocytes were seeded at 1,000,000 cells in a 10 cm dish (preadipocytes immortalized with large T antigen) with 10 ml medium (DMEM+10%FBS+5ug/ml Insulin). At confluence cells were differentiated with DMEM+10%FBS+DMI+GW1929 cocktail (DEX 1uM, IBMX 0.5 mM, Insulin 5ug/ml, GW1929 20nM). After 2-days, media replaced with DMEM+10%FBS+5ug/ml Insulin + GW1929, and replaced with fresh DMEM+10%FBS+5ug/ml Insulin + GW1929 every 2 days until day 10.

Lipolysis Assay: adipocytes differentiated for 10 days were incubated with Krebs Ringer buffer for 1 hour, media then replaced with or without 100nM CL-316,243 or PBS and incubated for 5 hours before media was removed.

Hepa1-6 was cultured in DMEM + 10% FBS. For condition medium treatment, confluent Hepa1-6 hepatocytes were treated with ringer buffer for 1 hour. Then, the Hepa1-6 cells were treated with condition media for 5 hrs.

Hepatocyte organoids differentiation and culture were described previously(Broutier et al., 2016). Organoids were treated with condition media for 5 hrs.

Tissue RNA isolation and quantitative real-time PCR

Total RNA of mouse liver tissue was isolated using TRIzol reagent (Invitrogen, Carlsbad, CA). cDNA library was prepared by High-Capacity cDNA RT kit (Catlog: 4368814, Thermo Fisher). Gene expression quantification was performed with KAPA SYBR FAST qPCR 2x Master Mix Lightcycle (Catalog: 7959591001, Kapabiosystems) on an Applied Biosystems QuantStudio 6 Flex Real-Time PCR System.

Lipid Extraction and Lipidomic analysis

25ul serum, 2-6mg homogenized tissue or .5mL culture media used for lipidomic analysis. For homogenized tissue, 50-100 mg of tissue were collected in a 2mL homogenizer tube pre-loaded with 2.8mm ceramic beads (Omni #19-628). .75mL PBS was added to the tube and homogenized in the Omni Bead Ruptor Elite (3 cycles of 10 seconds at five m/s with a 10 second dwell time).

Homogenate containing 2-6mg of original tissue was transferred to a glass tube for extraction. A modified Bligh and Dyer extraction (Hsieh et al., 2020) was carried out on all samples. Prior to biphasic extraction, a standard internal mixture consisting of 70 lipid standards across 17 subclasses was added to each sample (AB Sciex 5040156, Avanti 330827, Avanti 330830, Avanti 330828, Avanti 791642). (Note only AB Sciex 5040156 used in early experiments).

Following two successive extractions, pooled organic layers were dried down in a Thermo SpeedVac SPD300DDA using a ramp setting 4 at 35 degrees C for 45 minutes with a total run time of 90 minutes.

Lipid samples were resuspended in 1:1 methanol/dichloromethane with 10mM Ammonium Acetate and transferred to robovials (Thermo 10800107) for analysis.

Samples were analyzed on the Sciex 5500 with DMS device (Lipidyzer Platform) with an expanded targeted acquisition list consisting of 1450 lipid species across 17 subclasses (or the original acquisition list of 1100 lipids across 13 subclasses). Differential Mobility Device on Lipidyzer was tuned with EquiSPLASH LIPIDOMIX (Avanti 330731). Data analysis performed on an in-house data analysis platform comparable to the Lipidyzer Workflow Manager(Su et al.,

2021b). Instrument method including settings, tuning protocol, and MRM list available in Su et. al. Quantitative values were normalized to plasma/media volume or mg of tissue.

Metabolites Extraction and LC-MS

25ul serum, or 25uL culture media used for metabolites analysis. Add 500uL cold MeOH to each tube, vortex, wait 1 minute. Add 20uL Milli-Q water containing norvaline to each tube. Add 500L chloroform to each vial. Centrifuge samples for 6 min at 10,000 g at 4oC. The upper MeOH/H2O layer contains polar metabolites. Evaporate each sample.

Indirect Calorimetry and isotope analysis of $^{13}CO_2$

Oxygen consumption (ml/h), energy expenditure (kcal/h), and respiratory exchange ratio (RER) were monitored for individually housed WT mice using the Phenomaster metabolic cages (TSE Systems Inc., Chesterfield, MO). The climate chamber was set to 21°C, 50% humidity, with a 12:12 light-dark cycle as the home-cage environment. Data were collected at 22-minute intervals, and each cage was recorded for 2.75 min before time point collection. Mice were food-restricted during the stable isotope experiment, which was performed in the light phase. Mice were gavaged once with U-C13 palmitic acid (Catalog: CLM-409-0.5) or U-C13 linoleic acid (CLM-6855-0.25), followed by intraperitoneal injection an hour later with saline or CL-316,243. Exhaled $^{13}CO2$ for each cage was normalized to total CO2 abundance to quantify changes in systemic palmitic acid or linoleic acid utilization.

Quantification of ^{13}C-labeled fatty acids by GC-MS

Fatty acid methyl esters were extracted from liver and serum samples using mild acid methanolysis, which included a mixture of hydrochloric acid/methanol/toluene supplemented with triheptadecenoin (Nu-Chek Prep, T-404) as an internal standard. Fatty acid methyl esters were measured by gas chromatography-mass spectrometry (GC-MS) using an Agilent

7890B/5977A. Both labeled (^{13}C) and unlabeled (^{12}C) linoleic acid and palmitic acid methyl esters were quantified based on standards consisting of serial dilutions of ^{13}C-palmitate (Cambridge Isotope Laboratories, CLM-409), ^{13}C-linoleate (Cambridge Isotope Laboratories, CLM-6855), and a standard fatty acid mix containing ^{12}C-palmitate and ^{12}C-linoleate (Nu-Chek Prep, GLC-96). Incorporation of ^{13}C-labeled palmitate and linoleate in liver and serum was calculated as a ratio of the respective ^{13}C-labeled to total ^{12}C and ^{13}C-labeled fatty acid.

Analysis of lipidome from serum and Liver tissue

The lipidome data pie and bar graphs were plotted by Prism 7. The heatmap was performed by R language pheatmap (clustered by R cluster WardD.2 or Ward).

Corticosterone measurement

To allow quantification of mice serum corticosterone, a standard dilution series comprising ten known concentrations of corticosterone between 39pg/mL and 10000pg/mL was run with the biological samples using the competitive ELISA assay kit (Arbor Assay Catlog: K014-H1W). The ELISA read was measured the absorbance at 450nm.

ACTH measurement

To allow quantification of mice serum ACTH, a standard dilution series comprising ten known concentrations of ACTH between 7.81pg/mL and 500pg/mL was run with the biological samples using the competitive ELISA assay kit (Abcam Catlog: Ab263880). The ELISA read was measured the absorbance at 450nm.

β-hydroxybutyrate quantification (Ketogenesis measurement)

To allow quantification of mice serum β-hydroxybutyrate, a standard dilution series comprising six known concentrations of β-hydroxybutyrate between 2nmole/well and 10nmole/well was run with the biological samples using the β-hydroxybutyrate colorimetric

assay kit (Sigma Aldrich Catlog: MAK041). β-hydroxybutyrate was measured the absorbance at 450nm.

Triglyceride quantification

To allow quantification of mice serum and liver (tissue homogenized samples) triglyceride, a standard dilution series comprising six known concentrations of triglyceride between 2nmole/well and 10nmole/well was run with the biological samples using the triglyceride colorimetric assay kit (Sigma Aldrich Catlog: MAK266). triglyceride was measured the absorbance at 570nm.

Bioinformatics

Processing and analyses of liver bulk or cells RNA-seq data

For whole liver RNA-seq libraries, paired-end reads were mapped to the mouse genome assembly mm10 using the Bowtie2 and Samtools. Quantification of the number of mapped reads of each gene were performed using Htseq and DESeq2 (padj < 0.05) with default settings. The ingenuity pathway analysis was completed by University of Utah bioinformatics core.

CHIP seq track, TF motif activity, target sites and genes

CHIP-seq data was available for open access (*Cell Reports*, *37*(5), p.109938.), the CHIP track was performed by IGV. Motif analysis was performed by Homer motif analysis.

Supplement Figures

Supplemental Figure 2-1-1. The concentration of specific lipid species in serum after 30 minutes of CL administration.

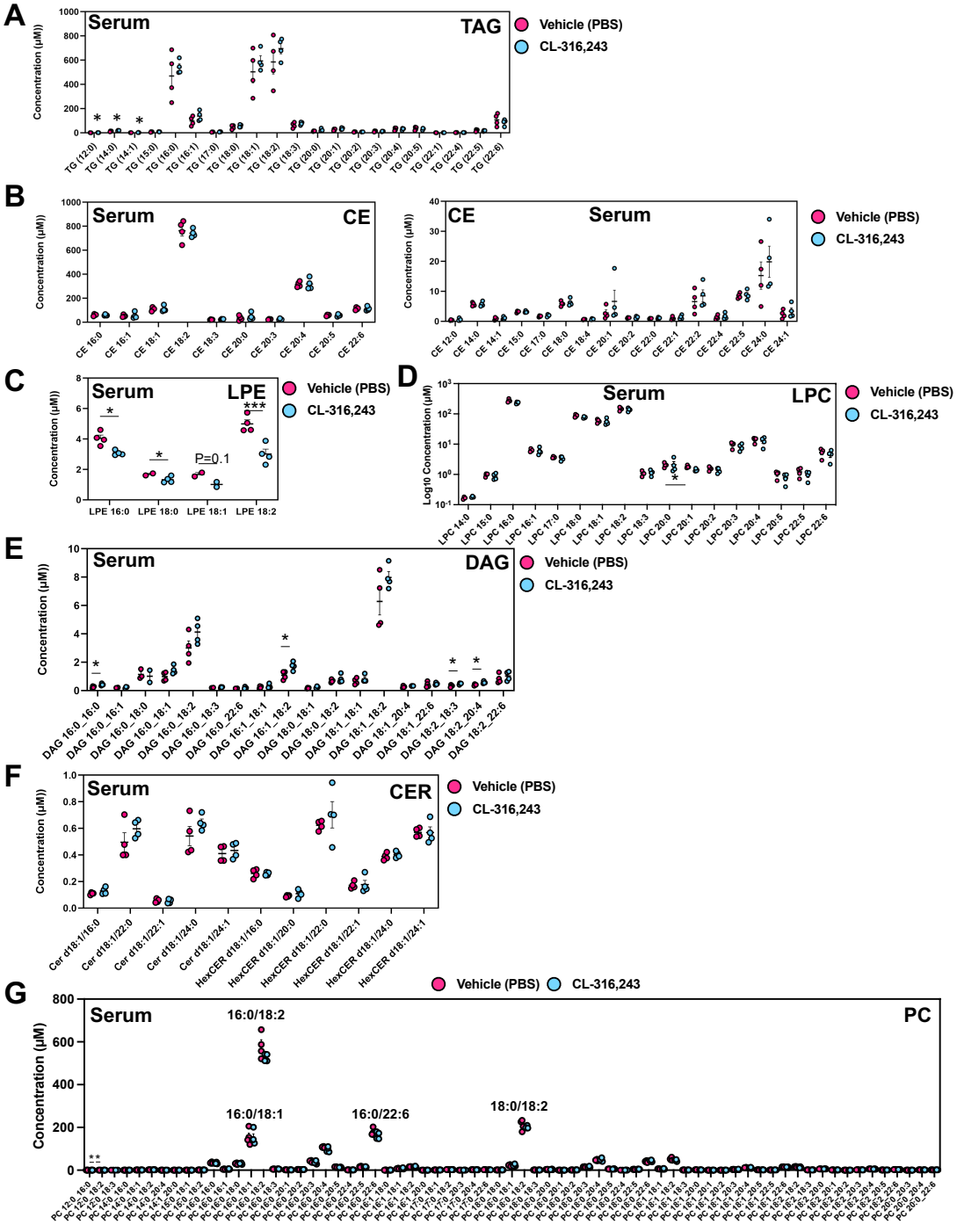

Supplement Figure 2-1-1. The concentration of specific lipid species in serum after 30 mins of CL administration.

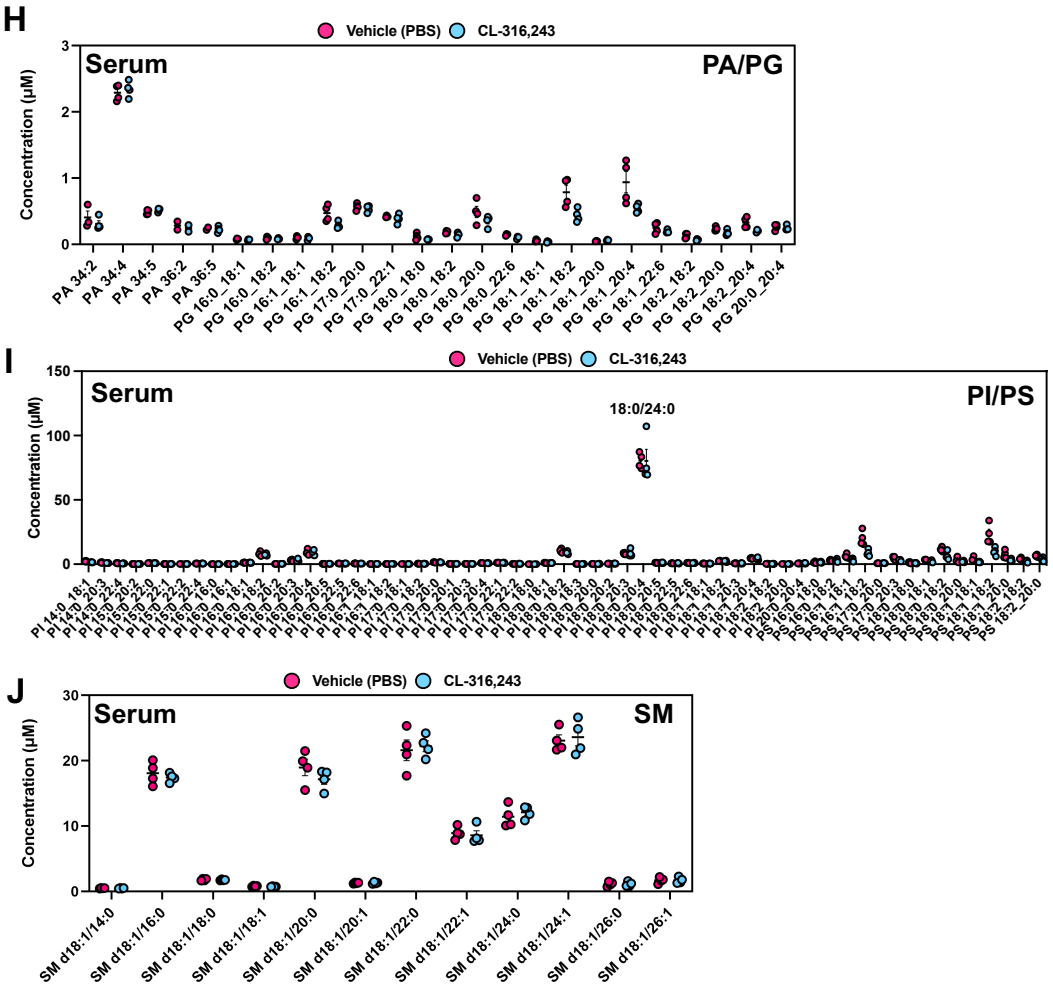

Supplement Figure 2-1-2. Serum and liver metabolites after 30 minutes of CL-316,243 administration.

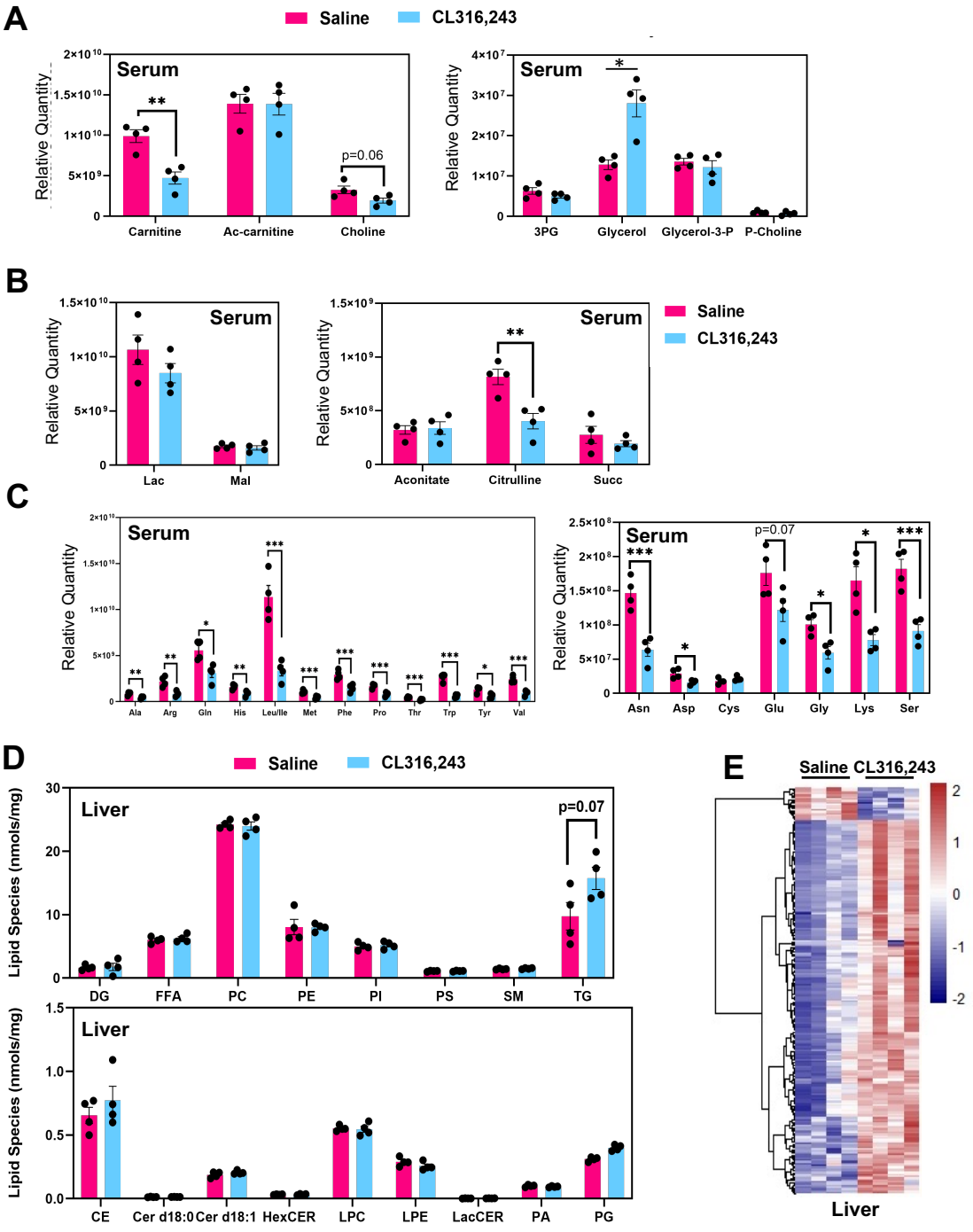

A. Serum carnitine, ac-carnitine, choline, 3-PG (3-phosphoglhycerate), glycerol, G-3-P (Glycerol-3-phosphate), and p-choline (phosphotidylcholine) 30 minutes after saline or CL-316,243 administration. B. Serum Lac (Lactose), Mal (malate), aconitate, citrulline, and succ (succinate) 30 minutes after saline or CL-316,243 administration. C. Serum amino acids after 30 minutes of saline or CL-316243 administration. D. Liver lipid classes change in the liver after 30 minutes of CL administration. E. Cluster analysis of liver lipids comparing saline and CL-316,243 administration, $p<0.05$. (n=4, *: $p<0.05$, **: $p<0.01$, ***: $p<0.005$)

Supplement Figure 2-2-1. Time Course for Serum and liver after Administration.

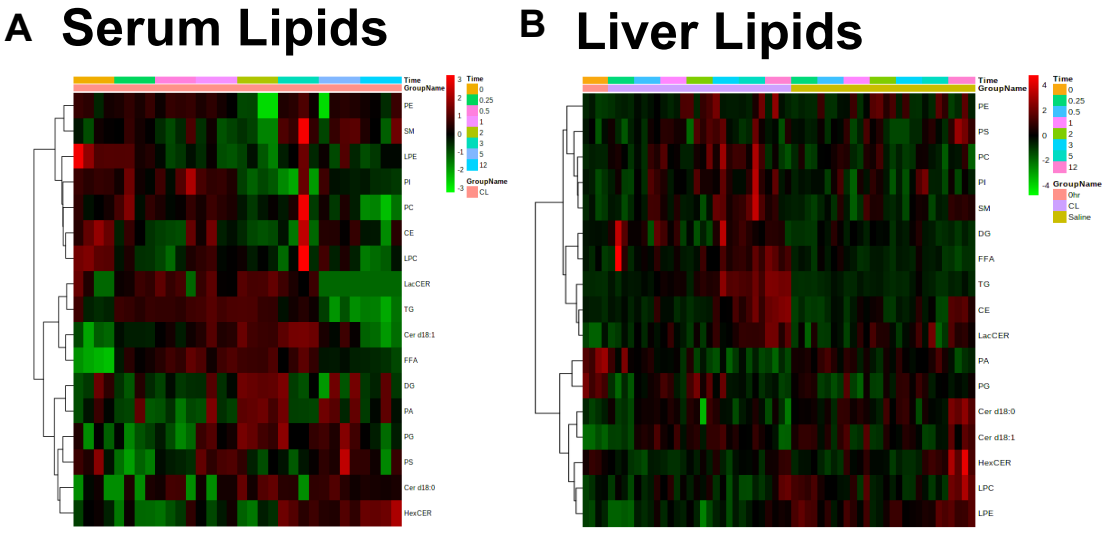

A. Heatmap cluster the serum lipid class species change after CL administration. B. Heatmap cluster the serum lipid classes change after CL administration.

Supplement Figure 2-2-2. Dietary palmitate and linoleate utilization in response to activation of lipolysis.

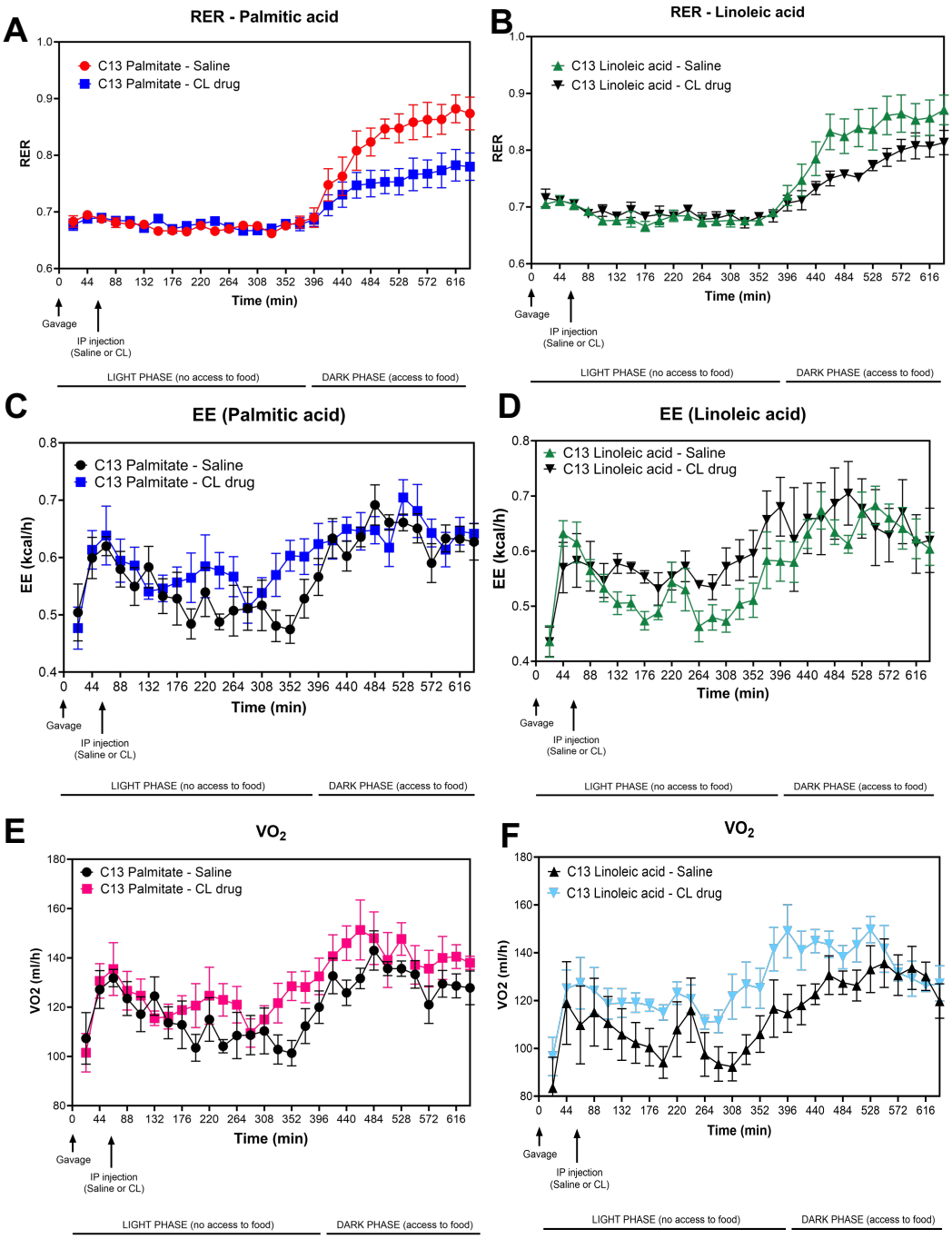

A. B. The respiratory exchange ratio (RER) CO_2 in systemic oxidation after ^{13}C fully labelled palmitic acid or linoleic acid gavage, CL was treated by IP injection after 1hr gavage. C. D. The Energy Expenditure (EE) CO_2 in systemic oxidation after ^{13}C fully labelled palmitic acid or linoleic acid gavage, CL was treated by IP injection after 1hr gavage. . E. F. VO_2 Test in systemic oxidation after ^{13}C fully labelled palmitic acid or linoleic acid gavage, CL was treated by IP injection after 1hr gavage.

Supplement Figure 2-3-1. Significantly changed lipids, Overlapped between *Pnpla2*$^{F/F}$ mice and *Pnpla2*$^{F/F}$*::Adipoq*^{CRE} mice.

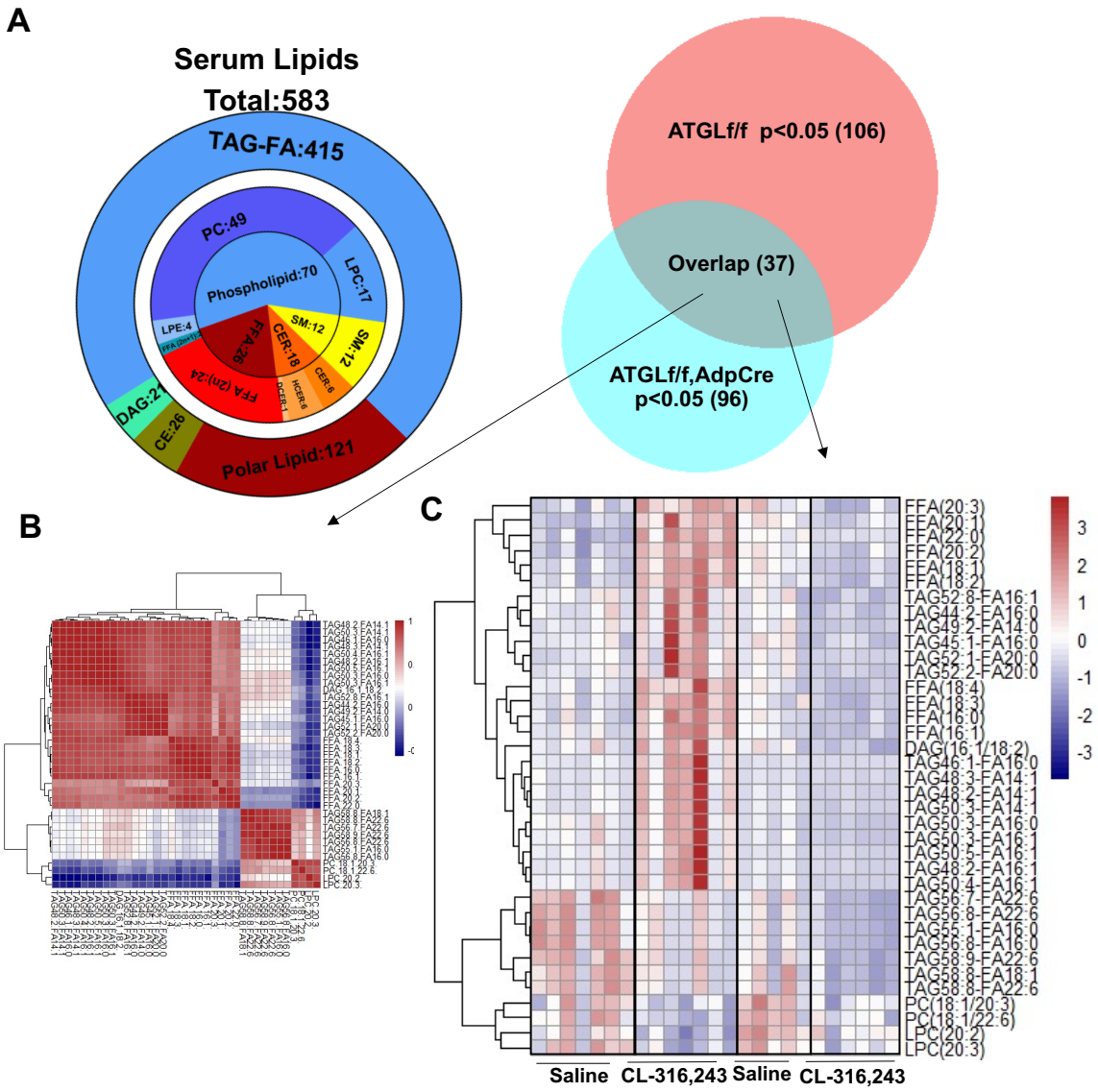

Supplement Figure 2-3-1. Significantly changed lipids, Overlapped between *Pnpla2*$^{F/F}$ mice and *Pnpla2*$^{F/F}$*::Adipoq*^{CRE} mice.

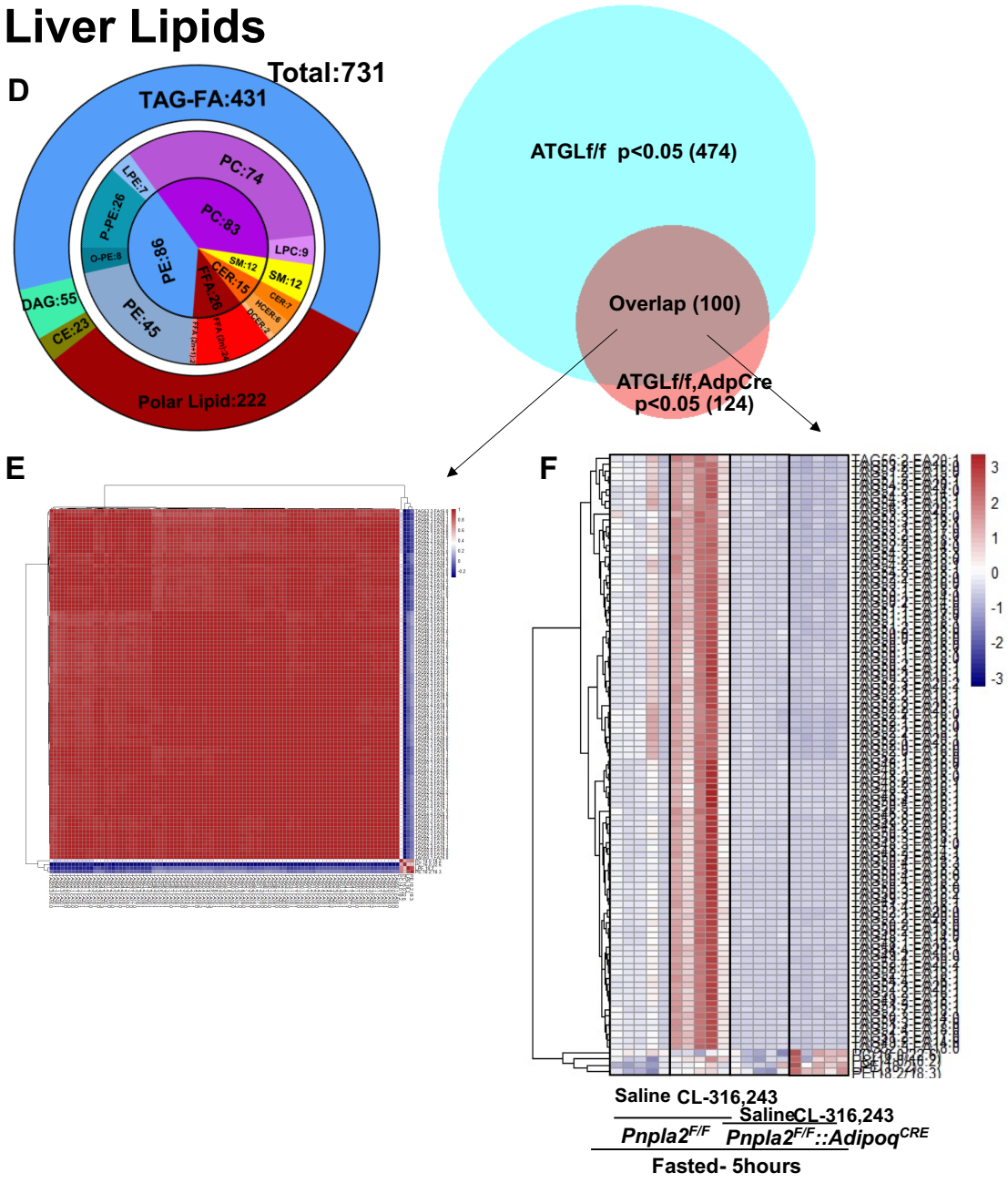

A. Pie graphic represents mice serum lipid molecular species grouped by the corresponding lipid classes**.** Totally dentified 583 lipids in serum lipids. **B.** Overlapped Significant CL-induced and CL-reduced serum lipids between between *Pnpla2*$^{F/F}$ mice and *Pnpla2*$^{F/F}$*::Adipoq*^{CRE} mice. **C.** Heatmap for all four groups in overlapped serum lipids. **D.** Pie graphic represents mice liver lipid molecular species grouped by the corresponding lipid classes**.** Totally dentified 583 lipids in serum lipids. **E.** Overlapped Significant CL-induced and CL-reduced serum lipids between *Pnpla2*$^{F/F}$ mice and *Pnpla2*$^{F/F}$*::Adipoq*^{CRE} mice. **F.** Heatmap for all four groups in overlapped hepatic lipids.

Supplement Figure 2-3-2. The concentration of specific lipid species in the serum after 5hrs CL administration by LC-MS

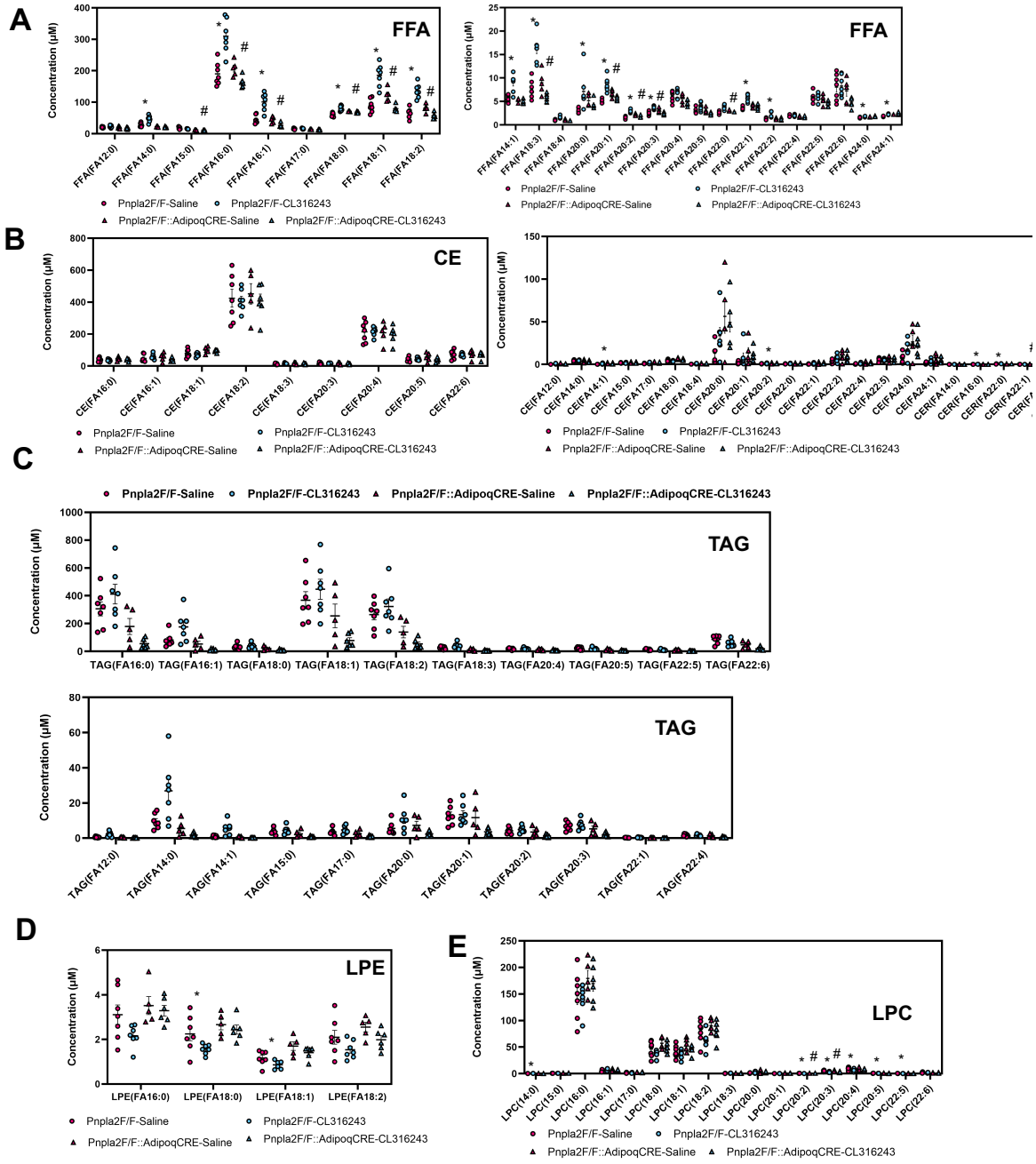

Supplement Figure 2-3-2 The concentration of specific lipid species in the serum after 5hrs CL administration by LC-MS

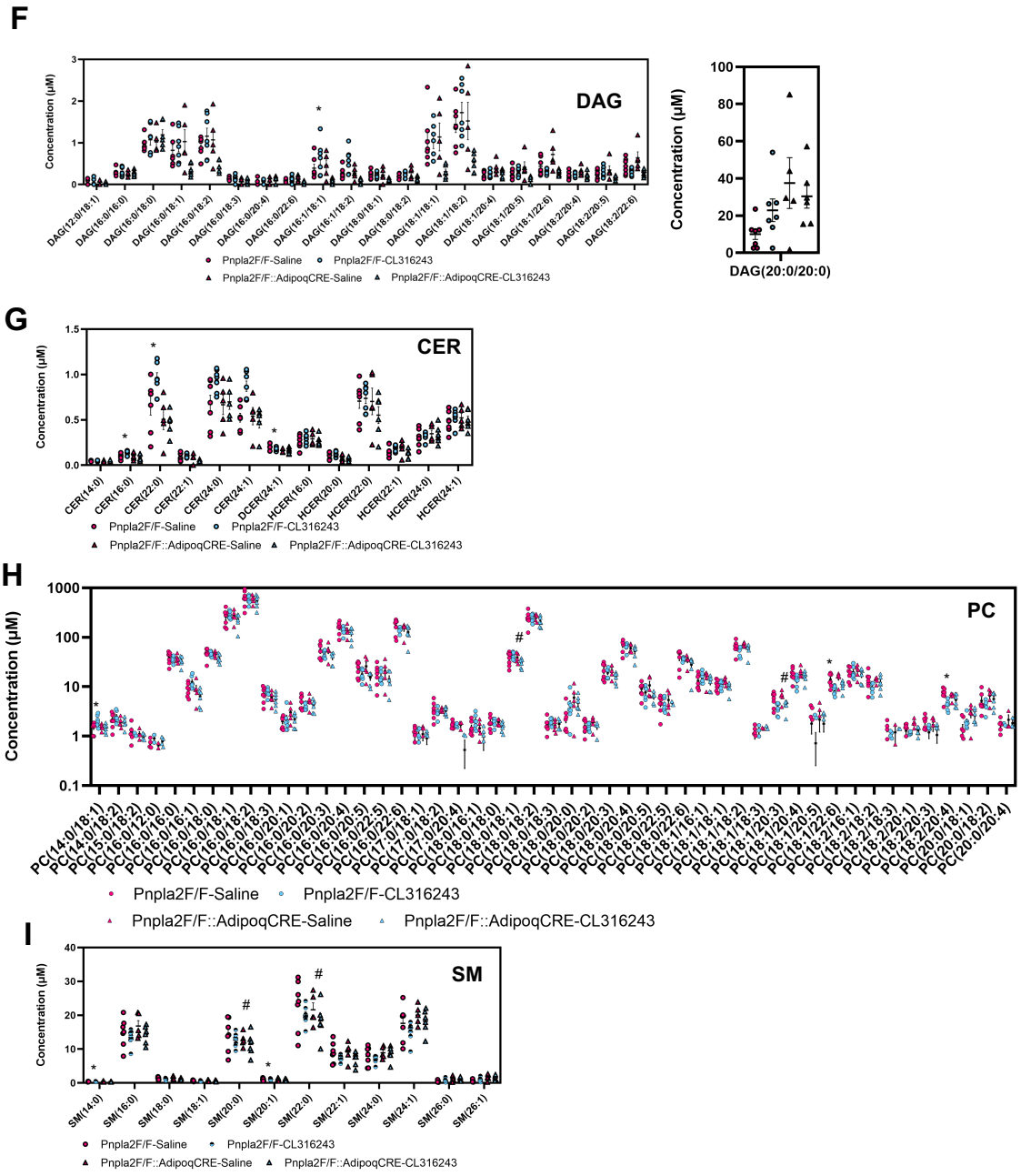

Supplement Figure 2-3-3. The concentration of specific lipid species in the liver after 5hrs CL administration by LC-MS

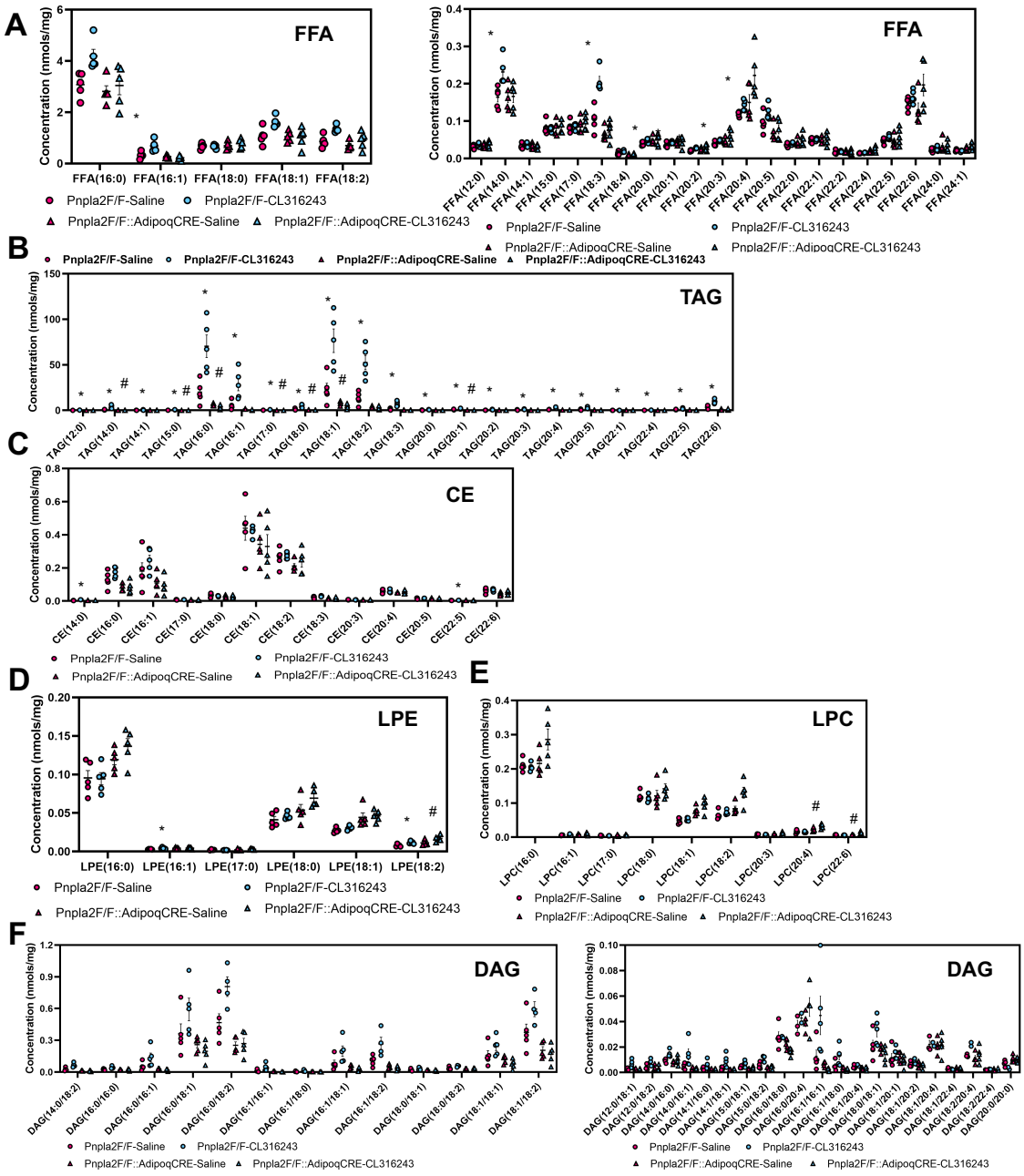

Supplement Figure 2-3-3. The concentration of specific lipid species in the liver after 5hrs CL administration by LC-MS

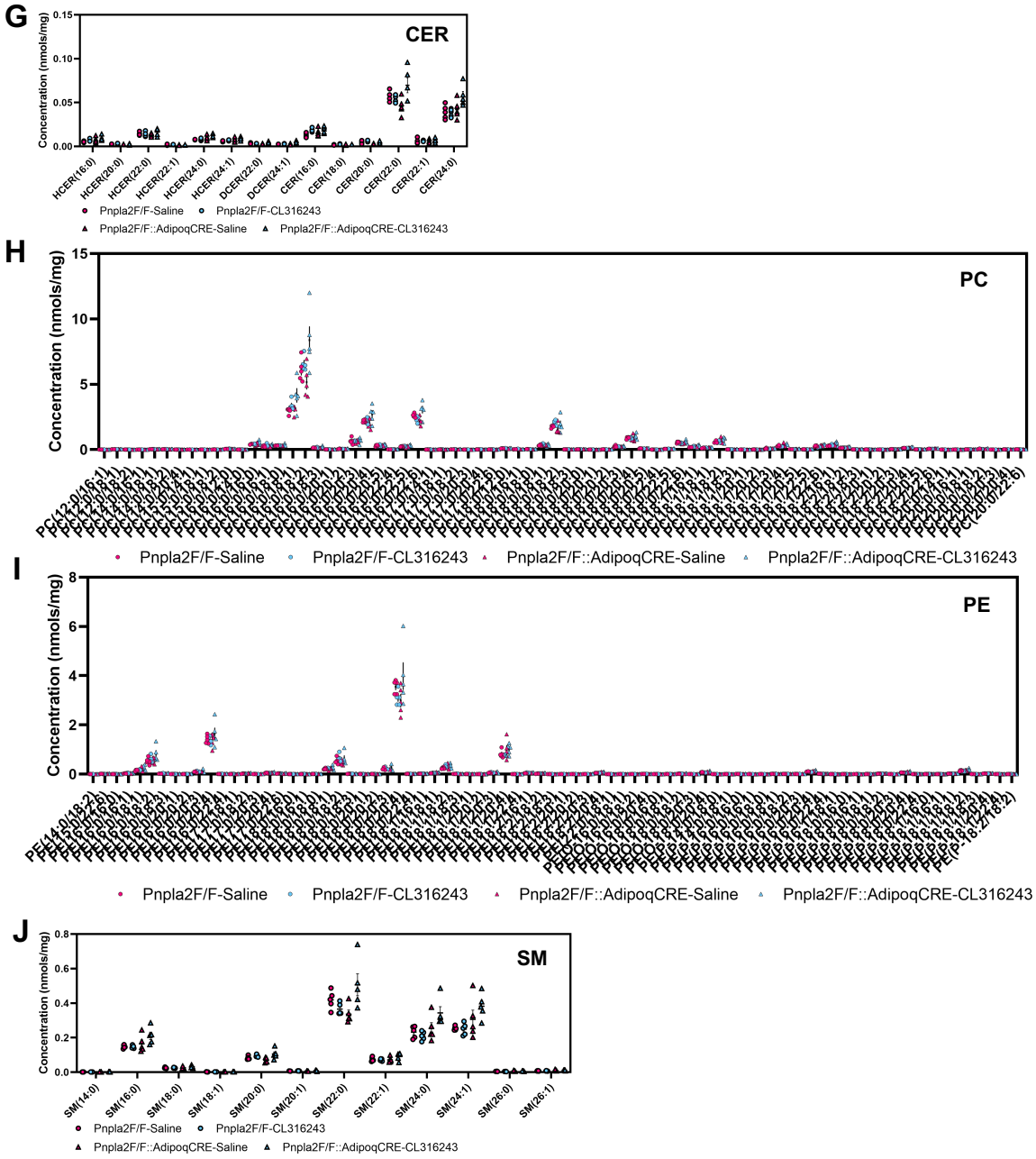

Supplement Figure 2-4-1. Untargeted lipidomic analysis and Condition medium metabolites.

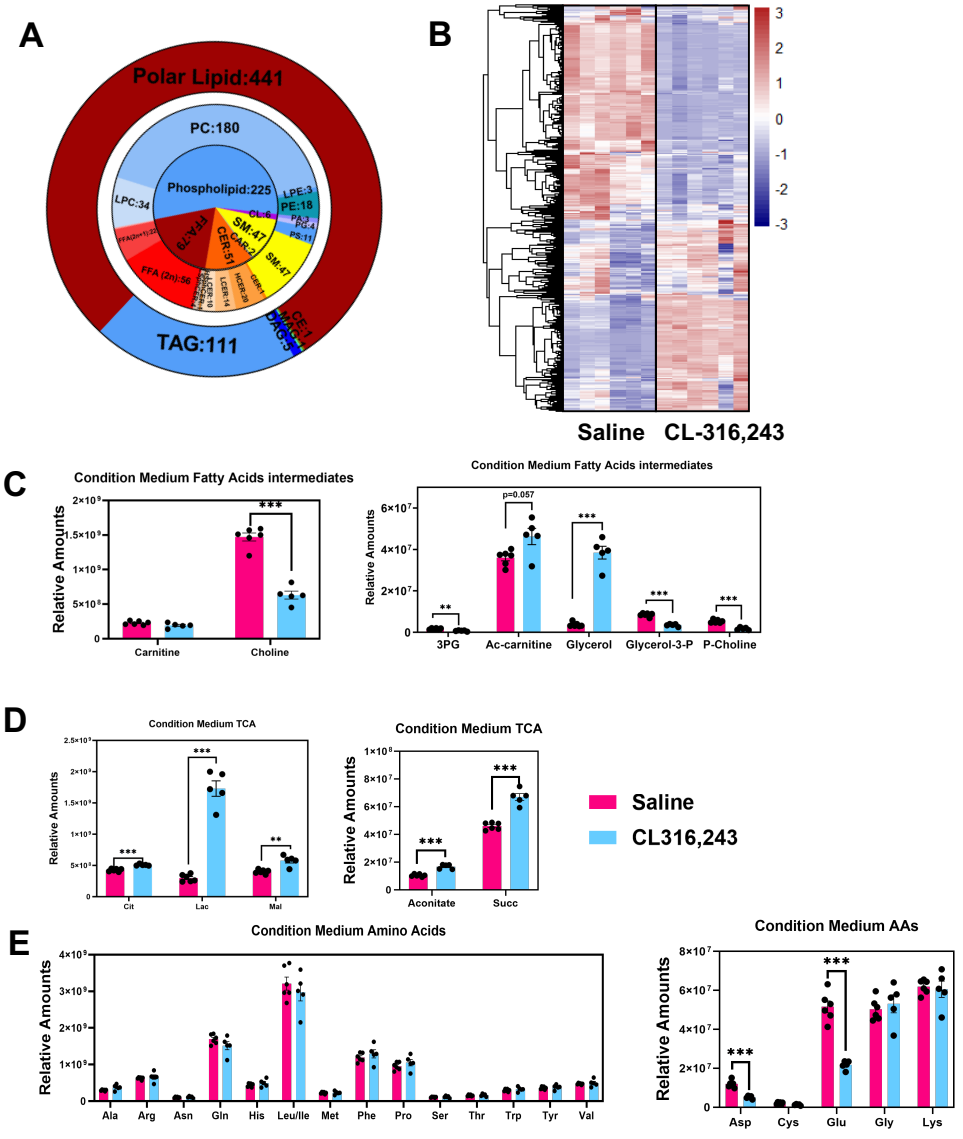

A. Pie graphic represents untargeted LC-MS analysis of mature adipose tissue secreted lipid molecular species grouped by the corresponding lipid class. B. Heatmap displays statistically significantly regulated lipid molecular species (untargeted LC-MS) between CL and vehicle treatment (n=6, $p<0.05$). C. FAs intermediates, we measured carnitine, ac-carnitine, choline, 3-PG, glycerol, G-3-P, and p-choline. The unit is relative amounts. D. glucose metabolism or TCA-related substrates, Lactose, malate, aconitate, citrulline, and succinate. E. 20 amino acids level change in condition medium after vehicle or CL treatment. (n=5-6, *: $p<0.05$, **: $p<0.01$, ***: $p<0.005$)

Supplement Figure 2-4-2. The concentration of specific lipid species in the condition medium after vehicle or CL administration by LC-MS.

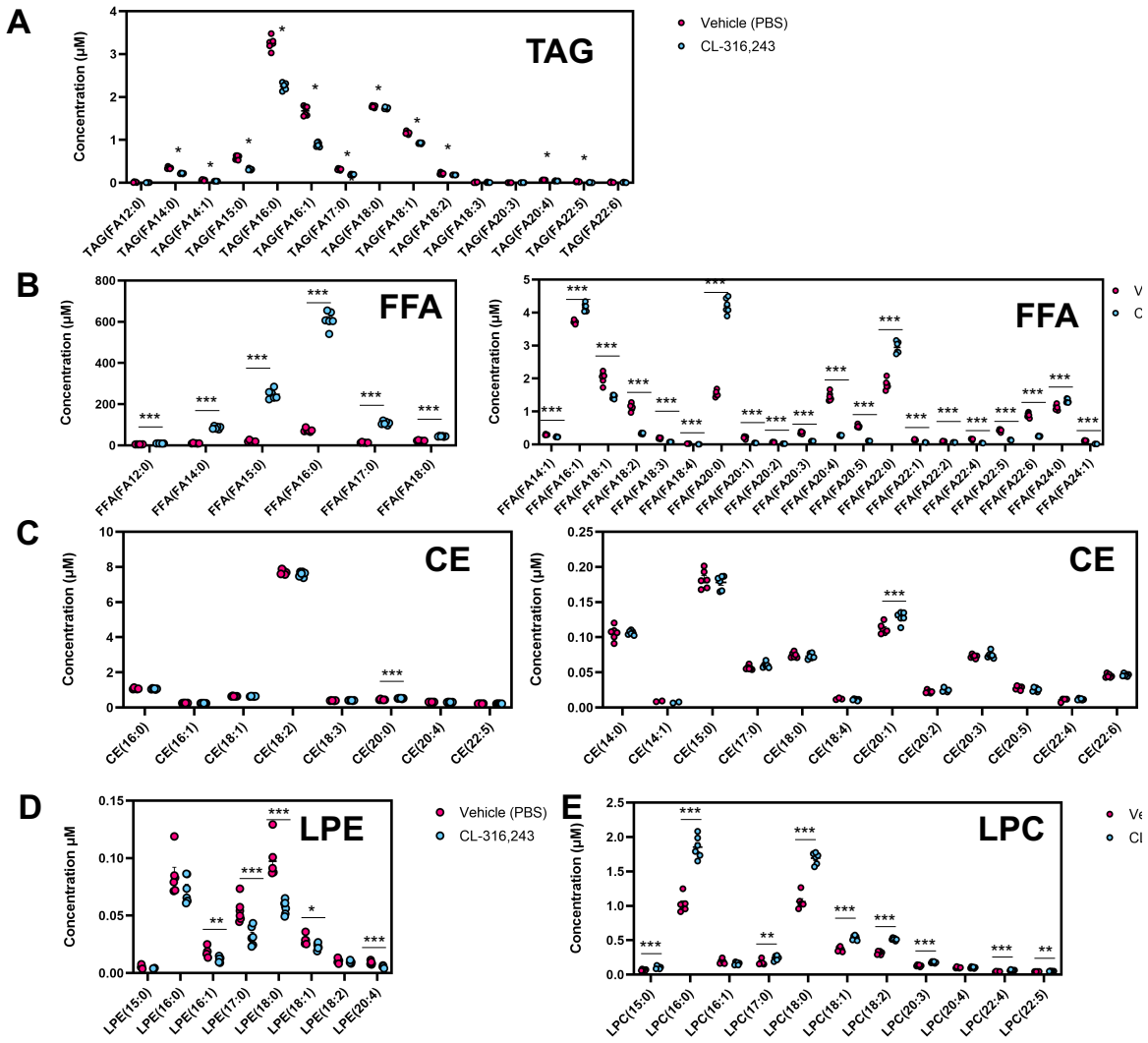

Supplement Figure 2-4-2. The concentration of specific lipid species in the condition medium after vehicle or CL administration by LC-MS.

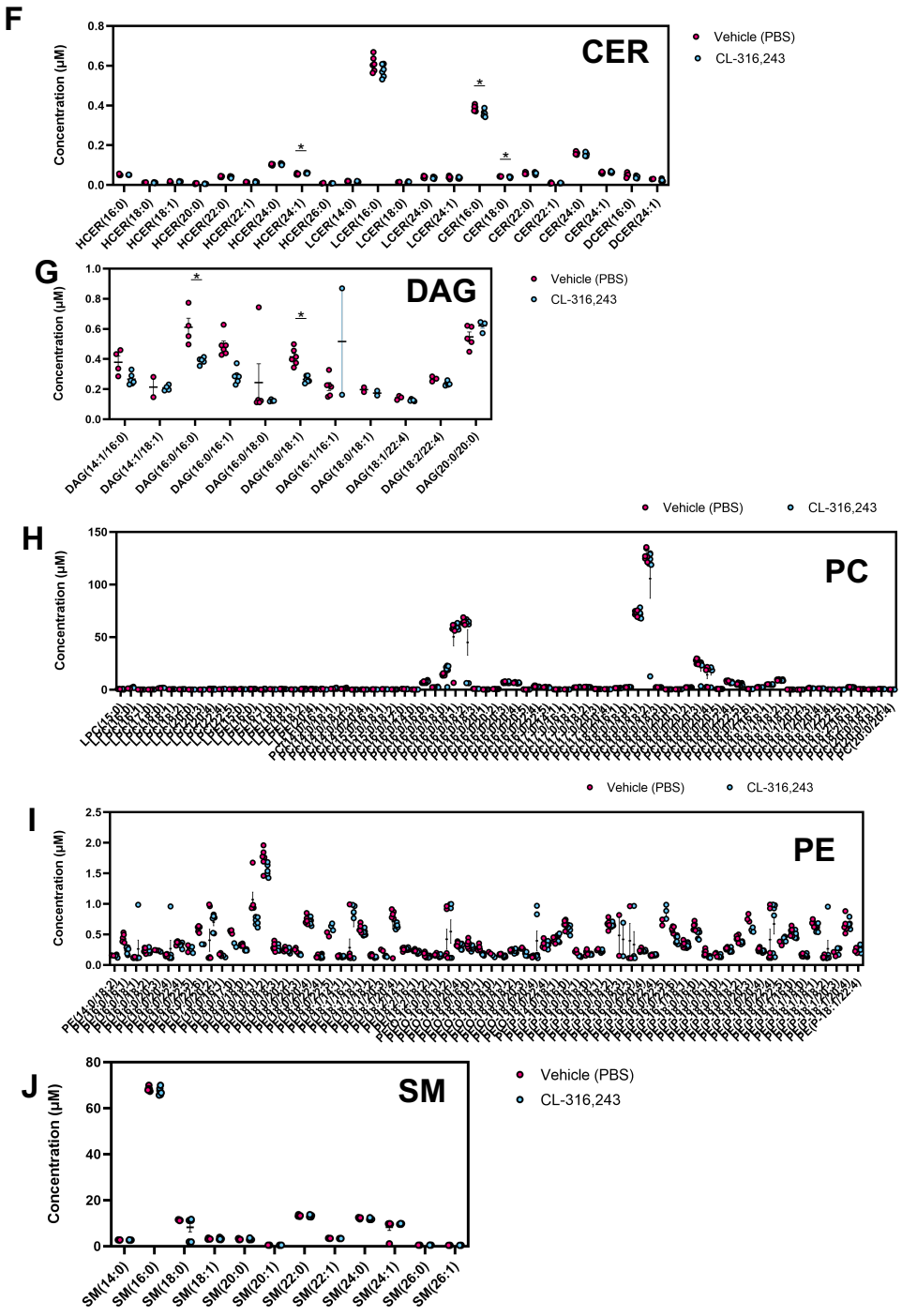

Supplement Figure 2-4-3. The concentration of specific lipid species in hepatocytes after condition medium treatment

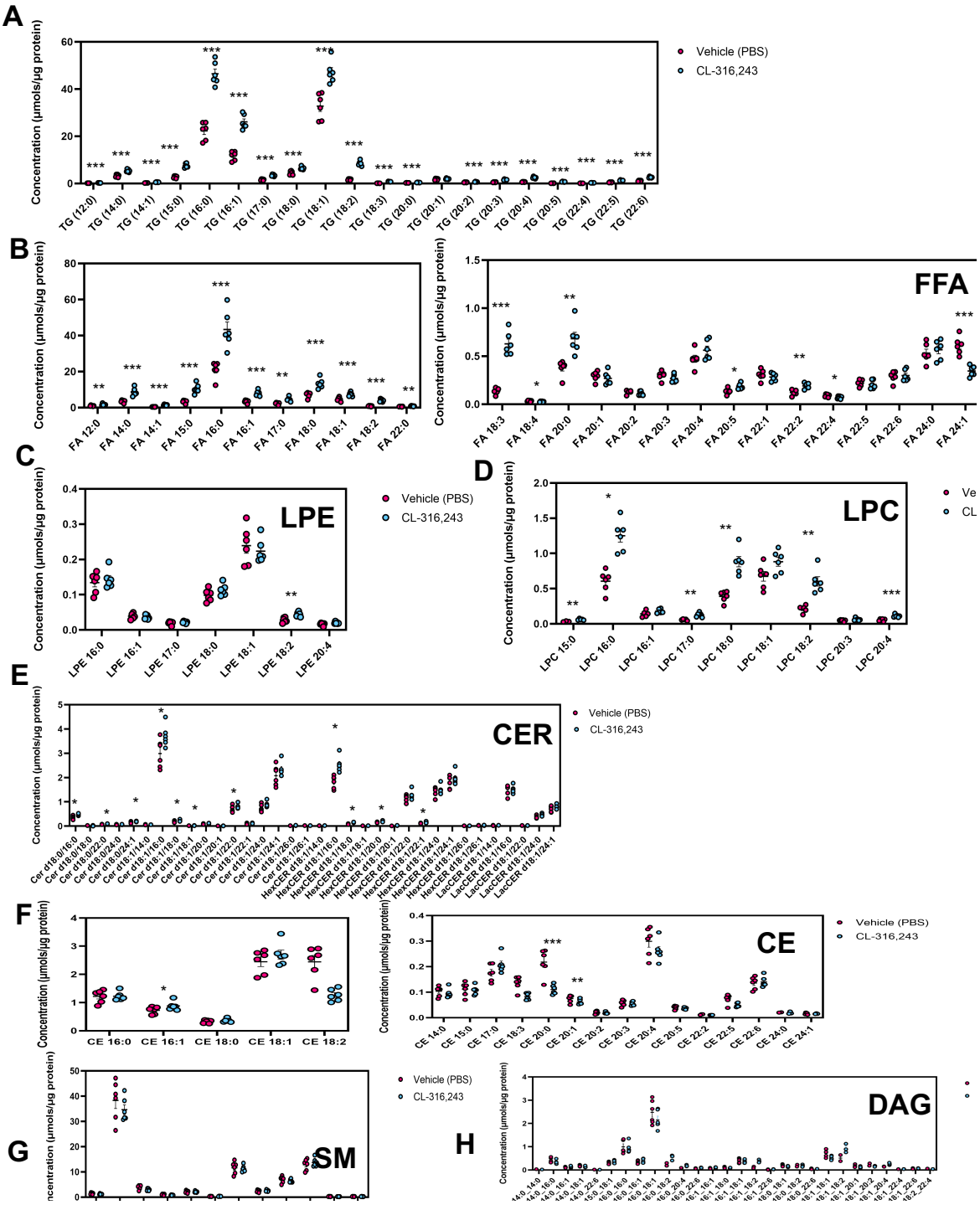

Supplement Figure 2-4-3. The concentration of specific lipid species in hepatocytes after condition medium treatment

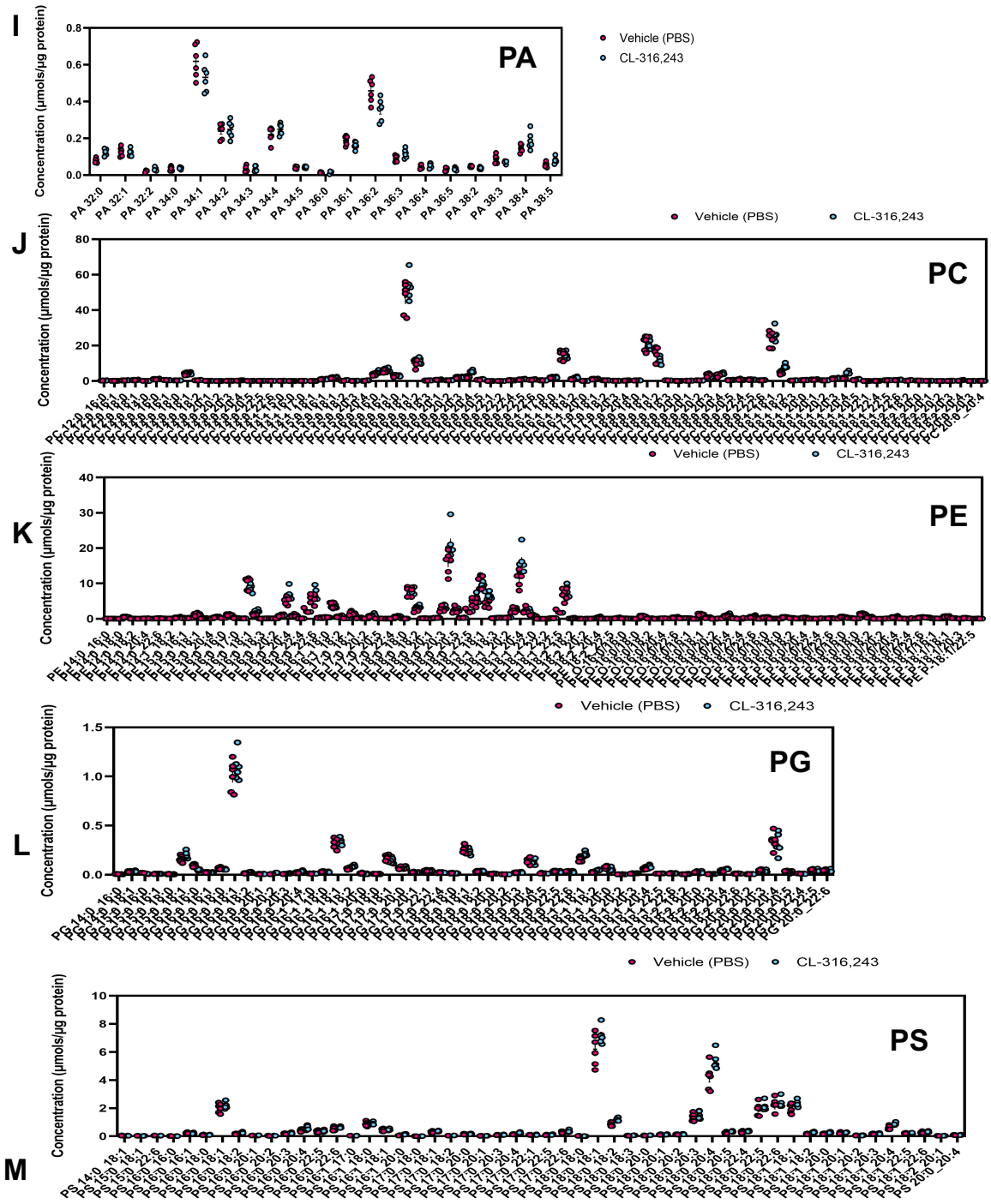

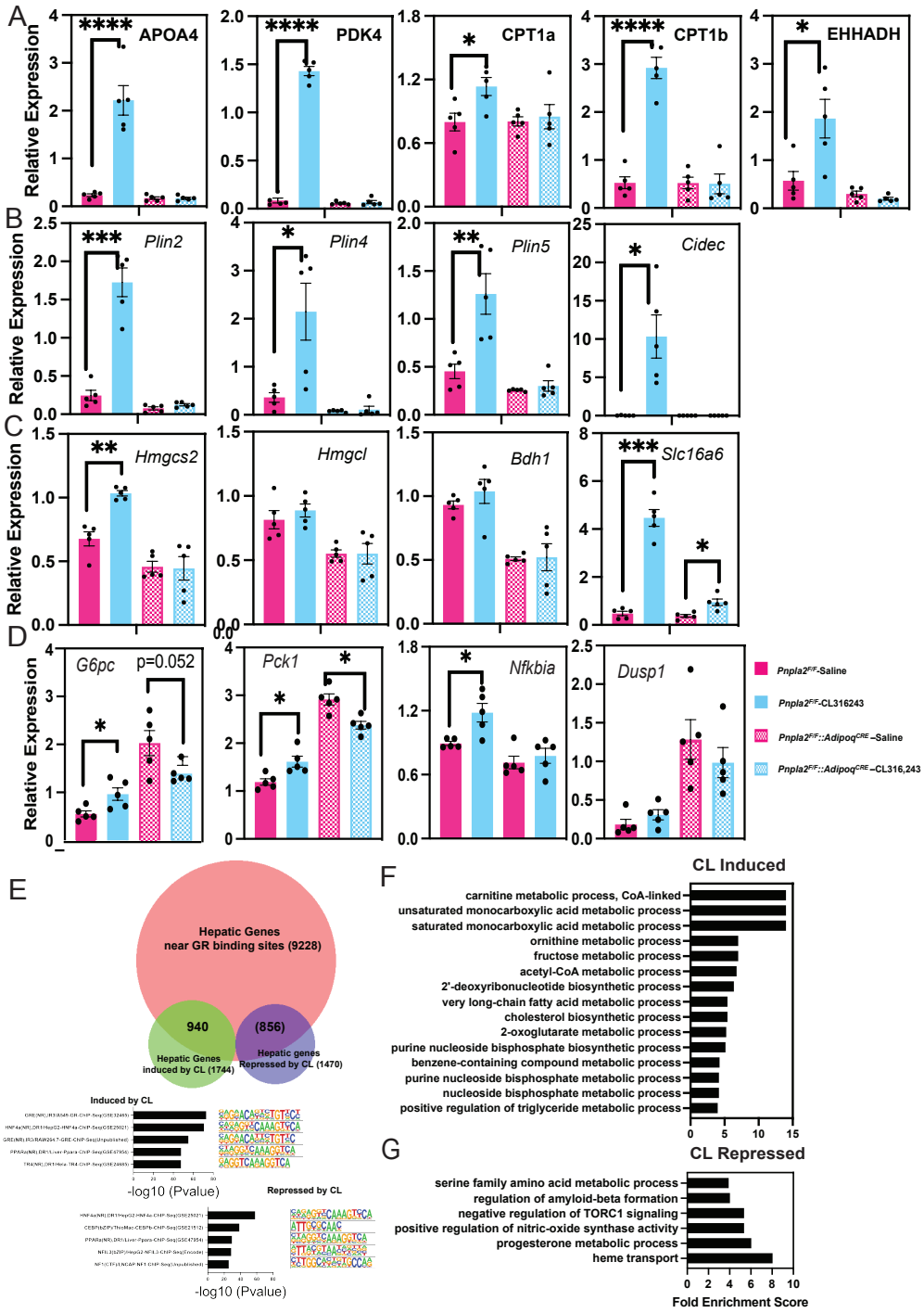

Figure S3-1-1. Transcription analysis from mice liver with selective deletion of ATGL in adipocytes. A. RT-PCR to quantify the gene expression of fatty acid oxidation gene expression and lipids markers gene expression. B. Lipid droplets coating gene expression. C. Ketogenesis pathway gene expression. D. GR targeted gene expression. (*: p<0.05, **: p< 0.01, ***: p<0.005, ****: p<0.001, n=5). E. Hepatic genes near GR binding sites overlapped with hepatic gene CL induced and induced expression, the overlapped motifs were analyzed by Homer-motif analysis. F. Gene set enrichment analysis (GSEA) for control groups by RNA-seq data. Up is CL upregulated pathways, while down represents downregulated pathways.

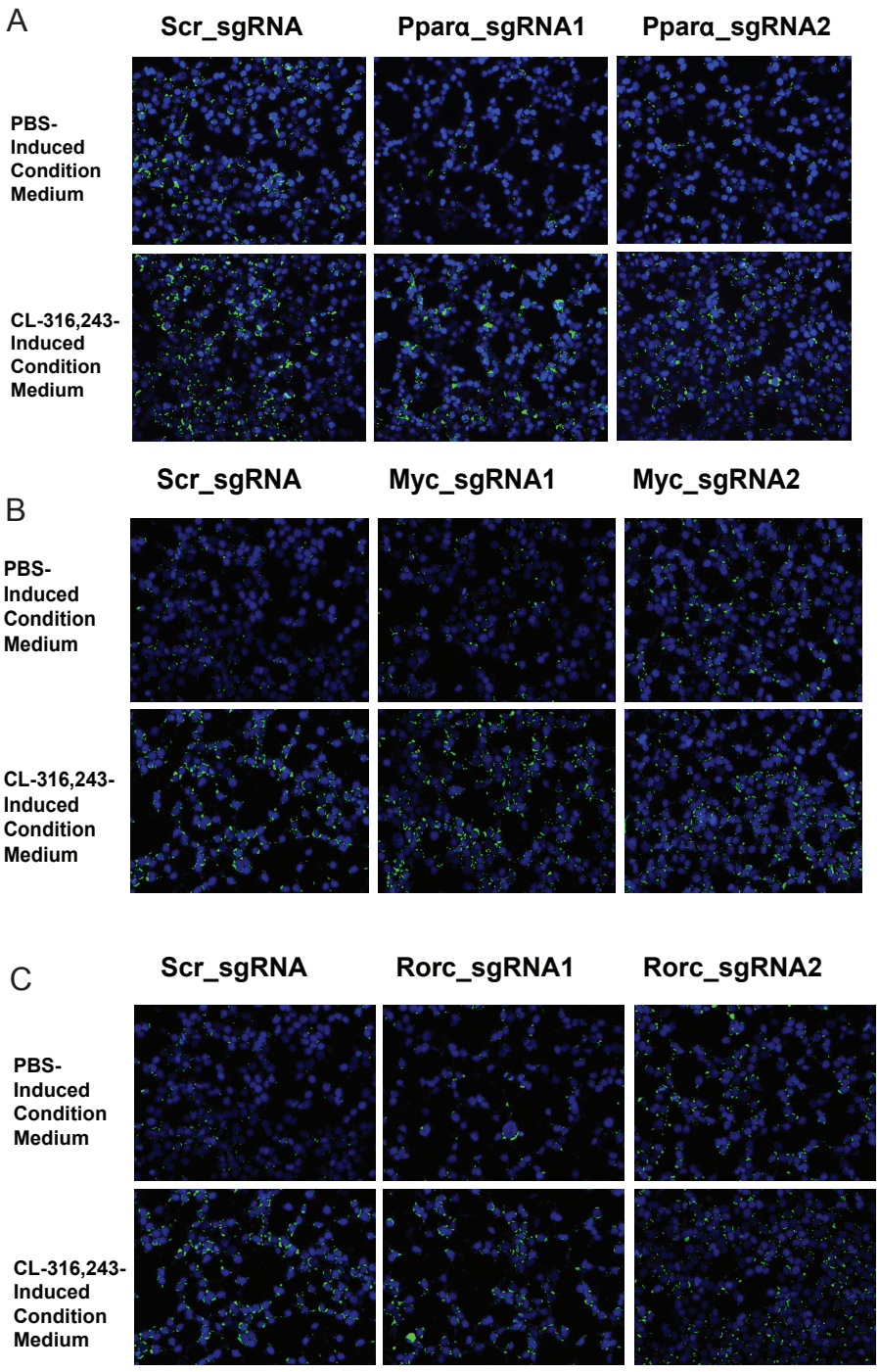

Figure S2. Imaging to assess the accumulation of lipids in different mutated hepatocyte cell lines after treating them with conditioned medium for 6 hours (Green: BPDIPY, Blue: DAPI, n=3). (*Ppara, myc*, and *Rorc*)

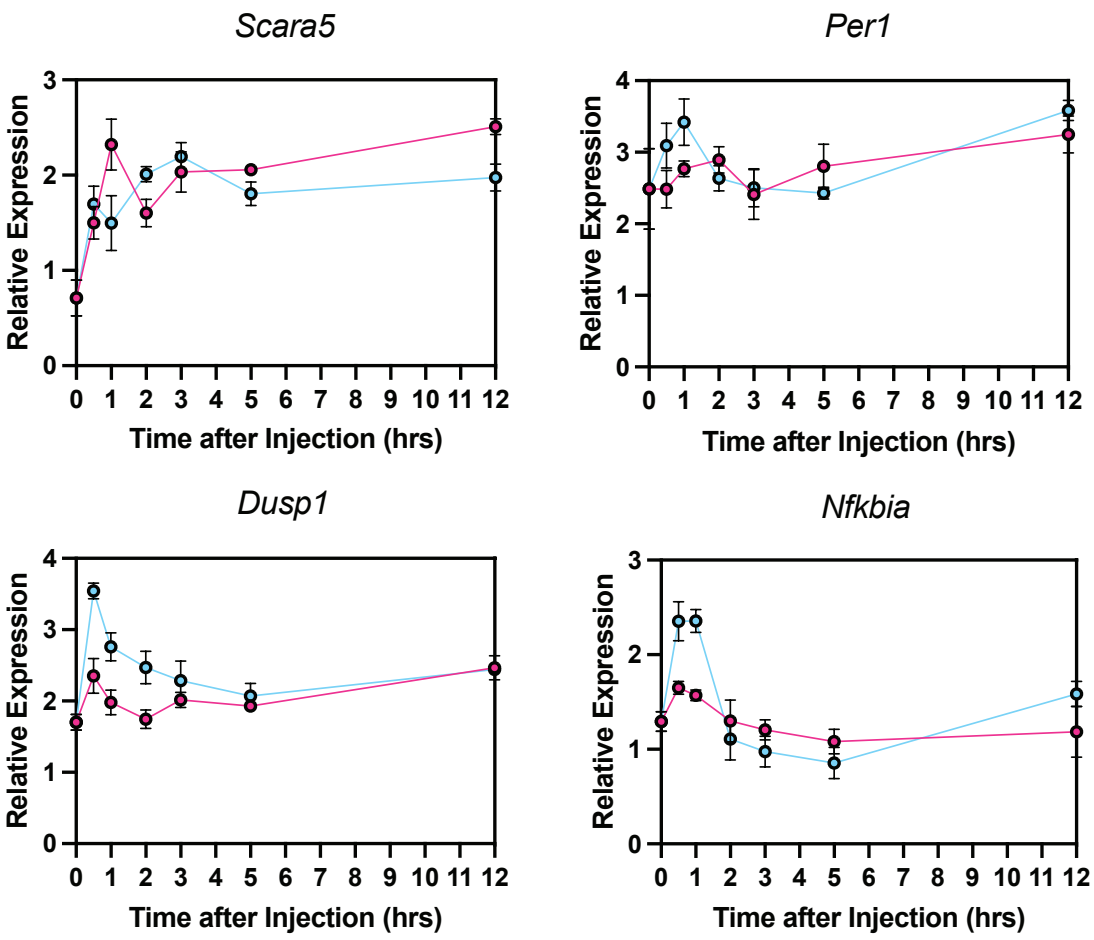

Figure S3-2. Time course for additional GR targeted genes (n=4).

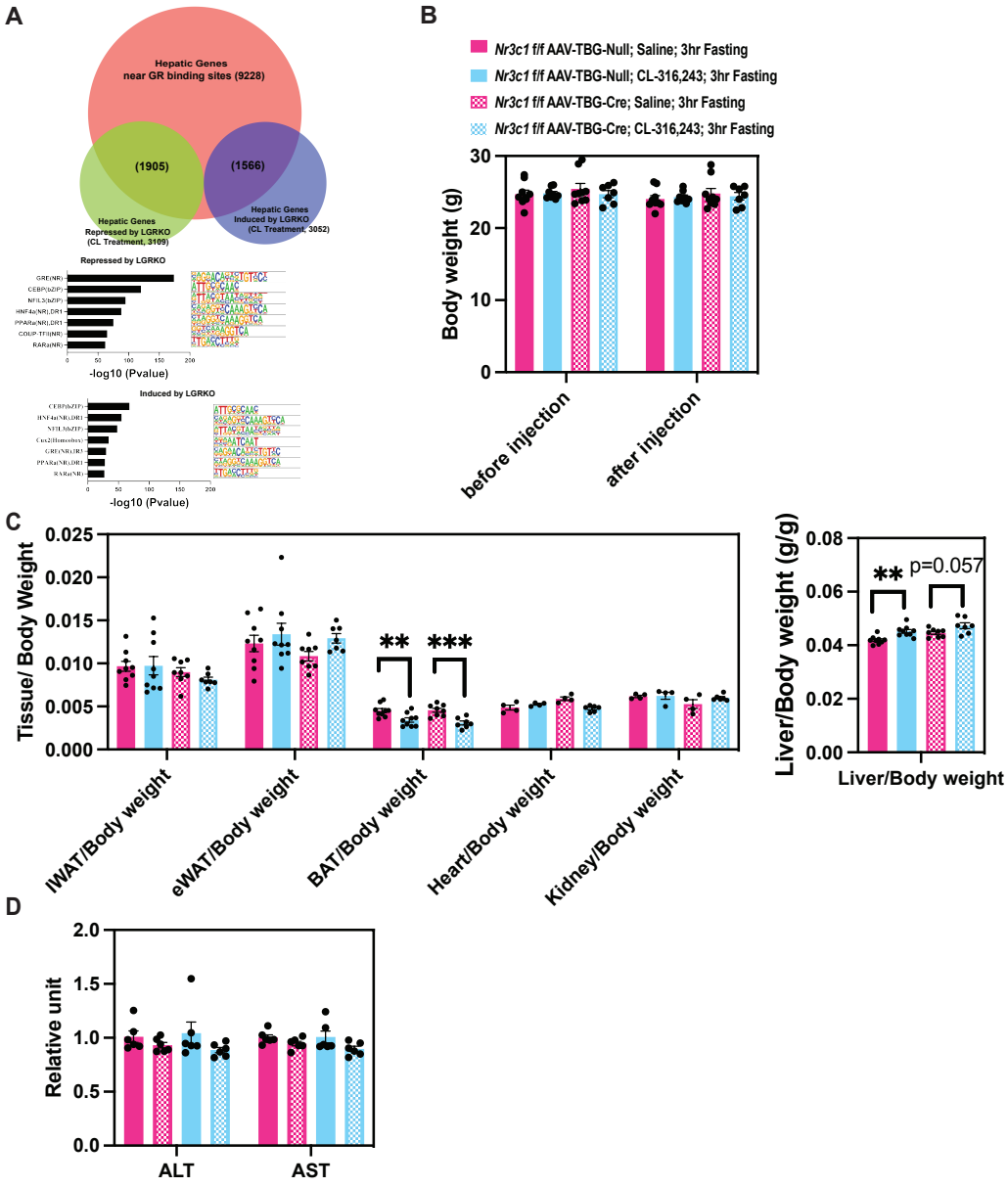

Figure S3-3-1. Hepatic GR deficiency mice has no significant body and organs weight change. A. Hepatic genes near GR binding sites overlapped with hepatic gene GRLKO reduced and induced expression (Saline treatment), the overlapped motifs were analyzed by Homer-motif analysis. B. Body weight before and after CL treatment. C. Tissue weight after 3 hours CL treatment. D. ALT and AST level in GRLKO. (Control groups CL vs Saline, *: p<0.05, **: p< 0.01, ***: p<0.005, ****: p<0.001, n=7-9).

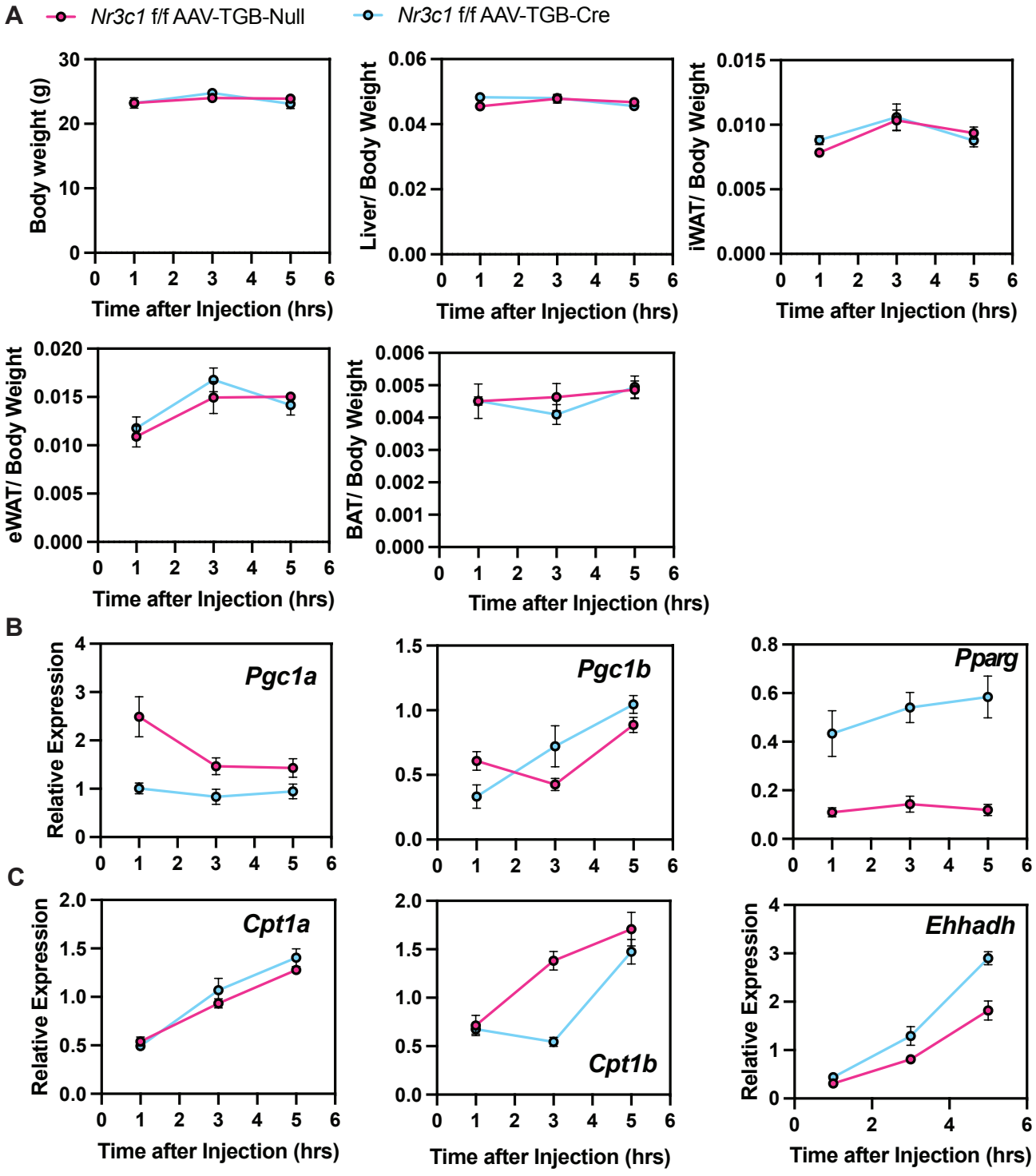

Figure S3-3-2. Time course for gene expression from hepatic GR deficiency liver in response to adipose tissue lipolysis. A. Time course for body weight and organs weight after CL administration. B. Transcriptional gene expression after CL treatment in the GRLKO mice liver. C. Fatty acid oxidation gene expression after CL treatment in the GRLKO mice liver. (n=5-7)

Reference.

Adler, D., et al. (2012). "Rearrangement of the ETS genes ETV-1, ETV-4, ETV-5, and ELK-4 is a clonal event during prostate cancer progression." Human pathology **43**(11): 1910-1916.

Ahmadian, M., Y. Wang and H. S. Sul (2010). "Lipolysis in adipocytes." The International Journal of Biochemistry & Cell Biology **42**(5): 555-559.

Akalestou, E., L. Genser and G. A. Rutter (2020). "Glucocorticoid metabolism in obesity and following weight loss." Frontiers in endocrinology **11**: 59 %@ 1664-2392.

Albaugh, V. L., et al. (2011). "Olanzapine promotes fat accumulation in male rats by decreasing physical activity, repartitioning energy and increasing adipose tissue lipogenesis while impairing lipolysis." Molecular psychiatry **16**(5): 569-581.

Arner, P. and M. Rydén (2022). "Human white adipose tissue: A highly dynamic metabolic organ." Journal of Internal Medicine **291**(5): 611-621 %@ 0954-6820.

Avril, T., E. Vauleon and E. Chevet (2017). "Endoplasmic reticulum stress signaling and chemotherapy resistance in solid cancers." Oncogenesis **6**(8): e373-e373 %@ 2157-9024.

Azzu, V., et al. (2020). "Adipose tissue-liver cross talk in the control of whole-body metabolism: implications in nonalcoholic fatty liver disease." Gastroenterology **158**(7): 1899-1912 %@ 0016-5085.

Bai, L., et al. (2011). "Transcription coactivator mediator subunit MED1 is required for the development of fatty liver in the mouse." HEPATOLOGY **53**(4): 1164-1174 %@ 0270-9139.

Barr, J., et al. (2012). "Obesity-dependent metabolic signatures associated with nonalcoholic fatty liver disease progression." Journal of proteome research **11**(4): 2521-2532 %@ 1535-3893.

Barta, E. (2011). "Command line analysis of ChIP-seq results." EMBnet. journal **17**(1): 13-17.

Besse-Patin, A., et al. (2019). "PGC1A regulates the IRS1: IRS2 ratio during fasting to influence hepatic metabolism downstream of insulin." Proceedings of the National Academy of Sciences **116**(10): 4285-4290 %@ 0027-8424.

Blüher, M. (2013). "Adipose tissue dysfunction contributes to obesity related metabolic diseases." Best practice & research Clinical endocrinology & metabolism **27**(2): 163-177 %@ 1521-1690X.

Bose, S. K., I. Hutson and C. A. Harris (2016). "Hepatic glucocorticoid receptor plays a greater role than adipose GR in metabolic syndrome despite renal compensation." Endocrinology **157**(12): 4943-4960.

Brocker, C. N., et al. (2017). "Hepatocyte-specific PPARA expression exclusively promotes agonist-induced cell proliferation without influence from nonparenchymal cells." American Journal of Physiology-Gastrointestinal and Liver Physiology **312**(3): G283-G299 %@ 0193-1857.

Brunt, E. M., et al. (2011). "Nonalcoholic fatty liver disease (NAFLD) activity score and the histopathologic diagnosis in NAFLD: distinct clinicopathologic meanings." HEPATOLOGY **53**(3): 810-820 %@ 0270-9139.

Buenrostro, J. D., et al. (2015). "ATAC-seq: a method for assaying chromatin accessibility genome-wide." Current protocols in molecular biology **109**(1): 21.29. 21-21.29. 29.

Cao, J., et al. (2006). "Molecular identification of microsomal acyl-CoA: glycerol-3-phosphate acyltransferase, a key enzyme in de novo triacylglycerol synthesis." Proceedings of the National Academy of Sciences **103**(52): 19695-19700.

Capellino, S., M. Claus and C. Watzl (2020). "Regulation of natural killer cell activity by glucocorticoids, serotonin, dopamine, and epinephrine." Cellular & molecular immunology **17**(7): 705-711 %@ 1672-7681.

Carotti, S., et al. (2020). "An overview of deregulated lipid metabolism in nonalcoholic fatty liver disease with special focus on lysosomal acid lipase." American Journal of Physiology-Gastrointestinal and Liver Physiology **319**(4): G469-G480 %@ 0193-1857.

Carpentier, A. C., et al. (2023). "Brown adipose tissue—A translational perspective." Endocrine Reviews **44**(2): 143-192 %@ 0163-0769X.

Caturano, A., et al. (2021). "Non-alcoholic fatty liver disease: From pathogenesis to clinical impact." Processes **9**(1): 135 %@ 2227-9717.

Chen, X., et al. (2011). "Melatonin alleviates lipopolysaccharide-induced hepatic SREBP-1c activation and lipid accumulation in mice." Journal of pineal research **51**(4): 416-425 %@ 0742-3098.

Cichoż-Lach, H. and A. Michalak (2014). "Oxidative stress as a crucial factor in liver diseases." World journal of gastroenterology: WJG **20**(25): 8082.

Collins, S. (2022). "β-Adrenergic receptors and adipose tissue metabolism: Evolution of an old story." Annual Review of Physiology **84**: 1-16 %@ 0066-4278.

Collins, S. and R. S. Surwit (2001). "The beta-adrenergic receptors and the control of adipose tissue metabolism and thermogenesis." Recent progress in hormone research **56**: 309-328 %@ 0079-9963.

Daas, S. I., B. R. Rizeq and G. K. Nasrallah (2019). "Adipose tissue dysfunction in cancer cachexia." Journal of cellular physiology **234**(1): 13-22.

Danysz, W., et al. (2018). "Browning of white adipose tissue induced by the ß3 agonist CL-316,243 after local and systemic treatment-PK-PD relationship." Biochimica et Biophysica Acta (BBA)-Molecular Basis of Disease **1864**(9): 2972-2982.

De Carvalho, F. G., et al. (2019). "Adipose tissue quality in aging: how structural and functional aspects of adipose tissue impact skeletal muscle quality." Nutrients **11**(11): 2553.

DeLany, J. P., et al. (2000). "Differential oxidation of individual dietary fatty acids in humans." The American journal of clinical nutrition **72**(4): 905-911.

den Uil, C. A., et al. (2014). "Conventional hemodynamic resuscitation may fail to optimize tissue perfusion: an observational study on the effects of dobutamine, enoximone, and norepinephrine in patients with acute myocardial infarction complicated by cardiogenic shock." PLoS One **9**(8): e103978 %@ 101932-106203.

Ding, L., et al. (2021). "Peroxisomal β-oxidation acts as a sensor for intracellular fatty acids and regulates lipolysis." Nature metabolism **3**(12): 1648-1661 %@ 2522-5812.

Dixon, E. D., et al. (2021). "The role of lipid sensing nuclear receptors (PPARs and LXR) and metabolic lipases in obesity, diabetes and NAFLD." Genes **12**(5): 645 %@ 2073-4425.

Dong, X. C. (2017). "FOXO transcription factors in non-alcoholic fatty liver disease." Liver research **1**(3): 168-173.

Enevoldsen, L. H., et al. (2007). "Post-exercise abdominal, subcutaneous adipose tissue lipolysis in fasting subjects is inhibited by infusion of the somatostatin analogue octreotide." Clinical physiology and functional imaging **27**(5): 320-326 %@ 1475-0961.

Fabbrini, E., et al. (2008). "Alterations in adipose tissue and hepatic lipid kinetics in obese men and women with nonalcoholic fatty liver disease." Gastroenterology **134**(2): 424-431.

Fain, J. N., et al. (2008). "Stimulation of human omental adipose tissue lipolysis by growth hormone plus dexamethasone." Molecular and cellular endocrinology **295**(1-2): 101-105.

Farzanegi, P., et al. (2019). "Mechanisms of beneficial effects of exercise training on non-alcoholic fatty liver disease (NAFLD): Roles of oxidative stress and inflammation." European journal of sport science **19**(7): 994-1003 %@ 1746-1391.

Fougerat, A., et al. (2022). "ATGL-dependent white adipose tissue lipolysis controls hepatocyte PPARα activity." Cell Reports **39**(10): 110910 %@ 112211-111247.

Fougerat, A., et al. (2022). "ATGL-dependent white adipose tissue lipolysis controls hepatocyte PPARα activity." Cell Reports **39**(10): 110910.

Geng, Y., et al. (2021). "How does hepatic lipid accumulation lead to lipotoxicity in non-alcoholic fatty liver disease?" Hepatology international **15**: 21-35.

Gluchowski, N. L., et al. (2017). "Lipid droplets and liver disease: from basic biology to clinical implications." Nature reviews Gastroenterology & hepatology **14**(6): 343-355 %@ 1759-5045.

Goncalves, M. D., et al. (2019). "High-fructose corn syrup enhances intestinal tumor growth in mice." Science **363**(6433): 1345-1349.

Grandi, F. C., et al. (2022). "Chromatin accessibility profiling by ATAC-seq." Nature protocols **17**(6): 1518-1552.

Granneman, J. G., et al. (2011). "Interactions of perilipin-5 (Plin5) with adipose triglyceride lipase." Journal of Biological Chemistry **286**(7): 5126-5135 %@ 0021-9258.

Green, C. R., et al. (2016). "Branched-chain amino acid catabolism fuels adipocyte differentiation and lipogenesis." Nature chemical biology **12**(1): 15-21.

Guilliams, M. and C. L. Scott (2022). "Liver macrophages in health and disease." Immunity **55**(9): 1515-1529 %@ 1074-7613.

Hall, Z., et al. (2021). "Lipid remodeling in hepatocyte proliferation and hepatocellular carcinoma." HEPATOLOGY **73**(3): 1028-1044.

Han, S.-F., et al. (2017). "Lipolysis and thermogenesis in adipose tissues as new potential mechanisms for metabolic benefits of dietary fiber." Nutrition **33**: 118-124.

Harms, M. and P. Seale (2013). "Brown and beige fat: development, function and therapeutic potential." Nature medicine **19**(10): 1252-1263.

Heine, M., et al. (2018). "Lipolysis triggers a systemic insulin response essential for efficient energy replenishment of activated brown adipose tissue in mice." Cell metabolism **28**(4): 644-655. e644 %@ 1550-4131.

Herrera-Marcos, L. V., et al. (2020). "Pgc1a is responsible for the sex differences in hepatic Cidec/Fsp27β mRNA expression in hepatic steatosis of mice fed a Western diet." American Journal of Physiology-Endocrinology and Metabolism **318**(2): E249-E261.

Hilton, C., F. Karpe and K. E. Pinnick (2015). "Role of developmental transcription factors in white, brown and beige adipose tissues." Biochimica et Biophysica Acta (BBA)-Molecular and Cell Biology of Lipids **1851**(5): 686-696 %@ 1388-1981.

Hirota, K. and A. Fukamizu (2010). "Transcriptional regulation of energy metabolism in the liver." Journal of Receptors and Signal Transduction **30**(6): 403-409.

Hu, Z. and W.-W. Tee (2017). "Enhancers and chromatin structures: regulatory hubs in gene expression and diseases." Bioscience reports **37**(2): BSR20160183.

Huang, P., et al. (2022). "Lanzhang granules ameliorate nonalcoholic fatty liver disease by regulating the PPARα signaling pathway." Evidence-Based Complementary and Alternative Medicine **2022**.

Huijsman, E., et al. (2009). "Adipose triacylglycerol lipase deletion alters whole body energy metabolism and impairs exercise performance in mice." American Journal of Physiology-Endocrinology and Metabolism **297**(2): E505-E513.

Hunter, A. L., et al. (2022). "HNF4A modulates glucocorticoid action in the liver." Cell Reports **39**(3).

Iizuka, K. and Y. Horikawa (2008). "ChREBP: a glucose-activated transcription factor involved in the development of metabolic syndrome." Endocrine journal **55**(4): 617-624.

Ipsen, D. H., J. Lykkesfeldt and P. Tveden-Nyborg (2018). "Molecular mechanisms of hepatic lipid accumulation in non-alcoholic fatty liver disease." Cellular and molecular life sciences **75**: 3313-3327.

Jain, R., et al. (2020). "Liver nucleotide biosynthesis is linked to protection from vascular complications in individuals with long-term type 1 diabetes." Scientific Reports **10**(1): 11561.

Jenkins, B., J. A. West and A. Koulman (2015). "A review of odd-chain fatty acid metabolism and the role of pentadecanoic acid (C15: 0) and heptadecanoic acid (C17: 0) in health and disease." Molecules **20**(2): 2425-2444.

Jiang, D., et al. (2021). "Pyruvate dehydrogenase kinase 4-mediated metabolic reprogramming is involved in rituximab resistance in diffuse large B-cell lymphoma by affecting the expression of MS4A1/CD20." Cancer Science **112**(9): 3585-3597.

Kakazu, E., et al. (2016). "Hepatocytes release ceramide-enriched pro-inflammatory extracellular vesicles in an IRE1α-dependent manner [S]." Journal of lipid research **57**(2): 233-245.

Kaneko, M., et al. (2017). "ER stress and disease: toward prevention and treatment." Biological and Pharmaceutical Bulletin **40**(9): 1337-1343 %@ 0918-6158.

Kasano-Camones, C. I., et al. (2023). "PPARα activation partially drives NAFLD development in liver-specific Hnf4a-null mice." The Journal of Biochemistry: mvad005 %@ 0021-0924X.

Kasano-Camones, C. I., et al. (2023). "PPARα activation partially drives NAFLD development in liver-specific Hnf4a-null mice." The Journal of Biochemistry **173**(5): 393-411.

Kaur, S., C. Auger and M. G. Jeschke (2020). "Adipose tissue metabolic function and dysfunction: impact of burn injury." Frontiers in Cell and Developmental Biology **8**: 599576 %@ 592296-599634X.

Kawano, Y. and D. E. Cohen (2013). "Mechanisms of hepatic triglyceride accumulation in non-alcoholic fatty liver disease." Journal of gastroenterology **48**: 434-441.

Keating, S. E., et al. (2015). "Effect of aerobic exercise training dose on liver fat and visceral adiposity." Journal of hepatology **63**(1): 174-182 %@ 0168-8278.

Kim, M. S., et al. (2007). "Tumor necrosis factor and interleukin 1 decrease RXRα, PPARα, PPARγ, LXRα, and the coactivators SRC-1, PGC-1α, and PGC-1β in liver cells." Metabolism **56**(2): 267-279 %@ 0026-0495.

Kim, S.-J., et al. (2016). "AMPK phosphorylates desnutrin/ATGL and hormone-sensitive lipase to regulate lipolysis and fatty acid oxidation within adipose tissue." Molecular and cellular biology **36**(14): 1961-1976 %@ 0270-7306.

Klemm, S. L., Z. Shipony and W. J. Greenleaf (2019). "Chromatin accessibility and the regulatory epigenome." Nature Reviews Genetics **20**(4): 207-220.

Kondo, Y., et al. (2008). "Downregulation of histone H3 lysine 9 methyltransferase G9a induces centrosome disruption and chromosome instability in cancer cells." PLoS One **3**(4): e2037 %@ 1932-6203.

Kouzarides, T. (2007). "Chromatin modifications and their function." Cell **128**(4): 693-705.

Kuryszko, J., P. Slawuta and G. Sapikowski (2016). "Secretory function of adipose tissue." Polish journal of veterinary sciences **19**(2).

Lass, A., et al. (2011). "Lipolysis–a highly regulated multi-enzyme complex mediates the catabolism of cellular fat stores." Progress in lipid research **50**(1): 14-27.

Latteri, S., et al. (2023). "Mechanisms linking bariatric surgery to adipose tissue, glucose metabolism, fatty liver disease and gut microbiota." Langenbeck's Archives of Surgery **408**(1): 101 %@ 1435-2451.

Leach, S. and K. Suzuki (2020). "Adrenergic signaling in circadian control of immunity." Frontiers in Immunology **11**: 1235 %@ 1664-3224.

Lee, J.-M., S.-J. Park and D.-S. Im (2017). "Calcium signaling of lysophosphatidylethanolamine through LPA1 in human SH-SY5Y neuroblastoma cells." Biomolecules & Therapeutics **25**(2): 194.

Li, S., et al. (2021). "Proteomics of Vitreous Humor Reveals PPARA, RXR, and LXR Are Possible Upstream Regulators of Proliferative Diabetic Retinopathy." Frontiers in Medicine **8**: 724695 %@ 722296-724858X.

Li, Y., et al. (2019). "Yin Yang 1 facilitates hepatocellular carcinoma cell lipid metabolism and tumor progression by inhibiting PGC-1β-induced fatty acid oxidation." Theranostics **9**(25): 7599.

Li, Z., et al. (2019). "Identification of transcription factor binding sites using ATAC-seq." Genome biology **20**: 1-21.

Liang, Q., et al. (2014). "FGF21 maintains glucose homeostasis by mediating the cross talk between liver and brain during prolonged fasting." Diabetes **63**(12): 4064-4075.

Loft, A., et al. (2022). "A macrophage-hepatocyte glucocorticoid receptor axis coordinates fasting ketogenesis." Cell metabolism **34**(3): 473-486. e479.

Louet, J.-F., et al. (2010). "The coactivator SRC-1 is an essential coordinator of hepatic glucose production." Cell metabolism **12**(6): 606-618 %@ 1550-4131.

Lynes, M. D., et al. (2018). "Cold-activated lipid dynamics in adipose tissue highlights a role for cardiolipin in thermogenic metabolism." Cell Reports **24**(3): 781-790.

MacPherson, R. E., et al. (2016). "Reduced ATGL-mediated lipolysis attenuates β-adrenergic-induced AMPK signaling, but not the induction of PKA-targeted genes, in adipocytes and adipose tissue." American journal of physiology-cell physiology **311**(2): C269-C276.

MacPherson, R. E. K., et al. (2013). "Skeletal muscle PLIN proteins, ATGL and CGI-58, interactions at rest and following stimulated contraction." American Journal of Physiology-Regulatory, Integrative and Comparative Physiology **304**(8): R644-R650 %@ 0363-6119.

Mandrekar, P. (2011). "Epigenetic regulation in alcoholic liver disease." World journal of gastroenterology: WJG **17**(20): 2456.

Marengo, A., C. Rosso and E. Bugianesi (2016). "Liver cancer: connections with obesity, fatty liver, and cirrhosis." Annual review of medicine **67**: 103-117 %@ 0066-4219.

Martin, A. R., S. Chung and K. Koehler (2020). "Is exercise a match for cold exposure? Common molecular framework for adipose tissue browning." International Journal of Sports Medicine **41**(07): 427-442 %@ 0172-4622.

Martínez-Jiménez, C. P., et al. (2006). "Underexpressed coactivators PGC1α and SRC1 impair hepatocyte nuclear factor 4α function and promote dedifferentiation in human hepatoma cells." Journal of Biological Chemistry **281**(40): 29840-29849 %@ 20021-29258.

Martinez-Lopez, N. and R. Singh (2015). "Autophagy and lipid droplets in the liver." Annual review of nutrition **35**: 215-237 %@ 0199-9885.

Marzolla, V., et al. (2020). "The novel non-steroidal MR antagonist finerenone improves metabolic parameters in high-fat diet-fed mice and activates brown adipose tissue via AMPK-ATGL pathway." The FASEB Journal **34**(9): 12450-12465.

McGee, S. L. and M. Hargreaves (2008). "AMPK and transcriptional regulation." Front Biosci **13**: 3022-3033.

McTernan, P. G., et al. (2002). "Insulin and rosiglitazone regulation of lipolysis and lipogenesis in human adipose tissue in vitro." Diabetes **51**(5): 1493-1498.

Medak, K. D., et al. (2022). "The glucose lowering effects of CL 316,243 dissipate with repeated use and are rescued by cilostamide." Physiological reports **10**(4): e15187.

Migliorini, R. H., M. A. Garofalo and I. C. Kettelhut (1997). "Increased sympathetic activity in rat white adipose tissue during prolonged fasting." American Journal of Physiology-Regulatory, Integrative and Comparative Physiology **272**(2): R656-R661 %@ 0363-6119.

Mohajan, D. and H. K. Mohajan (2023). "Obesity and Its Related Diseases: A New Escalating Alarming in Global Health." Journal of Innovations in Medical Research **2**(3): 12-23 %@ 2788-7022.

Møller, C. L., et al. (2015). "Melanocortin agonists stimulate lipolysis in human adipose tissue explants but not in adipocytes." BMC research notes **8**(1): 1-9 %@ 1756-0500.

Monetti, M., et al. (2007). "Dissociation of hepatic steatosis and insulin resistance in mice overexpressing DGAT in the liver." Cell metabolism **6**(1): 69-78 %@ 1550-4131.

Morak, M., et al. (2012). "Adipose triglyceride lipase (ATGL) and hormone-sensitive lipase (HSL) deficiencies affect expression of lipolytic activities in mouse adipose tissues." Molecular & Cellular Proteomics **11**(12): 1777-1789.

Muise, E. S., et al. (2019). "Pharmacological AMPK activation induces transcriptional responses congruent to exercise in skeletal and cardiac muscle, adipose tissues and liver." PLoS One **14**(2): e0211568.

Nguyen, K. D., et al. (2011). "Alternatively activated macrophages produce catecholamines to sustain adaptive thermogenesis." Nature **480**(7375): 104-108 %@ 0028-0836.

NIDDK.NIH (2023). "https://www.niddk.nih.gov/health-information/health-statistics/overweight-obesity."

NIDDK.NIH (2023). "https://www.niddk.nih.gov/health-information/liver-disease/nafld-nash/definition-facts#:~:text=Experts%20estimate%20about%2024%25%20of,of%20U.S.%20adults%20have%20NASH.".

Nikolova-Karakashian, M. (2018). "Alcoholic and non-alcoholic fatty liver disease: Focus on ceramide." Advances in biological regulation **70**: 40-50.

Nishina, A., et al. (2006). "Lysophosphatidylethanolamine in Grifola frondosa as a neurotrophic activator via activation of MAPK." Journal of lipid research **47**(7): 1434-1443.

Noureddin, M., et al. (2022). "Predicting NAFLD prevalence in the United States using National Health and Nutrition Examination Survey 2017–2018 transient elastography data and application of machine learning." Hepatology Communications **6**(7): 1537-1548 %@ 2471-1254X.

Ou, J., et al. (2001). "Unsaturated fatty acids inhibit transcription of the sterol regulatory element-binding protein-1c (SREBP-1c) gene by antagonizing ligand-dependent activation of the LXR." Proceedings of the National Academy of Sciences **98**(11): 6027-6032.

Pagadala, M., et al. (2012). "Role of ceramides in nonalcoholic fatty liver disease." Trends in endocrinology & metabolism **23**(8): 365-371.

Pan, G., et al. (2021). "Multifaceted regulation of hepatic lipid metabolism by YY1." Life Science Alliance **4**(7).

Pan, X., et al. (2017). "FOXO transcription factors protect against the diet-induced fatty liver disease." Scientific Reports **7**(1): 44597.

Panic, V., et al. (2020). "Mitochondrial pyruvate carrier is required for optimal brown fat thermogenesis." Elife **9**: e52558 %@ 52050-52084X.

Parker, R., S.-J. Kim and B. Gao (2018). "Alcohol, adipose tissue and liver disease: mechanistic links and clinical considerations." Nature reviews Gastroenterology & hepatology **15**(1): 50-59.

Pawlak, M., P. Lefebvre and B. Staels (2015). "Molecular mechanism of PPARα action and its impact on lipid metabolism, inflammation and fibrosis in non-alcoholic fatty liver disease." Journal of hepatology **62**(3): 720-733.

Petrescu, M., et al. (2022). "Chronic inflammation—A link between nonalcoholic fatty liver disease (NAFLD) and dysfunctional adipose tissue." Medicina **58**(5): 641 %@ 1648-9144.

Pettersen, I. K. N., et al. (2019). "Upregulated PDK4 expression is a sensitive marker of increased fatty acid oxidation." Mitochondrion **49**: 97-110.

Pirzgalska, R. M., et al. (2017). "Sympathetic neuron–associated macrophages contribute to obesity by importing and metabolizing norepinephrine." Nature medicine **23**(11): 1309-1318 %@ 1078-8956.

Præstholm, S. M., et al. (2021). "Impaired glucocorticoid receptor expression in liver disrupts feeding-induced gene expression, glucose uptake, and glycogen storage." Cell Reports **37**(5): 109938.

Qian, H., et al. (2021). "Autophagy in liver diseases: A review." Molecular aspects of medicine **82**: 100973 %@ 100098-102997.

Qin, Y.-J., et al. (2020). "Loss of PDK4 expression promotes proliferation, tumorigenicity, motility and invasion of hepatocellular carcinoma cells." Journal of Cancer **11**(15): 4397.

Rahimi, L., A. Rajpal and F. Ismail-Beigi (2020). "Glucocorticoid-induced fatty liver disease." Diabetes, Metabolic Syndrome and Obesity: 1133-1145 %@ 1178-7007.

Rando, G., et al. (2016). "Glucocorticoid receptor-PPARα axis in fetal mouse liver prepares neonates for milk lipid catabolism." Elife **5**: e11853 %@ 12050-11084X.

Reed, B. D., et al. (2008). "Genome-wide occupancy of SREBP1 and its partners NFY and SP1 reveals novel functional roles and combinatorial regulation of distinct classes of genes." PLoS genetics **4**(7): e1000133.

Reid, J. and D. R. Husbands (1985). "Oxidative metabolism of long-chain fatty acids in mitochondria from sheep and rat liver. Evidence that sheep conserve linoleate by limiting its oxidation." Biochemical Journal **225**(1): 233-237.

Robin, P., et al. (2007). "Post-translational modifications of histones H3 and H4 associated with the histone methyltransferases Suv39h1 and G9a." Genome biology **8**: 1-10.

Rosso, C., et al. (2019). "Crosstalk between adipose tissue insulin resistance and liver macrophages in non-alcoholic fatty liver disease." Journal of hepatology **71**(5): 1012-1021.

Rui, L. (2014). "Energy metabolism in the liver." Comprehensive physiology **4**(1): 177.

Sakers, A., et al. (2022). "Adipose-tissue plasticity in health and disease." Cell **185**(3): 419-446 %@ 0092-8674.

Schoiswohl, G., et al. (2015). "Impact of reduced ATGL-mediated adipocyte lipolysis on obesity-associated insulin resistance and inflammation in male mice." Endocrinology **156**(10): 3610-3624.

Schreiber, R., et al. (2017). "Cold-induced thermogenesis depends on ATGL-mediated lipolysis in cardiac muscle, but not brown adipose tissue." Cell metabolism **26**(5): 753-763. e757 %@ 1550-4131.

Schrem, H., J. Klempnauer and J. Borlak (2002). "Liver-enriched transcription factors in liver function and development. Part I: the hepatocyte nuclear factor network and liver-specific gene expression." Pharmacological reviews **54**(1): 129-158 %@ 0031-6997.

Schulze, R. J., et al. (2017). "Hepatic lipophagy: new insights into autophagic catabolism of lipid droplets in the liver." Hepatology Communications **1**(5): 359-369 %@ 2471-2254X.

Seebacher, F., et al. (2020). Hepatic lipid droplet homeostasis and fatty liver disease, Elsevier.

Sekizkardes, H., et al. (2020). "Free fatty acid processing diverges in human pathologic insulin resistance conditions." The Journal of clinical investigation **130**(7): 3592-3602.

Shao, W. and P. J. Espenshade (2012). "Expanding roles for SREBP in metabolism." Cell metabolism **16**(4): 414-419.

Shin, H., et al. (2017). "Lipolysis in brown adipocytes is not essential for cold-induced thermogenesis in mice." Cell metabolism **26**(5): 764-777. e765.

Shin, J., et al. (2013). "SIRT7 represses Myc activity to suppress ER stress and prevent fatty liver disease." Cell Reports **5**(3): 654-665.

Simcox, J., et al. (2017). "Global analysis of plasma lipids identifies liver-derived acylcarnitines as a fuel source for brown fat thermogenesis." Cell metabolism **26**(3): 509-522. e506 %@ 1550-4131.

Simopoulos, A. P. (2008). "The importance of the omega-6/omega-3 fatty acid ratio in cardiovascular disease and other chronic diseases." Experimental biology and medicine **233**(6): 674-688.

Smith, B. W. and L. A. Adams (2011). "Nonalcoholic fatty liver disease and diabetes mellitus: pathogenesis and treatment." Nature Reviews Endocrinology **7**(8): 456-465.

Stradomska, T. J., et al. (2020). "Serum very long-chain fatty acids (VLCFA) levels as predictive biomarkers of diseases severity and probability of survival in peroxisomal disorders." PLoS One **15**(9): e0238796 %@ 0231932-0236203.

Su, B., et al. (2021). "A DMS shotgun lipidomics workflow application to facilitate high-throughput, comprehensive lipidomics." Journal of the American Society for Mass Spectrometry **32**(11): 2655-2663.

Summers, S. A., B. Chaurasia and W. L. Holland (2019). "Metabolic messengers: ceramides." Nature metabolism **1**(11): 1051-1058.

Tang, H.-N., et al. (2017). "Plasticity of adipose tissue in response to fasting and refeeding in male mice." Nutrition & Metabolism **14**: 1-14.

Teng, M. L. P., et al. (2022). "Global Incidence and Prevalence of Non-alcoholic Fatty Liver Disease." Clinical and Molecular Hepatology %@ 2287-2728.

Thymiakou, E., M. Tzardi and D. Kardassis (2023). "Impaired hepatic glucose metabolism and liver-α-cell axis in mice with liver-specific ablation of the Hepatocyte Nuclear Factor 4α (Hnf4a) gene." Metabolism **139**: 155371.

Tran, K.-V., et al. (2020). "Human thermogenic adipocyte regulation by the long noncoding RNA LINC00473." Nature metabolism **2**(5): 397-412.

Tsuru, A., et al. (2016). "Novel mechanism of enhancing IRE1α-XBP1 signalling via the PERK-ATF4 pathway." Scientific reports **6**(1): 24217 %@ 22045-22322.

Van Beneden, K., et al. (2013). "HDAC inhibitors in experimental liver and kidney fibrosis." Fibrogenesis & tissue repair **6**: 1-14.

Ventura, I., et al. (2022). "SP1 and NFY Regulate the Expression of PNPT1, a Gene Encoding a Mitochondrial Protein Involved in Cancer." International Journal of Molecular Sciences **23**(19): 11399.

Villeneuve, J., et al. (2018). "Unconventional secretion of FABP4 by endosomes and secretory lysosomes." Journal of Cell Biology **217**(2): 649-665.

Walker, B. (2006). "Cortisol—cause and cure for metabolic syndrome?" Diabetic Medicine **23**(12): 1281-1288.

Wallace, M., et al. (2018). "Enzyme promiscuity drives branched-chain fatty acid synthesis in adipose tissues." Nature chemical biology **14**(11): 1021-1031.

Wang, L., et al. (2021). "Lipid droplets and their interactions with other organelles in liver diseases." The International Journal of Biochemistry & Cell Biology **133**: 105937 %@ 101357-102725.

Washrawirul, C., et al. (2023). "The role of the topical nasal decongestant oxymetazoline as a novel therapeutic option for post-acne erythema: A split-face, double-blind, randomized, placebo-controlled trial." The Journal of Dermatology %@ 0385-2407.

Watanabe, M., et al. (2020). "Beneficial effects of the ketogenic diet on nonalcoholic fatty liver disease: A comprehensive review of the literature." Obesity Reviews **21**(8): e13024 %@ 11467-17881.

Weikum, E. R., et al. (2017). "Glucocorticoid receptor control of transcription: precision and plasticity via allostery." Nature reviews Molecular cell biology **18**(3): 159-174 %@ 1471-0072.

Welch, R. D., et al. (2022). "Emerging Role of Nuclear Receptors for the Treatment of NAFLD and NASH." Metabolites **12**(3): 238 %@ 2218-1989.

Wilhelmi de Toledo, F., et al. (2020). "Unravelling the health effects of fasting: a long road from obesity treatment to healthy life span increase and improved cognition." Annals of medicine **52**(5): 147-161 %@ 0785-3890.

Xiong, F. and L. Zhang (2013). "Role of the hypothalamic–pituitary–adrenal axis in developmental programming of health and disease." Frontiers in neuroendocrinology **34**(1): 27-46 %@ 0091-3022.

Younossi, Z., et al. (2019). "Global perspectives on nonalcoholic fatty liver disease and nonalcoholic steatohepatitis." HEPATOLOGY **69**(6): 2672-2682 %@ 0270-9139.

Yu, J., et al. (2018). "Update on glycerol-3-phosphate acyltransferases: the roles in the development of insulin resistance." Nutrition & diabetes **8**(1): 34.

Yu, X. X., et al. (2002). "Cold elicits the simultaneous induction of fatty acid synthesis and β-oxidation in murine brown adipose tissue: prediction from differential gene expression and confirmation in vivo." The FASEB Journal **16**(2): 155-168 %@ 0892-6638.

Zhang, S., et al. (2023). "Acute activation of adipocyte lipolysis reveals dynamic lipid remodeling of the hepatic lipidome." Journal of Lipid Research: 100434.

Zhang, X., et al. (2022). "Plin5 bidirectionally regulates lipid metabolism in oxidative tissues." Oxidative Medicine and Cellular Longevity **2022 %@ 1942-0900**.

Zhao, J., et al. (2020). "Anti-lipolysis induced by insulin in diverse pathophysiologic conditions of adipose tissue." Diabetes, Metabolic Syndrome and Obesity: 1575-1585.

Zhao, S., et al. (2010). "Regulation of cellular metabolism by protein lysine acetylation." Science **327**(5968): 1000-1004 %@ 0036-8075.

Zhao, Y., et al. (2020). "PDK4-deficiency reprograms intrahepatic glucose and lipid metabolism to facilitate liver regeneration in mice." Hepatology communications **4**(4): 504-517.

Zhao, Y., et al. (2020). "Liver governs adipose remodelling via extracellular vesicles in response to lipid overload." Nature communications **11**(1): 719.

Zhou, J., et al. (2008). "Hepatic fatty acid transporter Cd36 is a common target of LXR, PXR, and PPARγ in promoting steatosis." Gastroenterology **134**(2): 556-567. e551 %@ 0016-5085.

Zhu, Y., et al. (2021). "Adipose tissue hyaluronan production improves systemic glucose homeostasis and primes adipocytes for CL 316,243-stimulated lipolysis." Nature communications **12**(1): 4829 %@ 2041-1723.